POWER SYSTEM STABILITY ANALYSIS WITH A HIGH PENETRATION OF DISTRIBUTED GENERATION

by

Mohamed El Chehaly
B.Eng. Concordia University

A thesis submitted to the Department of Electrical and Computer Engineering in partial fulfillment of the requirements of the degree of Master in Engineering

Department of Electrical and Computer Engineering,
McGill University,
Montréal, Québec, Canada
February 2010

Abstract

The operation and structure of distribution system is changing with the integration of distributed generation, based on alternative energy sources, including renewable energy sources (wind, solar). Among the new issues, there is the question of stability of distribution systems in the presence of a large penetration of distributed generation (DG).

With power systems operating near their loadability limits, voltage stability becomes an important issue. Many utilities have implemented long-term solutions to counter this problem, such as adding transmission lines and new power plants in order to improve the reliability of the power system. An alternative solution consists in increase of generation at the distribution level. This is also a way of meeting growing economical, technical and environmental constraints. The size, the technology and the placement of DG play an important role in the operation of distribution systems.

For long-term voltage stability analysis, bus-based voltage indices are implemented using Power-Voltage curves (PV curves) to analyze the contribution of DG. Large-penetration of DG also has an impact on the short-term stability (voltage stability and transient stability) of the system. Indices are developed to rank contingencies and show how different DG interconnections affect the system during faults. Time-domain simulations are used to perform those studies. For short-term voltage stability, voltage dips at load buses are monitored following a large disturbance. The maximum rotor speed deviations of centralized synchronous generators are used to study the transient stability of the overall system.

All of the indices defined above are tested on three commonly used test systems: the IEEE RTS-96 24-bus system, the IEEE 39-bus New England system and the IEEE 118 bus system. The studies conclude that, regardless of its technology, DG mostly improves the long-term voltage stability particularly when located in areas near large loads. With DG injecting reactive power, the voltage security margin is increased. Synchronous machine based DG has the greatest impact on the short-term stability when located near large centralized generators. For short-term voltage stability, the contribution of DG is most noticeable when it absorbs reactive power, thus lowering the voltage dips.

Résumé

La pénétration de la production décentralisée (DG) ne cesse de croître dans les réseaux électriques. La structure des réseaux conventionnels est modifiée à cause de la présence des sources de puissance alternatives localisées au niveau de la distribution. La stabilité du système est donc étudiée afin de déterminer les conséquences de la grande pénétration de DG.

La stabilité de tension devient une préoccupation majeure de la plupart des utilités dont leur capacité de charge approche les limites. Plusieurs utilités ont mis en œuvre des solutions à long terme pour contrer ce problème, telles que l'implémentation de nouvelles lignes de transmission et de nouvelles centrales électriques afin de garantir la fiabilité du réseau électrique. D'autres utilités ont opté à des solutions plus modernes telles que la production décentralisée qui satisfait les contraintes économiques, techniques et environnementales.

Concernant l'analyse de la stabilité de tension à long terme, des indices basés sur la tension sont implémentés à l'aide des courbes PV pour analyser la contribution de la DG. La haute pénétration de la DG a également un impact sur la stabilité à court terme du système. Les indices sont mis au point pour classifier les défauts et exposer les effets des différentes interconnexions de la DG sur le réseau. Ces études ont été performées à l'aide de plusieurs simulations. Concernant la stabilité de tension à court terme, les creux de tension qui apparaissent à la charge lors d'un défaut sont utilisés pour déterminer la stabilité du système. Les plus grands écarts de vitesse du rotor des générateurs synchrones centralisés aident à déterminer la stabilité transitoire du réseau.

Ces indices sont testés en utilisant trois réseaux électriques. Indépendamment de la technologie, les DGs améliorent la stabilité de tension à long terme quand elles sont situées proches des grosses charges. La stabilité de tension est augmentée lorsque les DG opèrent avec un facteur de puissance inductif. Les DGs basées sur des machines synchrones améliorent le plus la stabilité à court terme, lorsqu'elles sont situées proche des grands générateurs centralisés. Pour la stabilité de tension à court terme, la contribution de la DG est plus visible quand elle opère avec un facteur de puissance capacitif.

Acknowledgements

I would like to thank Prof. Géza Joós, for his supervision during my Master's studies. Through his guidance, I have learned several aspects regarding engineering disciplines and industry needs. I am also very grateful for the significant contributions of Dr. Hugo Gil who helped me on the long-term voltage stability analysis along with Dr. Claudio Cañizares for guiding me early in the work.

I would like to extend my thanks to Prof. Boon Teck Ooi, Prof. Francisco Galiana, Prof. Anthony Rodolakis, and Prof. Jorge Marques. I am also grateful for the support and friendship of Carlos Martinez, Jonathan Robinson, Bassam Frem, Hamed Golestani Far, Sameh El Khatib, Ali Jahanbani Ardakani, Rodrigo Hidalgo Anfossi, Michael Ross, Chad Abbey, José Restrepo, Catalina Gomez-Quilles, Wei Li, Amir Kalantari, Aboutaleb Haddadi, Makram De Freige, Moustafa Momen,Yongzeng Zeng, and Hao Quresh.

Finally I would like to thank my parents, Nevine and Ibrahim, as well as my sister, Iman. Also, special thanks to Lesly Soriana Cruz Perez.

Table of Contents

List of Figures

List of Tables

List of Abbreviations

DG	*Distributed Generator*
HV	*High Voltage*
MV	*Medium Voltage*
LV	*Low Voltage*
GHG	*GreenHouse Gases*
HVDC	*High Voltage Direct Current*
CTC	*Critical Clearing Time*
PV	*Power-Voltage*
CPF	*Continuation Power Flow*
CHP	*Combined Heat and Power*
MLP	*Maximum Loadability Point*
NDSM	*Non-Divergent Solution Methodlogy*
SIB	*Singularity Induced Bifurcation*
SNB	*Saddle-Node Bifurcation*
LIB	*Limited Induced Bifurcation*
DFIG	*Doubly-Fed Induction Generator*
PCC	*Point of Common Coupling*
GENROU	*Round Rotor Synchronous Genertor*
PF	*Power Factor*
CIMTR3	*Induction Generator*
SVC	*Static Var Compensator*
FACTS	*Flexible AC Transmission System*
RTS	*Reliability Test System*
PL	*Penetration Level*
VSM	*Voltage Security Margin*
LTC	*Load Tap Changers*
BVI	*Bus Voltage Improvement*
LDC	*Load Duration Curve*
IESO	*Independent Electricity System Operator*
ISO	*Independent System Operator*
NYISO	*New York Independent System Operator*
AEMO	*Australian Energy Market Operator*
RTE	*Gestionnaire du Réseau de Transport d'Electricité*
STATCOM	*Static Compensator*
SMES	*Superconducting Magnetic Energy Storage*
SVSI	*Short-Term Voltage Stability Index*
MRSD	*Maximum Rotor Speed Deviation*

Nomenclature

$\overline{V}$	*Load bus voltage*
$\overline{E}$	*Generator terminal voltage*
$\overline{I}$	*Current of the two bus system*
X	*Impedance of the transmission line*
S	*Load complex power*
P	*Load real power*
Q	*Load reactive power*
P_{max}	*Maximum load real power*
Q_{crit}	*Critical load reactive power*
X_{crit}	*Critical impedance of the transmission line*
θ_{old}	*Old voltage phase angles*
θ_{new}	*New voltage phase angles*
V_{old}	*Old voltage magnitudes*
V_{new}	*New voltage magnitudes*
$\Delta\theta$	*Change vectors for voltage phase angles*
$\frac{\Delta V}{\Delta V_{old}}$	*Change vectors for bus voltage magnitudes*
α	*Non-divergent parameter*
T'_{do}	*Direct axis open-circuit transient time constant*
T'_{qo}	*Quadrature axis open-circuit transient time constant*
T''_{do}	*Direct axis open-circuit subtransient time constant*
T''_{qo}	*Quadrature axis open-circuit subtransient time constant*
X_d	*Unsaturated direct axis synchronous reactance*
X_q	*Unsaturated quadrature axis synchronous reactance*
X'_d	*Unsaturated direct axis transient reactance*
X'_q	*Unsaturated quadrature axis transient reactance*
X''_d	*Unsaturated direct axis subtransient reactance*
X''_q	*Unsaturated quadrature axis subtransient reactance*
X_l	*Leakage reactance*
H	*Machine inertia*
D	*Damping ratio*
PL	*Penetration level*
P_{DG}	*DG output power*
P_L	*Load real power*
λ_0	*Operating load level*
$\lambda_{\max}$	*Maximum loadability point*
$\lambda_{\max 1}$	*Maximum loadability point of contingency 1*
$\lambda_{\max 2}$	*Maximum loadability point of contingency 2*
$\lambda_{\max}^{DG}$	*Maximum loadability point with DG*
BVI_i	*Bus voltage improvement index with DG at bus i*
P_{DGi}	*DG output power at bus i*

BVI_{Ω}	*Bus voltage improvement index of the subset Ω*
$\lambda_{\max \Omega}^{DG}$	*Maximum loadability point of the subset Ω*
γ_i	*Weight factor*
$SVSI_{base}$	*Short-term voltage stability index for the base case*
S_{Li}	*Load apparent power*
ΔV_i	*Voltage dip at bus i*
N	*Number of load buses*
$SVSI_{DG}$	*Short-term voltage stability index with DG*
S_{DG}	*DG apparent power*
P_{DG}	*DG real power*
Q_{DG}	*DG reactive power*
p	*Penetration level*
PF	*Power factor*
$SVSI_{diff}$	*Contribution of DG connected at one load bus*
$SVSI_{tot}$	*Contribution of DG connected at all load buses*
$MRSD_{base}$	*Maximum rotor speed deviation for the base case*
$MRDD_{DGi}$	*Maximum rotor speed deviation with DG*
$MRDD_{diff\,j}$	*Contribution of DG connected at load bus j*
N_g	*Number of centralized synchronous generators*
$MRSD_{base}$	*Contribution of DG connected at all load buses*
V_{des}	*Desired voltage at the bus*
P_L	*Load real power*
Q_L	*Load reactive power*
P_G	*Generator real power*
Q_G	*Generator reactive power*
R	*Branch resistance*
X	*Branch reactance*
B	*Branch susceptance*
$S(1.0)$	*Saturation factor at 1 p.u.*
$S(1.2)$	*Saturation factor at 1.2 p.u.*
T'	*Transient time constant*
X'	*Transient reactance*
E_1	*Voltage in p.u.*
$S(E_1)$	*Saturation factor at E_1*
E_2	*Voltage in p.u.*
$S(E_2)$	*Saturation factor at E_2*

Chapter 1: Introduction

1.1 Distributed Generation

In most North American power systems, large power plants generate electric power to meet the demand. To maximize profits, many power systems are operated near their generation limits, and therefore may require adding additional generation to meet increases in energy demand due to population and industrial growth. Due to some constraints (geographical, political, economical, environmental), constructing additional large power plants may not be possible, and therefore a larger penetration of Distributed Generation (DG) may be required. The distribution system is shifting from being a "passive" network, containing only loads, to an "active" network.

Large penetration of DG can affect the stability of the system by either improving or deteriorating the stability of the system. Due to the variety of the DG technologies and the complexity of the power system, modeling DG becomes crucial to obtain a correct response of the impact on the power system stability. Indices are developed to assess the contribution of DGs on the system.

A *conventional* power system is organized in three separate areas (Figure 1.1.a):

- Generation
- Transmission
- Distribution

The generation system consists of large power plants that convert mechanical power into electrical power by using energy resources such as coal, gas, oil and hydro. In most cases, these plants are located very far from the loads. The connections between the generation plants and the loads are made through the transmission system where transmission lines transport high voltage (HV) and then medium voltage (MV) electrical power to the loads. In the distribution system, large loads are supplied from the transmission system at low voltages (LV) [1].

Distributed Generation has many definitions as some countries define DG with respect to the voltage level; others define it as generation present in the distribution system and finally some others define it based on characteristics such as renewable,

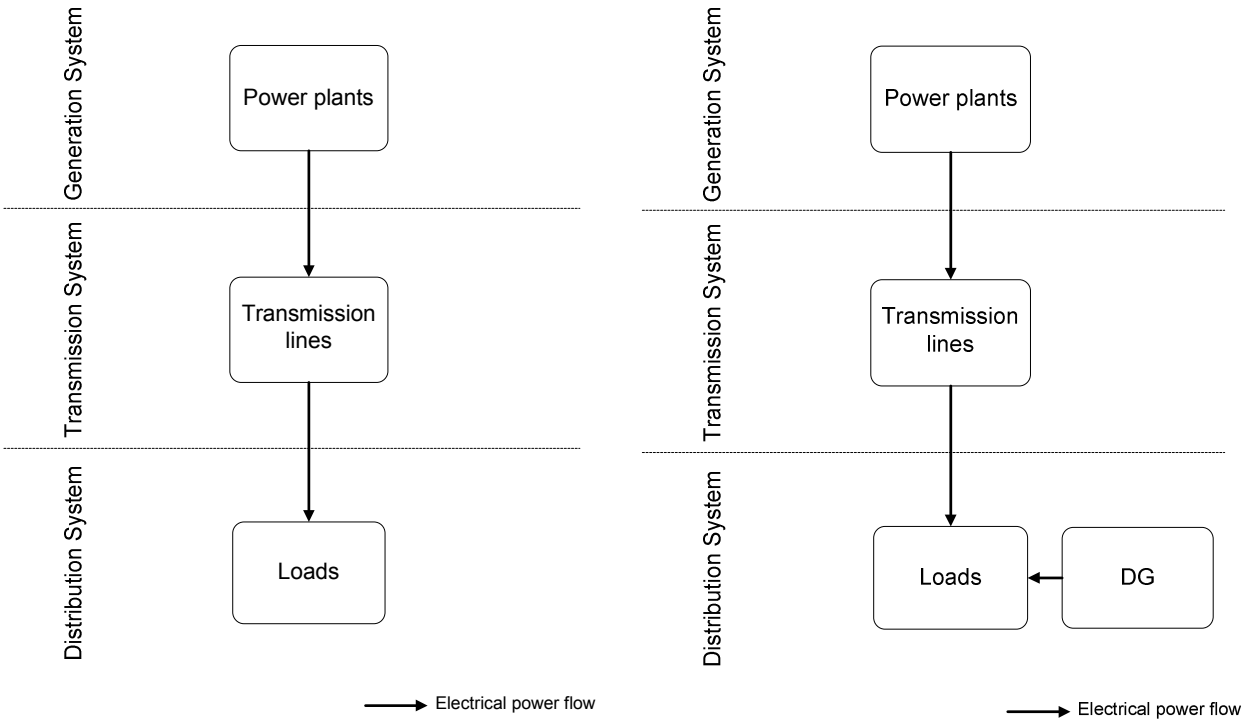

(a) Conventional Power System

(b) Power System with DG

Figure 1.1. Overview of a power system

cogeneration and non-dispatched (DG cannot be controlled from the system operator) [2,3].

CIGRE defines some attributes of DG as being not centrally planned, nor centrally dispatched, smaller than 50-100 MW, and connected to the distribution system [4]. Many authors define DG as a generation that ranges from a few kW to a few tens of MW and that is connected on the distribution side [5-9]. In [10,11], DG is defined as a generation that is directly connected to the distribution network regardless of its generation capacity level and its prime mover. This last definition is favored as it allows a large-penetration of DG using any available technology. Figure 1.1.b shows the new structure of the power system with DG connected to the distribution system.

Many environmental, political and economical factors are pushing towards a large-penetration of DG. CIRED has pointed out these drivers [2,12]:

- Reduction in greenhouse gases (GHG)
- Energy efficiency
- Deregulation and competition policy
- Diversification of energy resources

- National power requirement

Other studies stated more cost-effective reasons such as reduction of transmission lines due to the fact that DG is directly connected to the distribution system, low capital costs and short construction time of small plants and load growth uncertainty [4,12,13].

1.2 Power System Stability

Stability of the power system has been a major concern for more than 90 years. The IEEE/CIGRE Joint Task Force defines stability as follows [14]:

Power system stability is the ability of an electric power system, for a given initial operating condition, to regain a state of operating equilibrium after being subjected to a physical disturbance, with most system variables bounded so that practically the entire system remains intact.

Power system instability is a complex problem as it can take different forms and be associated with a large number of factors. Figure 1.2 shows a detailed classification, defining three main categories of power system stability. Considerations that are taken to counter system instability include [15]:

- The physical nature of the instability: loss of synchronism, low bus voltages, high frequency deviation
- The size of the disturbance
- Measures taken to enhance the power system stability and to prevent system instability
- Methods of calculation to study the different aspects of power system stability

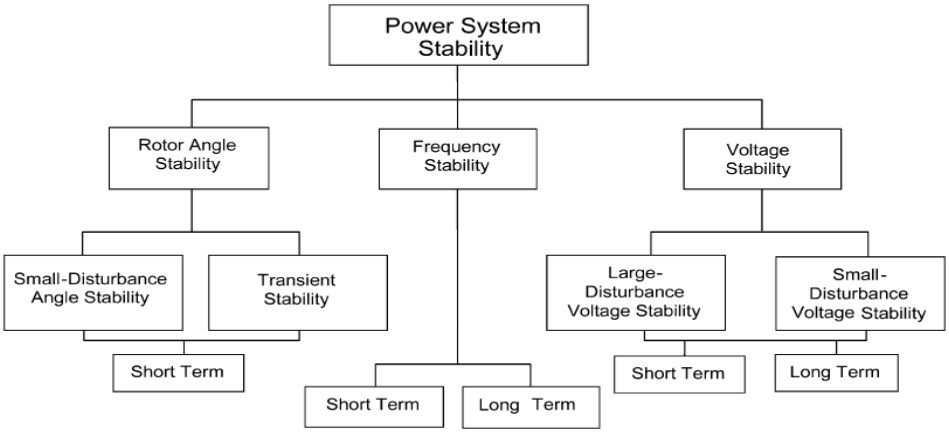

Figure 1.2. Classification of power system stability [15]

1.2.1 Voltage Stability

Voltage stability is defined as the maintenance of bus voltages within an acceptable level in the power system following a disturbance. Stability occurs when equilibrium between the load demand and the supply from the power system is found [14]. *Voltage instability* arises when load dynamics attempt to restore power consumption beyond the capabilities of the generation system. This could result in tripping loads, transmission lines and/or a loss of synchronism of some generators [16]. *Voltage collapse* often occurs during the final stage of voltage instability when very low bus voltages lead to a partial or total blackout in the system [14,15,17].

As referred in Figure 1.2, voltage stability is divided into two sections, i.e. large-disturbance and small-disturbance. *Large-disturbance voltage stability* consists of maintaining bus voltages at a certain acceptable level after the system is subjected to a large disturbance (system faults, loss of generation or presence of contingencies). Whereas, *small-disturbance voltage stability* involves maintaining steady voltages following small perturbations in the system such as load variations [14,15].

For all types of disturbances, the time frame of interest varies from a few seconds to several minutes. Figure 1.2 shows that the time frame is divided into short-term and long-term voltage stability. *Short-term voltage stability* consists of the dynamics of the components of the system shortly after a disturbance. Short-term instability often arises due to the presence of fast acting load components such as induction motor loads, high penetration of distributed generation that is consuming reactive power without voltage control, electronically controlled loads and HVDC converters [14,18]. *Long-term voltage stability* is mainly studied using static analysis for large-scale power systems under various conditions [14,19-23]. Equipment considered for this time scale consists mainly of tap-changing transformers, thermostatically controlled loads and generator current limiters. The main causes of long-term instability include [14,17]:

- Loss of a long-term equilibrium operating point
- Lack of reaching a stable post-disturbance equilibrium due to the effect of overexcitation limiters
- Tap changers reaching their limits or when operating near a small-disturbance instability

1.2.2 Rotor Angle Stability

Rotor angle stability is defined as the ability to maintain the system's synchronous machines of in synchronism after the occurrence of a disturbance. Equilibrium is reached when the electromagnetic torque and the magnetic torque are equal. Being subjected to a disturbance, the synchronous machines start "swinging" with respect to each other. If one machine starts running faster than another, the deviation in angular position will increase and the fast machine will supply more loads. Its speed will then decrease allowing the other machine's speed to increase until equilibrium is reached. Instability occurs when equilibrium is not reached and the speed of some machines increases until these machines are tripped [14,15]. Rotor angle stability is a highly nonlinear, multi-dimensional problem [24].

Instability can be categorized into two different parts: aperiodic (or nonoscillatory) instability and oscillatory instability. Aperiodic instability is caused by a lack of synchronizing torque that is associated with rotor angle deviation. Oscillatory instability is caused by a lack of damping torque associated with speed deviation. Rotor angle stability consists only of short-term phenomena as the time frame is in the order of a few seconds to a few tens of seconds [14,15].

1.2.2.1 Transient Stability

Large-disturbance angle stability (Transient stability) is a subcategory of rotor angle stability and consists of the ability of the power system to maintain angle stability after being subjected to a large disturbance (such as a short-circuit on a transmission line, or the disconnection of a generator …). Instability problems are aperiodic and are mainly due to insufficient synchronizing torque [14,15]. The *critical clearing time* (CCT) is defined as the maximum time duration between the occurrence of the fault and its clearing that the power system can regain stability. Due to the highly nonlinear characteristics of transient stability, time domain simulation is used to solve the differential and algebraic equations of a power system using a step-by-step calculation procedure. Direct method can also be used to determine stability using Lyapunov's second method. This method is not often used due to the complication of finding an adequate Lyapunov function and to the inability of defining a practical stability domain

[15,24]. Pattern recognition can also be a method for transient stability analysis by referring to past experience and applying it on current stability properties [24].

1.2.2.2 Small-Signal Stability

Small-disturbance angle stability (small-signal stability) is another subcategory of rotor angle stability (Figure 1.2) and consists of the ability of the power system to maintain angle stability after being subjected to a small disturbance. A disturbance is considered to be small if the linearized system still represents the dynamics of the original system under this disturbance [14,15]. Once the system is linearized, modal analysis methods could be applied. Modal analysis allows for the computation of the characteristics of modes (mode shapes, participation factors and transfer functions) that can be useful for damping enhancement [15,25]. Time-domain simulations can be used to validate the results [26]. Bifurcation method is another alternative which, unlike modal analysis that considers all system parameters to be fixed, evaluates the impact of large changes on the small-signal stability [27,28]. As discussed previously, two forms of rotor angle instability may arise. The presence of complex conjugate eigenvalues with positive real parts incites an oscillatory instability (Figure 1.3). If the eigenvalue is positive and real, the instability is an aperiodic type (Figure 1.4). Small-signal stability is not in the scope of this thesis.

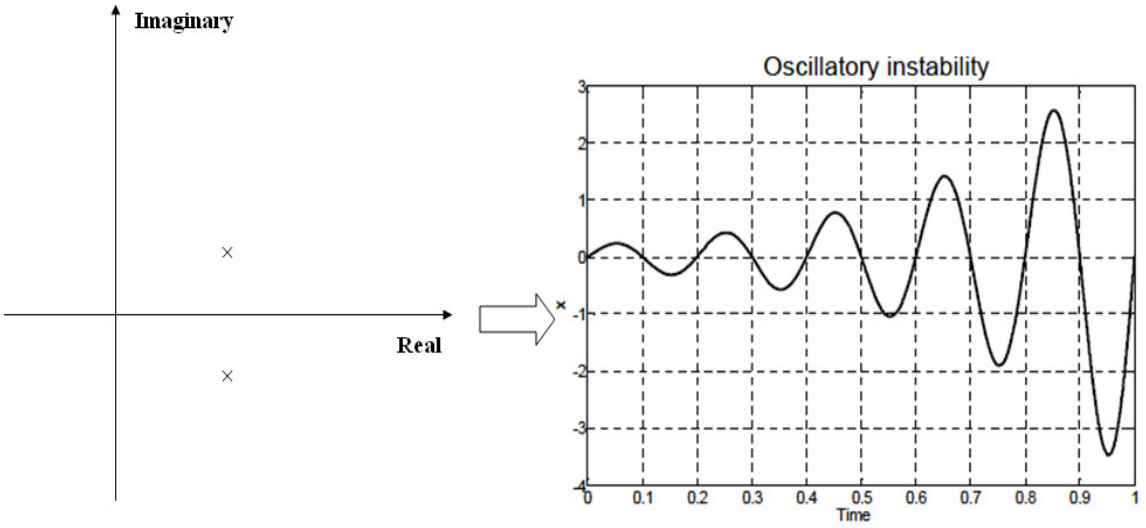

Figure 1.3. Oscillatory instability

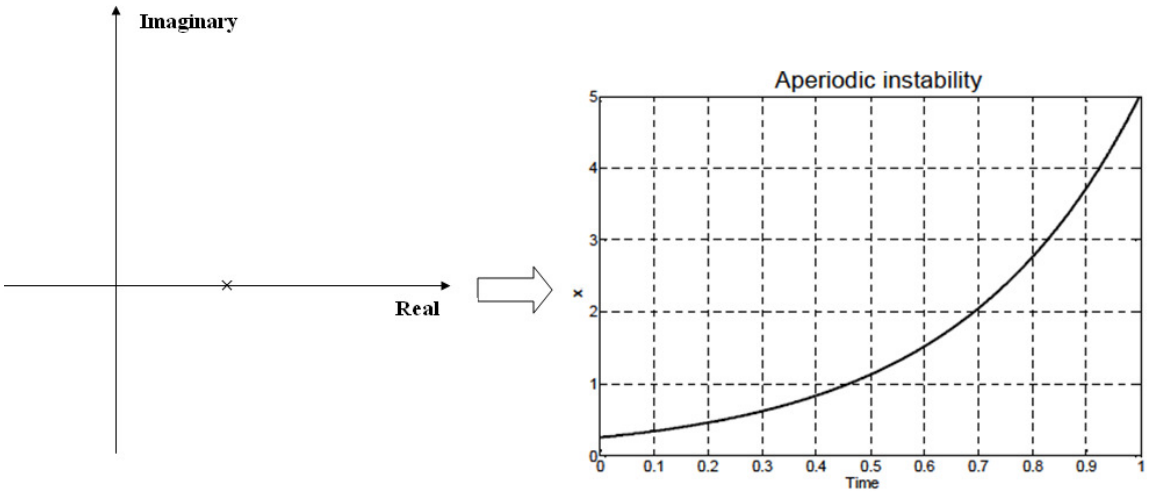

Figure 1.4. Aperiodic instability

1.2.2.3 Frequency Stability

Frequency stability is defined as the ability of a power system to maintain a stable frequency following a disturbance due to an imbalance between generation and load. The system is said to have frequency stability if it can maintain or restore balance between the generation and the load with minimum load tripping [14]. Time domain simulations are mainly used for frequency stability analysis with adequate representation of some dynamic devices [15]. Frequency stability is not in the scope of this thesis.

1.3 Impact of DG on the Power System Stability

With a fast increase in the DG penetration level, the power system stability can vary due to the presence of the new power generation at the distribution level. Recent studies have focused on analyzing the short-term and the long-term impact of connecting DG on the power system.

1.3.1 Impact of DG on the Long-Term Stability

Voltage and frequency stability can be regarded as long-term studies where the time frame can be extended from a few minutes to a few hours (Figure 1.1). Steady-state analysis and dynamic simulations are used to evaluate the long-term voltage stability.

In [29], a method for placement of DGs is defined based on an objective function. PV curves have been used to determine the voltage stability of the system. The method used to draw these curves is the Continuation Power Flow (CPF) that encounters the location

of the voltage collapse without diverging as opposed to conventional power flow methods. The objective function defined in this thesis is to determine the weak buses and to boost the voltage profile that was decreased due to an increase in total load demand. Following the execution of the defined algorithm to place the DG, the bus voltages are close to one, the power losses have decreased significantly and the maximum loading and the voltage stability margin have increased, indicating that the long-term voltage stability is improved.

In [30], the optimal location and optimal penetration level are studied. The CPF method is used to obtain the PV curves and a stability index is defined to find the critical power by increasing the load power at one bus at a time. The indices are then ranked to find the optimal placement by locating the weakest bus associated with the smallest index. The primal dual interior point method is used to find the optimal DG reactive power by minimizing the power losses.

In [31], the effect of excitation system control modes of synchronous machine based DG is discussed. The PV curves were found by varying the real and reactive power of the loads and by keeping constant the DG power. Two types of exciters were defined:

- Voltage Regulator: the terminal voltage of the DG is kept constant by varying the reactive power
- Power Factor Regulator: the DG power factor is constant by matching the required reactive power. The power factor can either be lagging, leading or unitary

In all cases, the voltage stability is improved when DG is added to the system. It is shown that when the synchronous machine based DG is equipped with a voltage regulator, the voltage stability is improved the most. It is then followed by a DG with constant lagging power factor, constant unitary power factor and finally by constant leading power factor.

In [32], [33] and [34], the impact of induction machine based DGs on the long-term voltage stability is examined. Compared with the base case, the voltage stability margin is worsened with induction generator based DGs. This is only the case when induction generators operate at their nominal power. It is then explained that an increase in load at the nose point of the PV curve can cause a constant increase in speed due to a decrease of

electrical torque that is proportional to the terminal voltage. When the induction generator is operating at a lower value, the voltage stability is improved compared with the base case.

In [35], the impact of a small hydro power plant, modeled by two synchronous generators with a voltage regulator on the stability of the northern region of the Brazilian system is studied. Using PV curves, it was shown that the voltage stability is improved with the increase of the DG penetration level. Several simulations were executed using different load models (constant power, constant current, constant impedance and induction motors). The voltage stability margin is highest when loads are modeled as constant impedance and lowest when 60 % of the loads are modeled as induction motors.

1.3.2 Impact of DG on the Short-Term Stability

All segments of stability (rotor angle, voltage and frequency) can be considered for short-term analysis. The time frame can vary from a few hundreds of milliseconds to a few seconds.

In [36], the impact of DG on the transient stability of a distribution network is studied. The method used to determine the stability is the Critical Clearing Time (CCT). Several time domain simulations are performed to obtain the CCT of each fault and the critical generator is identified. Detailed dynamic models of different DG technologies include three squirrel cage induction generator wind turbines, a diesel generator, a microturbine and two Combined Heat and Power (CHP) generators. The fault with the smallest CCT is considered the most critical. The critical generator associated with this fault is the microturbine due to its low inertia. This study shows that not all DG should be tripped according to the IEEE Std. 1547 because some DG technologies can surpass the CCT given by that standard.

In [37], two indices are defined to compare the impact of several DG technologies on the transient stability of the power system. The technologies include induction generators, synchronous generators and power electronic converters. Studies are also made with connecting voltage and frequency controllers to the synchronous generators and the converters. The two indices consist of measuring the maximum rotor speed deviation of central generators and the oscillation duration which consists of the time interval until the

rotor speed deviation stabilizes. Results show that induction generators do not have a noticeable impact on the transient stability, unlike synchronous generator based DG, which decreases the maximum rotor speed deviations but increases the oscillation duration due to inter-area oscillations. Power electronic converters decrease the generator speeding, but are then disconnected which can lead to voltage drops with high DG penetration.

In [38], the effect of synchronous machine based DG on voltage sags due to phase-to-ground and phase-to-phase faults is discussed. Synchronous generators are modeled in detail and are equipped with a power factor controller. Results show that the response of such excitation systems is relatively slow following a fault. The presence of synchronous machines improves the voltage sags but it can extend the duration of these sags because loads will not trip and therefore the recovery time increases.

In [31], the effect of different types of synchronous machine based DG excitation systems on transient stability is shown. Synchronous machines equipped with a voltage controller and operating at a lagging power factor prevent the system from reaching instability following a three-phase fault. When the power factor is set to unity or is leading, the system becomes unstable. The voltage sags are shown for the stable cases and with power factor control, the voltage reaches a smaller value than with voltage control.

In [32], synchronous and induction machine based DG are compared for transient stability and short-term voltage stability. Synchronous machines equipped with a voltage controller improve the stability by providing reactive power during and after a three-phase fault. Those equipped with a power factor controller improve the stability during the fault by supplying reactive power due to the slow response of the controller. Following the fault, the controller reduces the supplied reactive power to maintain a constant power factor and therefore has a negative impact on the transient stability. Similarly, the induction generator provides reactive power support during the fault and requires a large amount of reactive power after the fault is cleared which weakens the system significantly leading to a collapse. With DG, voltage sags, caused by a phase-to-ground fault, are worsened in almost all cases except when the DG is equipped with a

voltage controller and is located far from the fault. In [35], similar to the observations made in [32], voltage sags are worsened with the increase of the DG penetration level.

The transient and the voltage stability are considered in this thesis. Time domain simulations are carried out to show the impact of DG on the short-term stability.

1.4 Research Objectives

Many concerns are raised regarding power system stability with a large penetration of DG. DG has an impact on voltage and rotor angle stability in the short-term and the long-term time frames [4,12,13]. With a large variety of DG technologies, DG modeling becomes crucial to obtain accurate results. There is a need to classify the different DG technologies in a reduced set of categories, namely rotating machines and static converter based DG.

1.4.1 Problem Definition

Current regulations only consider small DGs that do not have a large impact on the system. Therefore, DGs are tripped during a fault and are not permitted to regulate voltage. Aggregated DGs can be viewed as large generators from the transmission level and if tripped instantaneously, power system instability can occur due to the large amount of lost generation.

With power systems operating near their loadability limits, voltage stability becomes an important issue. Many utilities have implemented long-term solutions to counter this problem, such as adding transmission lines and new power plants in order to improve the reliability of the power system. An alternative solution consists in increase of generation at the distribution level. This is also a way of meeting growing economical, technical and environmental constraints. The size, the technology and the placement of DG play an important role in the operation of distribution systems. There is a need, addressed on this thesis, to quantify the impact of DG on the stability of the system.

1.4.2 Research Goals

Utilities request fast and accurate methods to determine the stability of the system with large penetration of DG. Indices are developed to show the contribution of aggregated DGs connected at load buses. A fast method to study the stability of the

system is implemented to determine the optimal location where DG should be placed and to estimate the contribution of several DGs connected simultaneously. Large-penetration of DG also has an impact on the transient stability of the system. Indices are developed to rank contingencies and show how different DG interconnections affect the system during faults. To the best of the author's knowledge, the following are the contributions of this thesis, grouped under relevant power systems performance headings:

- Assessing the long-term and the short-term voltage stability of the system
- Defining indices to study the effects of DG penetration on the voltage stability
- Exploring the notion of linearity regarding the contribution of DG on voltage stability
- Determining different applications of these indices
- Evaluating the rotor angle stability of the system (transient stability)
- Showing the effects of DG penetration on the rotor angle stability using defined indices with different scenarios

1.4.3 Claim of Originality

The thesis developed a new approach to study the impact of DG on the voltage and transient stability of the power system. The new features by the proposed methodology consist of:

(a) General approach: Using automated process, consisting in running several scenarios with connecting DG at load buses with different penetration levels, technologies and power factors and using either PV curves for long-term voltage stability or time-domain simulations for short-term voltage stability as well as transient stability, data is generated for assessment of different types of stabilities.

(b) Long-term voltage stability: Appropriate indices for the long-term voltage stability that can help rank the contingencies and define the weak areas where DG can provide support to the system in terms of power, are developed. Concepts of linearity are defined where the contribution of DG on the long-term voltage stability can be predicted when connected at several load buses and at any penetration level. The bus based indices applied to determine the "DG assistance" where DG can be useful to prevent voltage collapse using load duration curves.

(c) Short-term voltage stability: the contribution of DG to the short-term voltage stability is assessed by defining indices that allow a contingency ranking and the comparison of the impacts of different DG technologies. A concept of linearity is identified for the short-term voltage stability index that is applicable for power electronic interfaced DG in small and medium power system cases.

(d) Transient stability: a transient stability index is defined to quantify the different contributions of each DG technology with different penetration levels. This index can be used to define the critical contingencies for transient stability.

1.5 Thesis Outline

The succeeding chapters are composed as follows:

Chapter 2 describes the different methods to draw the Power-Voltage curve. It focuses as well on modeling DG depending on the technology and the stability study. It also gives a brief description of the power system test cases presented as well as the software used.

Chapter 3 analyzes the impact of DG on the long-term voltage stability. Indices are defined using PV-curves to determine the contribution of DG at different locations, sizes and power factors. Some applications are described to emphasize the use of these indices.

Chapter 4 discusses the influence of DG on the voltage dips following large disturbances. Indices are defined to measure these voltage dips with different sizes, locations and technologies of DG.

Chapter 5 emphasizes on the transient stability with the presence of DG by monitoring the maximum rotor speed deviations of centralized synchronous generators. Similarly, these indices determine the best location and sizes of DG in each test case.

Finally, Chapter 6 gives a brief summary as well as few conclusions and future works.

Chapter 2: Power System Stability Concepts and DG Modeling

2.1 Power-Voltage Analysis

PV analysis, a widely used method, is very useful in conceptual analysis of voltage stability. The parameter P can either represent the total active power load in an area or the power flow across an interconnection between two areas and the state variable V is the voltage at a certain bus. The PV curve is obtained by increasing the load demand and solving the new power flow.

2.1.1 PV Curve of a Two-Bus System

A two-bus system is considered with a source, representing an infinite bus, connected to a single load through a lossless transmission line (Figure 2.1).

The load bus voltage is described as

$$\overline{V} = \overline{E} - jX\overline{I} \tag{2.1}$$

The complex load power is written as

$$S = \overline{V}\overline{I}^{*} = \overline{V}\left(\frac{\overline{E} - \overline{V}}{jX}\right)^{*} \tag{2.2}$$

$$S = -\frac{EV}{X}\sin\theta + j\left(\frac{EV}{X}\cos\theta - \frac{V^2}{X}\right) \tag{2.3}$$

Eq. (2.3) can be decomposed into the well-known power flow equations of a lossless system:

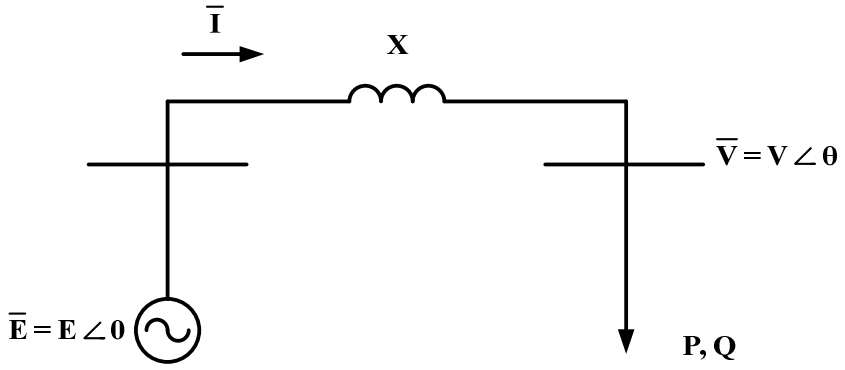

Figure 2.1. Two-bus system

$$P = -\frac{EV}{X}\sin\theta \tag{2.4}$$

$$Q = \frac{EV}{X}\cos\theta - \frac{V^2}{X} \tag{2.5}$$

By eliminating the angle θ from Eq. (2.4) and Eq. (2.5), the following second-order equation is obtained by

$$\left(V^2\right)^2 + \left(2QX - E^2\right)^2 V^2 + X^2\left(P^2 + Q^2\right) = 0 \tag{2.6}$$

There is at least one solution to Eq. (2.6) only if the following condition is met:

$$\left(2QX - E^2\right)^2 - 4X^2\left(P^2 + Q^2\right) \geq 0 \tag{2.7}$$

By solving Eq. (2.6), the two solutions for voltage will be

$$V = \sqrt{\frac{E^2}{2} - QX \pm \sqrt{\frac{E^4}{4} - X^2P^2 - XE^2Q}} \tag{2.8}$$

Plotting of Eq. (2.8) will give the well-known PV curve (also known as the nose curve). Figure 2.2 shows an example of a PV curve with the following values:

$$E = 1.0\ pu$$
$$X = 1.0\ pu$$
$$Q = 0.0\ pu$$

It is interesting to note that for each load power lower than the loadability limit there are two solutions: one with a high voltage and low current and the second is with a low voltage and high current. It is desirable to operate at a voltage close to the one of the infinite bus and therefore it is rare for a power system to operate at the lower part of the curve.

The maximum load can then be obtained by setting the following from Eq. (2.8) to zero:

$$\frac{E^4}{4} - X^2P^2 - XE^2Q = 0$$

$$P_{\max} = \frac{\sqrt{\frac{E^4}{4} - XE^2Q}}{X} \tag{2.9}$$

It can be seen that by reducing the reactive power and/or the reactance, the maximum loadability is increased. Reactive compensation improves the voltage stability of the

system. It should be noted that voltage overcompensation can lead to a voltage increase that can trigger over-voltage relays that protect the equipment.

Theoretically, the maximum loadability may be equal to zero if

$$\frac{E^4}{4} - XE^2Q = 0 \tag{2.10}$$

A critical reactive power and line impedance can be formulated as

$$Q_{crit} = \frac{E^2}{4X} \tag{2.11}$$

$$X_{crit} = \frac{E^2}{4Q} \tag{2.12}$$

2.1.2 PV Analysis for Large Systems

The analysis described in Section 2.1.1 is easy to implement for a two-bus system. It becomes more complicated with more buses and therefore another approach is used to build the PV curve. Simulation tools solve the power flow at the base case using full, decoupled or fixed slope Newton-Raphson method [17]. A problem arises when the solution of the power flow nears the "nose point" because the Newton method diverges and the *maximum loadability point* (MLP) cannot be reached [16].

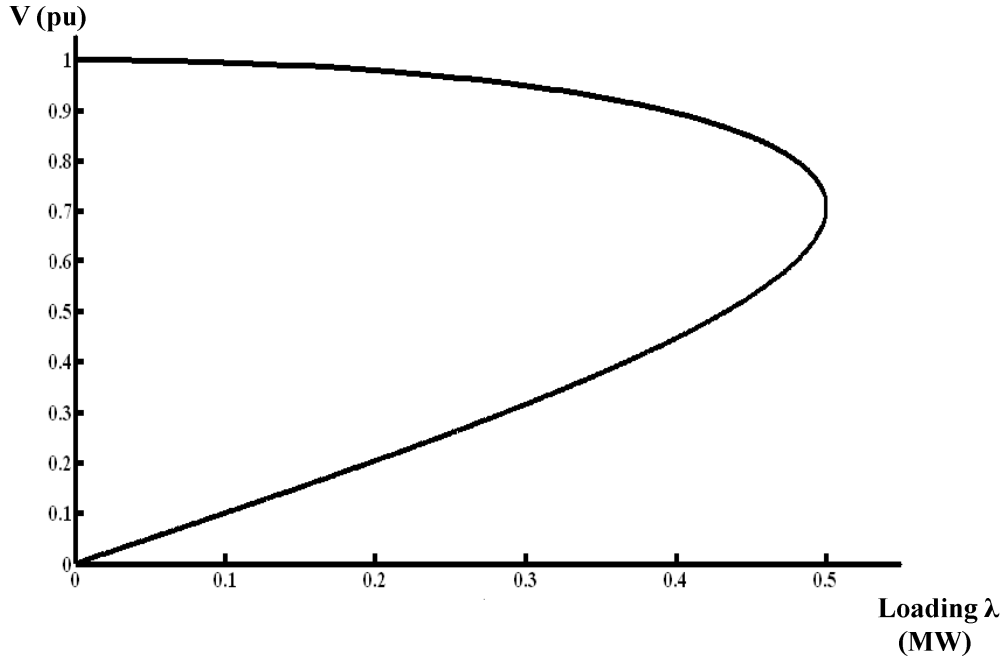

Figure 2.2. PV curve of the two-bus system

Several solutions have been implemented to counter this problem. A very well-known solution, called the *continuation power flow* (CPF), consists of a two-stage algorithm. The predictor approximates the next solution by taking a step using either the Tangent or the Secant method. The corrector decreases the error between the approximated value found by the predictor and the true value. The parameter μ becomes the continuation parameter and is then incorporated as a variable and computed at each iteration [23,39]. Figure 2.3 shows an example of how the CPF method is used to obtain the MLP of the PV-curve.

The software used in this study is PSS®E 31 and the method implemented to draw the PV curve is the *Non-Divergent Solution Methodology* (NDSM). If the power flow diverges using Newton's method, NDSM is then used to find a solution. If the NDSM fails to converge, the system is considered unstable. The following equations are used when NDSM is activated:

$$\theta_{new} = \theta_{old} + (\alpha \Delta\theta) \tag{2.13}$$

$$V_{new} = V_{old} + \left(1 + \alpha \frac{\Delta V}{\Delta V_{old}}\right) \tag{2.14}$$

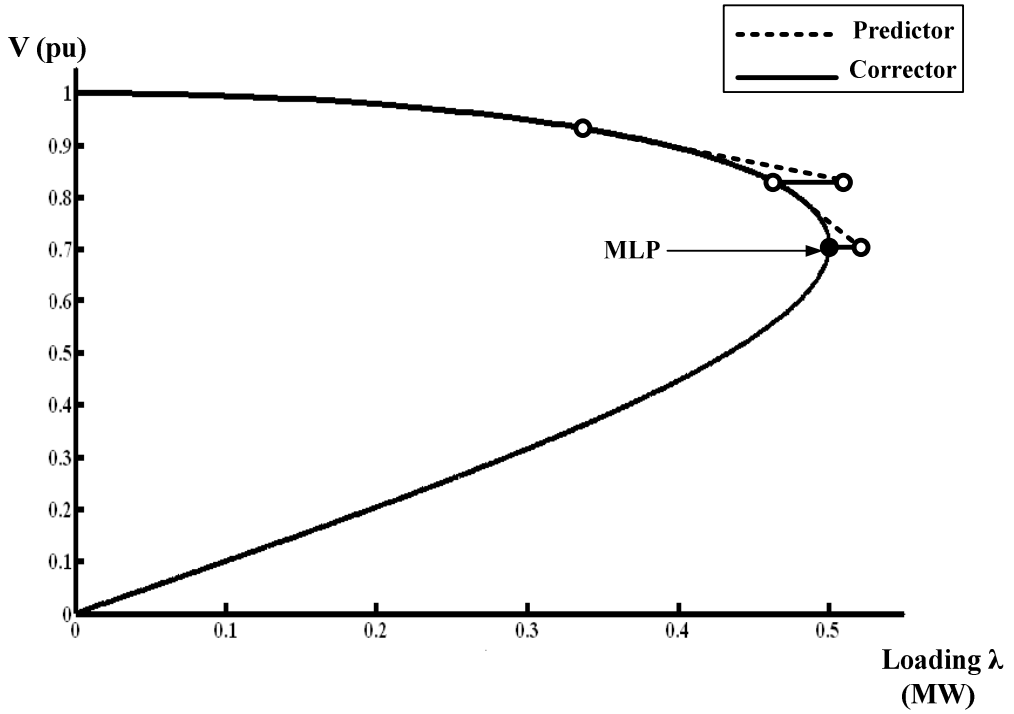

Figure 2.3. PV-Curve using the CPF method

Where θ_{old} , θ_{new} , V_{old} and V_{new} represent the old and the new voltage phase angles and voltage magnitudes respectively. $\Delta\theta$ and $\frac{\Delta V}{\Delta V_{old}}$ are change vectors for voltage phase angles and bus voltage magnitudes. α is called *the non-divergent parameter* that is set to 1.0 when the NDSM is deactivated [40]. Figure 2.4 shows the algorithm implemented in PSS®E to solve the power flow using the NDSM. If the power flow diverges, NDSM is activated and the non-divergent parameter is halved. If is converges, the power flow is solved by surpassing the point known as *Singularity Induced Bifurcation* (SIB), where the Jacobian of the algebraic equations with respect to the dependent variable *y* does not coincide with the point of collapse [41]. If the power flow does not converge, the process is repeated until the non-divergent parameter becomes very small. Then, the system reaches a voltage collapse that can be either associated with the *Saddle-Node Bifurcation* (SNB) or with the *Limited Induced Bifurcation* (LIB). SNB occurs when the system is on the verge of instability. Voltage collapse is directly related to SNB and therefore it is important to identify this point in order to employ countermeasures to enhance stability. LIB is defined as the point where the control limits are reached and the system collapses due to the disappearance of equilibrium [41].

2.2 Interconnection of DG at the Distribution Level

2.2.1 State-of-the-art DG Technology

As discussed previously, clean power is one of the main drivers towards the implementation of DG. Extensive research involves integration of renewable resources into the grid in order to decrease GHG emissions. Some of these resources involve wind energy, photovoltaic panels, small-scale hydro-plants, biomass, geothermal and wave energy [12,42,43]. DG with fossil energy resources, such as microturbine generators and combined heat and power (CHP) generators, are considered environmentally friendly due to their low emissions [44,45].

2.2.1.1 Fuel-Based DG

Nowadays, most DG technologies consist of *diesel and gas-powered engines* due to their low costs, high efficiency and good reliability. Reciprocating engines produce

power at a range of 1 to 30 MW and have relatively high emissions [10]. Diesel reciprocating generating units are used as a back-up in order to maintain power during interruptions for certain loads (such as hospitals, factories and shopping malls)[46]. Gas turbines are mainly used as CHP generators by some countries such as the UK in order to reduce CO_2 emissions [47].

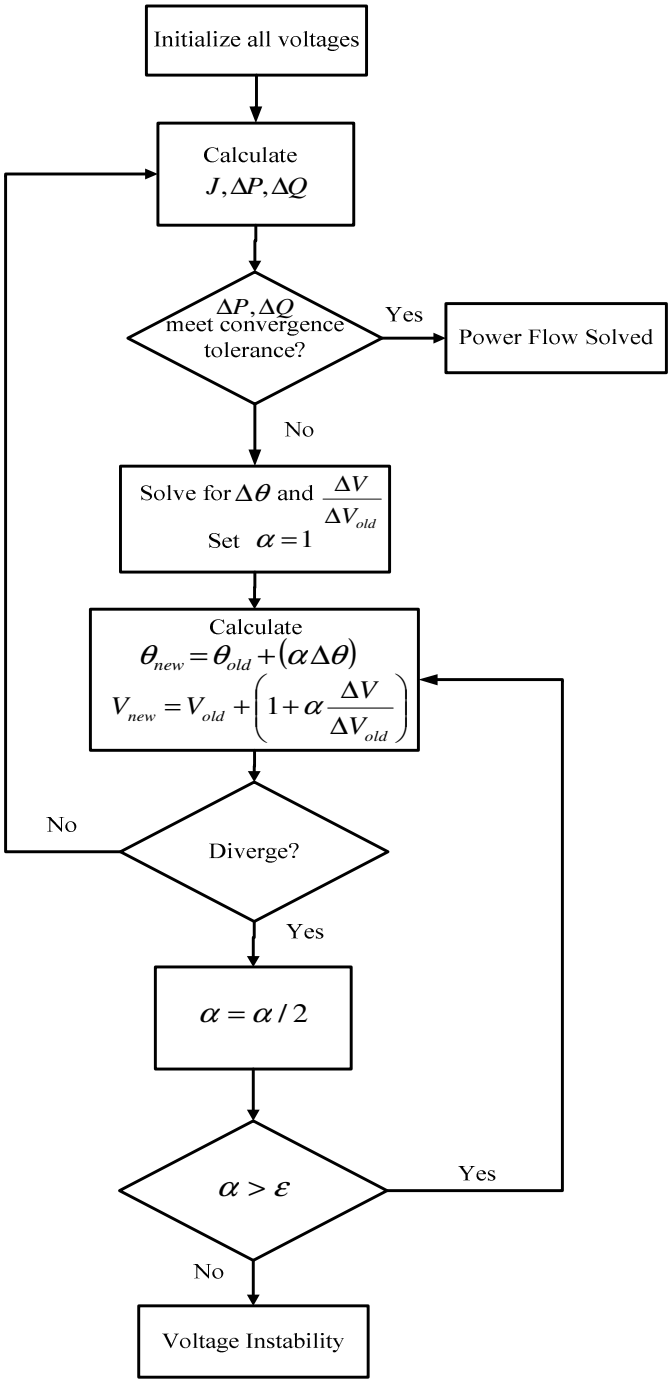

Figure 2.4. Non-Divergent Solution Methodology algorithm

Microturbines are a new technology that attracts interest due to its quick start capability and the flexibility of its control which could be useful for peak shaving [48]. It is a very small gas turbine that produces 30 to 400 kW; it operates at high speeds (up to 120,000 RPM) and generates high-frequency AC current. Microturbines have extremely low emissions and can be used as a source of electrical power or CHP. The disadvantages of microturbines are the high costs and short track record [44].

Fuel cells are another interesting technology that has had rapid development in the automotive industry. Fuel cells are stationary electrochemical energy conversion devices that have very high efficiency (higher than reciprocating engines because of the transition from chemical to electrical energy), high reliability and almost non-existence of GHG emissions. Fuel cells have a few major disadvantages as well, such as high costs, power density (power production per unit volume) and usage of hydrogen gas as a fuel which is expensive obtain and store. Other fuels can be used, such as natural gas, but will reduce efficiency [49-51].

2.2.1.2 Renewable Resources

Photovoltaic systems produce power when illuminated by the sun which makes the capacity factors very low. A photovoltaic panel consists of several photovoltaic modules in series-parallel configurations that produce each a few hundred watts and DC current. Advantages of this renewable energy consist of availability of sun energy during peak time, long life cycle, low capital costs and simple maintenance. CO_2 emission is low as it is only associated with production of photovoltaic panels [52].

Small-scale wind generation is a very common renewable resource that is used as an alternative to photovoltaic panels. The main focus of this technology is on large-scale implementation (wind farms) where a scale of 100 MW to few GW is considered. Wind farms are not considered as DG, only small-scale wind generators (a few kW) that are placed near the loads (near farms, on top of high buildings) [53].

Small hydroelectric power plants generate electricity from the motion of a mass of water from a river and can produce up to a few MW. Some advantages consist of low maintenance costs and a short construction schedule. Small hydroelectric plants have less environmental and social impacts than large plants [54,55].

Due to high power fluctuations and unpredictability of renewable resources, the implementation of energy storage near each DG, with photovoltaic panels or small wind turbines, may be a solution to counter this problem [56-58]. However, the cost of an energy storage system is quite high. A proposed solution to the variability of renewable resources takes the form of a dispatchable DG network. The design philosophy of the network revolves around balancing the power generation between the controllable DG (such as diesel engines, gas engines, microturbines, and small hydroelectric power plants) and the non-controllable DG (such as wind turbines and photovoltaic panels) [59].

2.2.2 DG Interconnection with the Grid

Except for a few DG technologies (internal combustion engines) that use synchronous generators or induction generators, interconnection with the grid is made indirectly through power electronics converters [60-62]. DG with DC current (photovoltaic panels, fuel cells, etc…) are connected to a DC/DC converter which is attached to a DC/AC converter. The DC link between the two converters smoothen the fluctuations caused by the ripple current. The output of the DC/AC converter is connected to the grid (Figure 2.5).

Variable speed (wind turbine) and high frequency (microturbines) based DG cannot be directly connected to the grid and therefore the link is formed by an AC/DC converter connected to a DC/AC converter (Figure 2.6).

Wind turbines are coupled to either a synchronous or an induction generator. In the past, wind turbines were directly connected to the grid and operated at fixed speeds. Wind turbines with a fixed speed and coupled with an induction generator are widely implemented [61]. Another alternative is using a doubly-fed induction generator (DFIG) where the stator is directly connected to the grid and the rotor is connected through a power electronic interface (Figure 2.7).

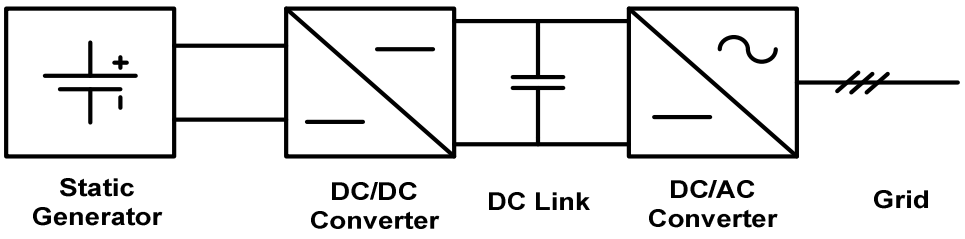

Figure 2.5. Interconnection of DG with DC output with the grid

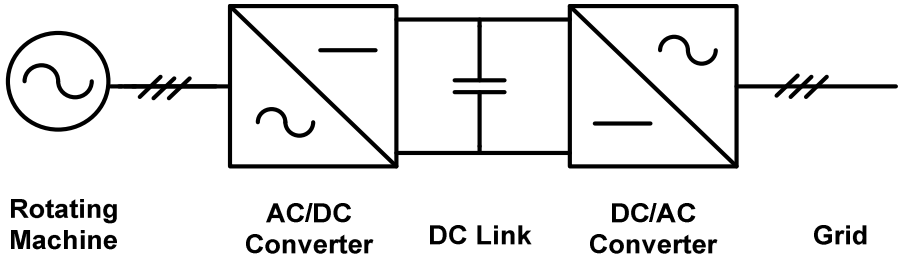

Figure 2.6. Interconnection of DG with high frequency or variable speed with the grid

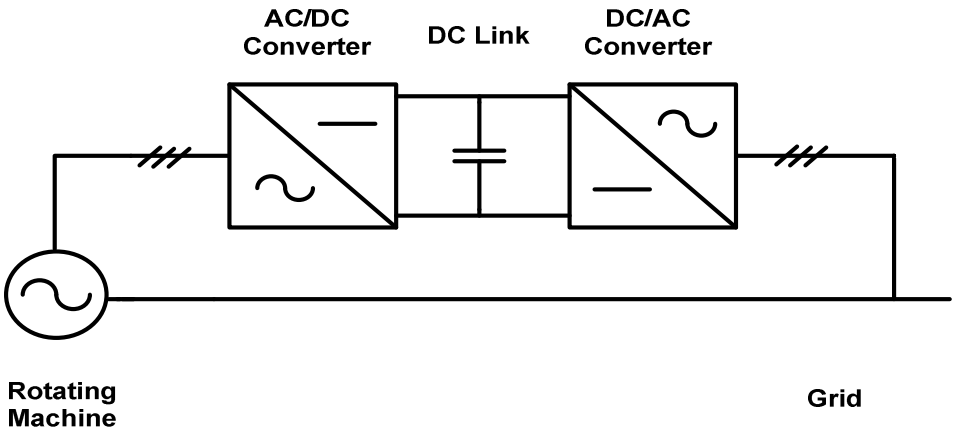

Figure 2.7. Doubly fed induction generator

2.2.3 Impact of DG on the Distribution System

A high penetration of DG will affect the steady-state and the dynamics of the distribution system. These impacts mainly consists of [12,63-65]:

- **Voltage regulation** – Utilities do not allow DG to regulate the voltage at the point of common coupling (PCC). DG should only operate with a constant power factor control.
- **Short-circuit level –** During a fault, when several DG are connected at the same feeder, a miscoordination between the fuse and the breaker can occur and this can lead to an unrequested fuse operation. The reliability of the system is strongly affected.
- **Islanding –** Unintentional islanding should be avoided in all cases due to the unpredictable behavior of the islanded system. Anti-islanding protection should be implemented to disconnect the DG in order to avoid the possibility of harming nearby loads. The concept of "intentional islanding" is still under consideration

due to the complexity of the islanded systems and that the DG owners should be reliable and can maintain the voltage and the frequency of local loads.

- **Voltage flicker** – Connecting and disconnecting single DGs can cause voltage flicker. Also, the variation of the output of each DG along with the load variation can lead to noticeable lighting flicker. In order to reduce these fluctuations, mitigation approaches can be implemented. Induction generators require having a reduced voltage start, synchronous generators should have tighter synchronization and voltage matching and power electronic interfaced DGs should limit inrush currents and changes in power output.
- **Harmonic distortion** – DGs can introduce harmonics to the system depending on the converter technology and the interconnection configuration. Any DG technology should meet the requirements set by the IEEE 1547-2007 standard (Table 2.1).

Table 2.1. Maximum allowable harmonic current distortion in percent of current (I)[a] [63]

Individual harmonic order h (odd harmonics)[b]	h < 11	11 ≤ h < 17	17 ≤ h < 23	23 ≤ h < 35	35 ≤ h	Total demand distortion (TDD)
Percent (%)	4.0	2.0	1.5	0.6	0.3	5.0

[a] I = the greater of the Local EPS maximum load current integrated demand (15 or 30 minutes) without the DR unit, or the DR unit rated current capacity (transformed to the PCC when a transformer exists between the DR unit and the PCC).
[b] Even harmonics are limited to 25% of the odd harmonic limits above.

2.3 Modeling DG for Power System Stability Studies

With a constant increase in DG penetration, an accurate modeling of DG is required to obtain adequate results. DG has an impact on the dynamic and the steady-state operation of the power system.

2.3.1 Modeling DG for Short-Term Stability Studies

Short-term stability studies require detailed modeling of the components of the system (such as generators, governors, exciters, and loads). As mentioned in Section 2.2.2, DGs are classified into two main categories:

- Direct connection to the grid (reciprocal engines)

- Indirect connection to the grid (with a power electronic interface)

2.3.1.1 Modeling DG as Reciprocal Engines

Directly connected DGs are represented by standard synchronous or asynchronous machine models that are well developed in the PSS®E library.

Synchronous generators are modeled by sixth order differential equations (GENROU), shown in [66]. The parameters of this well-known model consist of:

- **T'_{do} –** Direct axis open-circuit transient time constant (in seconds)
- **T'_{qo}** – Quadrature axis open-circuit transient time constant (in seconds)
- **T''_{do}** – Direct axis open-circuit subtransient time constant (in seconds)
- **T''_{qo} –** Quadrature axis open-circuit subtransient time constant (in seconds)
- **X_d –** Unsaturated direct axis synchronous reactance (in p.u. of the machine's MVA base)
- **X_q –** Unsaturated quadrature axis synchronous reactance (in p.u. of the machine's MVA base)
- **X'_d** – Unsaturated direct axis transient reactance (in p.u. of the machine's MVA base)
- **X'_q –** Unsaturated quadrature axis transient reactance (in p.u. of the machine's MVA base)
- **X''_d –** Unsaturated direct axis subtransient reactance (in p.u. of the machine's MVA base)
- **X''_q –** Unsaturated quadrature axis subtransient reactance (in p.u. of the machine's MVA base)
- **X_l –** Leakage reactance (in p.u. of the machine's MVA base)
- **H –** Machine inertia (in p.u. of the machine's MVA base)
- **D –** Damping ratio (in p.u. of the machine's MVA base)

The unsaturated quadrature axis subtransient reactance is equal to the direct axis subtransient reactance. The machine's reactance, inertia and damping ratio are in per unit base of the machine's rated power. A completion to the current model is provided by saturation parameters. DG owners would have the incentive to operate at maximum power and therefore a governor is not necessary. Current utilities do not allow DGs to

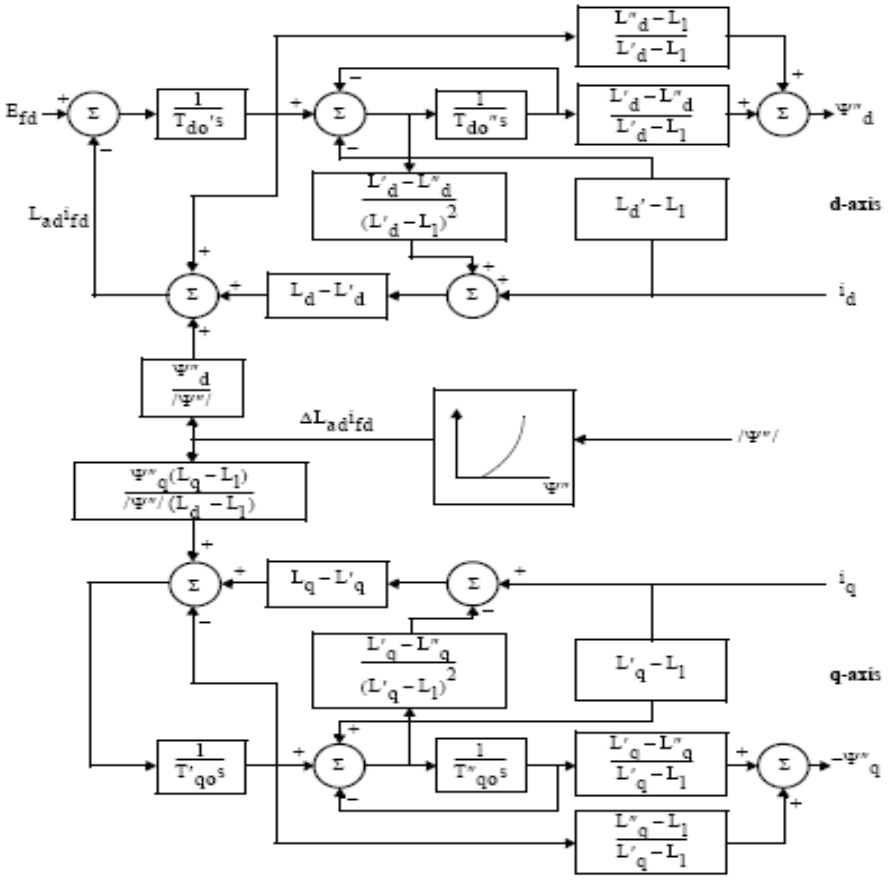

Figure 2.8. Electromagnetic model of round rotor generator (GENROU)

regulate voltage and thus, the exciter employed is a var/PF regulator that keeps a constant power factor. During a sudden disturbance, var/PF regulators do not react fast enough to control voltage dips. Thus, exciters for synchronous based DG are not considered [38,67]. . The data for the parameters of the synchronous machine interfaced DG are shown in Appendix B.

The common third-order model (CIMTR3) is used to represent DGs interconnected with induction generators. This model includes a detailed representation of the rotor flux transients (Figure 2.9) [66]. The parameters are similar to the synchronous generator with only a single transient time constant and a single transient reactance, as well as a single subtransient time constant and a subtransient reactance. This model can represent either a single-cage or a double-cage induction generator. Induction machine interfaced DG are single-cage generators, and therefore the subtransient time constant and reactance are set to zero. Induction generation absorbs reactive power when it supplies power and therefore there is a "hidden" shunt capacitor connected at the terminal of the machine to

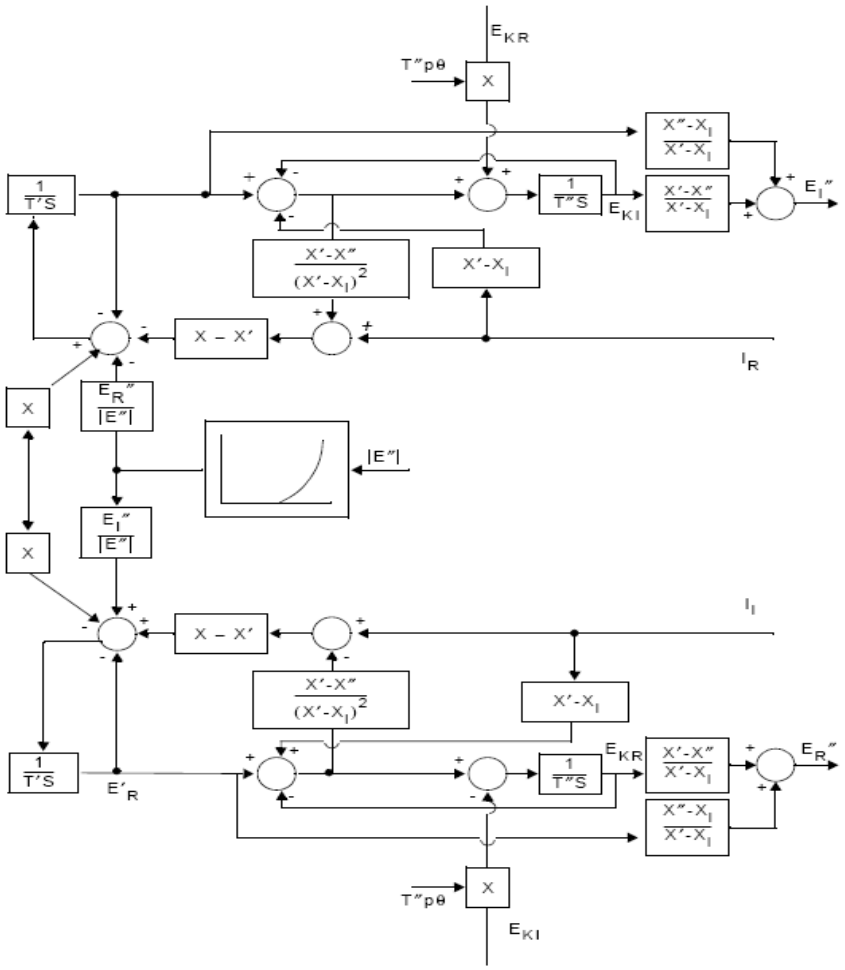

Figure 2.9. Electromagnetic model of induction generator (CIMTR3)

compensate the reactive difference between the reactive power of the machine in steady-state and the one absorbed by the machine in dynamic study. The data of the parameters are shown in Appendix B.

2.3.1.2 Modeling DG with Power Electronics Interface

Although most DGs are currently reciprocal engines, high interest in renewable resources led to an increase in DGs with power electronic interfaces. For short-term stability studies, power electronics act faster than the electromechanical devices. The response of the converters, during a fault, is dependent on the controllers and their parameters. Therefore, a general model of such devices for transient studies is complicated. In [68], a study shows that the output of the current source is a good estimation of the output of a converter during voltage dips. If DGs with power electronic

interfaces are not connected to the slack bus and operate with a constant power factor, they can be modeled by a constant current source [69]. In PSS®E, these are modeled by negative constant current loads.

2.3.1.3 Tripping DG during Faults

With current protection settings on the distribution side, the IEEE 1547-2003 standard recommends the disconnection of DG during a fault to protect the system and the DG itself [63]. A miscoordination of the protection equipment can lead to a false tripping of a healthy feeder, a late detection of fault current on the feeder, or a prevention of automatic reclosing. False tripping is mainly caused by synchronous machine interfaced DG that is connected to a healthy feeder that supplies current to a faulted adjacent feeder. The healthy feeder then disconnects due to the large current supplied by the DG. To overcome this issue, a bi-directional overcurrent relay can be used. The fault current seems reduced to the level of the protection relay on the feeder with the presence of a large DG or several small ones. Protection relays are then "blinded" and would not disconnect the feeder during a fault. The settings of the relay should then be modified to be more sensitive. DGs can prevent early auto-reclosing by energizing the arc for an extended period. This can lead to out-of-phase reclosing that can damage synchronous generators [70].

The IEEE 1547-2003 standard defines the voltage and frequency level and the clearing time at which a DG should cease to energize the circuit. For small DGs (less than or equal to 30 kW), these clearing times represent the CCT, and for large DGs (more than 30 kW), the CCT is adjustable. Table 2.2 and Table 2.3 show the clearing time at which the protective relay of the DG should be set when sensing abnormal voltage and frequency. The relay connected near the DG should then be composed of undervoltage, overvoltage, underfrequency and overfrequency protection.

Table 2.2. System response to fault voltages

Voltage range (% of the base voltage)	Clearing time (s)
V<50	0.16
50≤V<88	2.00
110<V<120	1.00
V≥120	0.16

Table 2.3. System response to fault frequencies

DR size	Frequency range (Hz)	Clearing time (s)
≤30 kW	>60.5	0.16
	<59.3	0.16
>30 kW	>60.5	0.16.
	<{59.8 to 57.0} (adjustable set point)	Adjustable 0.16 to 300
	<57.0	0.16

The specifications of the IEEE 1547-2003 standard are applicable to small stand-alone DGs. With a high penetration of DG, a sudden disconnection can weaken the system and thus lead to a voltage collapse due to the lack of generation. The protection scheme should be reviewed in order to keep DGs online during faults and to prevent any harm to the system. Therefore, in this thesis, it is assumed that a proper protection scheme is implemented and DGs are not disconnected during short-circuit faults.

2.3.2 Modeling DG for Long-Term Stability Studies

In the short-term scale, power electronic converters behave like a current source as mentioned in Section 2.3.1.2. Given the resources, the output of the converters becomes a constant power that can be set by the owner. The owners of DGs that run with fuel have the incentive to operate at maximum power to maximize profit. The output of DGs powered by renewable resources (such as wind and sunlight) varies depending on the availability of the energy source. Figure 2.10 shows the output of a wind plant during one month in Denmark in 2000. The plant is spread among a large area to reduce wind variability [71]. In Figure 2.11, the output of a photovoltaic array during a 24-hour period is exposed. With multiple photovoltaic arrays, the aggregated output is similar to the one shown in that figure. The load, shown in Figure 2.10, can also be considered as constant power loads for power flow studies. During long-term stability analysis, the power output of DGs powered by renewable resources can be considered as a constant during the time frame of several seconds to a few hours. DGs with renewable resources are modeled as negative constant power loads. Although power electronic interfaced DGs can regulate voltage at the PCC, as mentioned in Section 2.2.3, utilities do not allow DGs to provide voltage support.

Induction machine interfaced DGs are increasing due to the high interest in wind energy and due the low cost of these machines. Induction generators operate at a constant power given the resource and cannot supply reactive power. As mentioned previously, it is assumed that a Static Var Compensator (SVC) is connected at the machine terminal to compensate for the reactive power absorbed by the induction machine.

Currently, most DGs are synchronous machine interfaced and are used for back-up due to the high efficiency. Synchronous machine interfaced DG can operate continuously at any power factor in a certain range. It can then supply reactive power (overexcited) and absorb reactive power (underexcited) with a voltage controller.

As mentioned in Section 2.2.3, utilities do not allow DGs to have a voltage controller but instead recommend DGs to have a var/PF controller to keep the reactive power or the power factor constant. Table 2.4 displays a few power factor ranges for the interconnection of DGs on the grid given by some North American utilities who request that DGs operate at a constant power factor [73-80]. Synchronous machine based and power electronics based DGs can operate at any power factor given in Table 2.4.

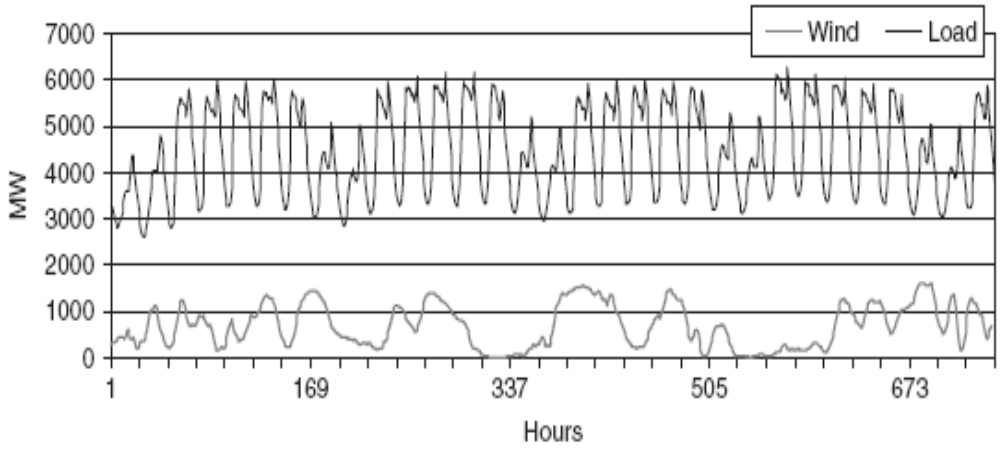

Figure 2.10. Wind power output and demand variation during one month in Denmark [71]

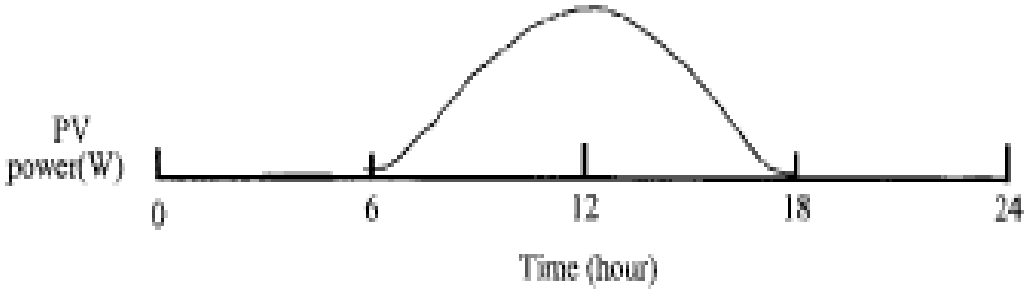

Figure 2.11. Output power of a PV array during one day [72]

Table 2.4. Power factor range from different utilities

Utilities	Lagging Power Factor	Leading Power Factor
Alberta	0.9	0.9
British Columbia	0.9	0.9
Manitoba	0.9	0.9
Ontario	0.9	0.95
Saskatchewan	0.95	0.9
Quebec	0.95	0.95
New York	0.9	0.9
California	0.9	0.9

2.4 Simulation Setup

2.4.1 Test Cases Used to Study the Stability of the System

The main focus of this thesis deals with the impact of a high penetration of DG on the transmission system. Several models are used to show different scenarios with the main focus on the stability of the system. Three test systems (small, medium and large systems) are used to assess these impacts. The bus and the branch data are given in Appendix A.

2.4.1.1 The IEEE Reliability Test System 1996

The IEEE Reliability Test System 1996 (RTS96) is a small system with 24 buses (Figure 2.12 and Table 2.5). Ten generators supply 17 loads with a total demand of 2850 MW. The system is considered a small system with only 34 transmission lines and two areas (230 kV and 138 kV). The dynamic data of the generators, exciters and governors are taken from [81]. Most generation is in the north of the system, and the largest loads are located in the south. It is interesting to note that if the transmission line from bus 7 to bus 8 is tripped, an island will be formed at bus 7 and therefore, a contingency on this line is disregarded. There is also a fixed shunt at bus 14 (13.7 MVAR) that supplies reactive power to the system [82].

2.4.1.2 The IEEE 39-Bus New England Test System

The IEEE 39-bus New England test system is used widely for stability studies (Figure 2.13 and Table 2.6). This system is considered as a medium system with 10

generators and 19 loads with a total demand of 6041.15 MW. A large concentration of loads is

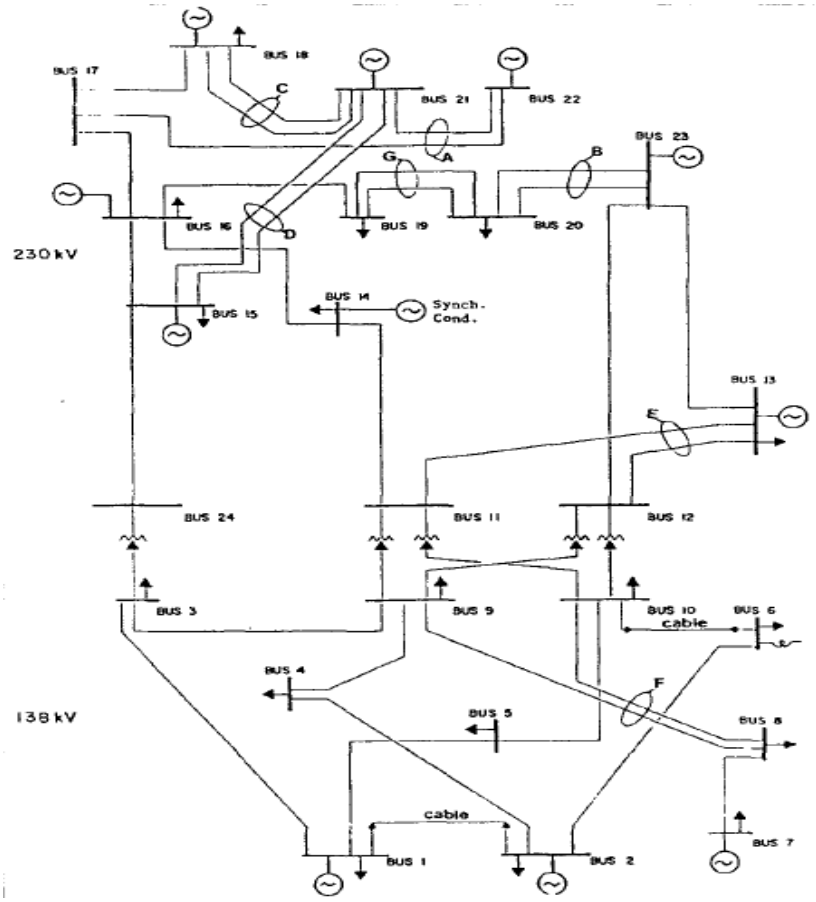

Figure 2.12. IEEE RTS96 24-bus test system [82]

located in the west of the system and large loads are in the south east. The detailed dynamic data for this system is provided with the characteristics of the system [83].

Table 2.5. System Characteristics of the IEEE RTS96 24-bus test system

System Characteristics	Value
Buses	24
Generators	10
Loads	17
Transmission lines	34
Total load real power	2850 MW
Total load reactive power	580 MVAR

2.4.1.3 The IEEE 118-Bus Test System

The IEEE 118-bus test case is a model of a portion of the American Electric Power System (Midwestern states) in December of 1962 (Figure 2.14 and Table 2.7). This

system is a large system with 58 generators, 99 loads and 179 transmission lines [84]. The system is quite robust with many interconnections between the buses.

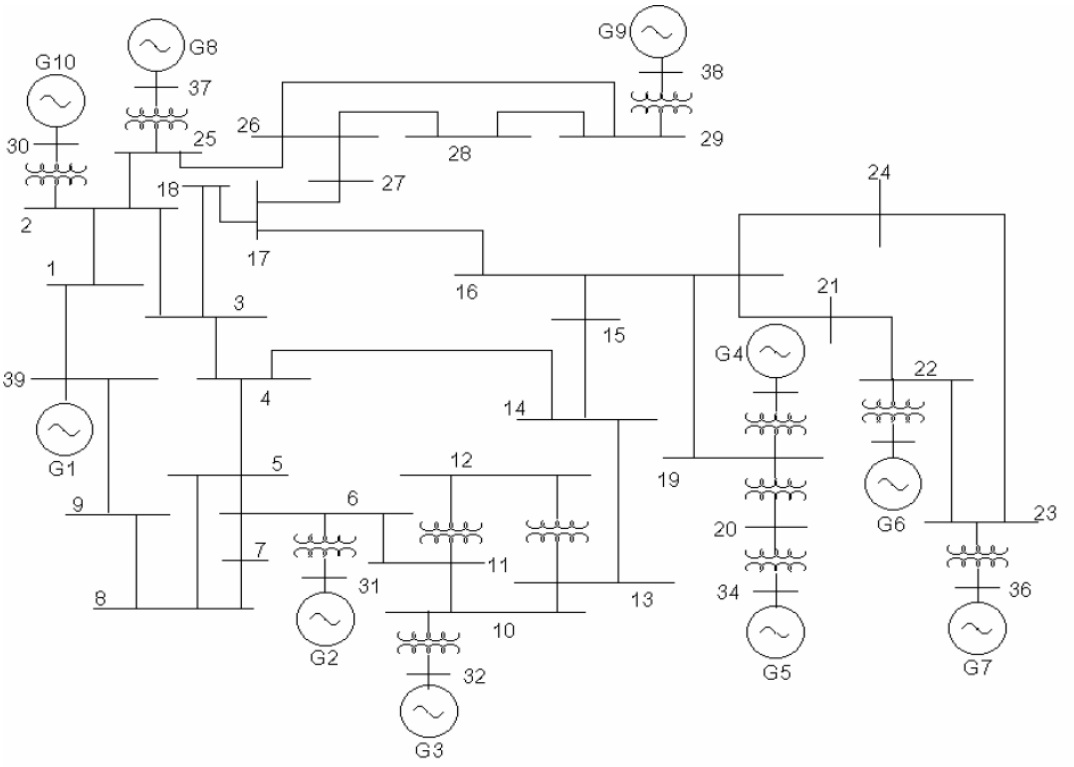

Figure 2.13. IEEE 39-bus New England test system [83]

The dynamic data for the generators, governors and exciters is taken from [81].

Table 2.6. System Characteristics of the IEEE 39-bus New England test system

System Characteristics	Value
Buses	39
Generators	10
Loads	19
Transmission lines	46
Total load real power	6041.15 MW
Total load reactive power	1359.64 MVAR

Several islands are formed by tripping some of the lines. Due to the size of the system, these islands cannot be easily detected. The function "TREE" defined in PSS®E detects any island that is not connected to the swing bus (Table 2.8).These contingencies are not considered because some of these islands have generators which can damage the loads. The rest can also be affected if DGs are connected.

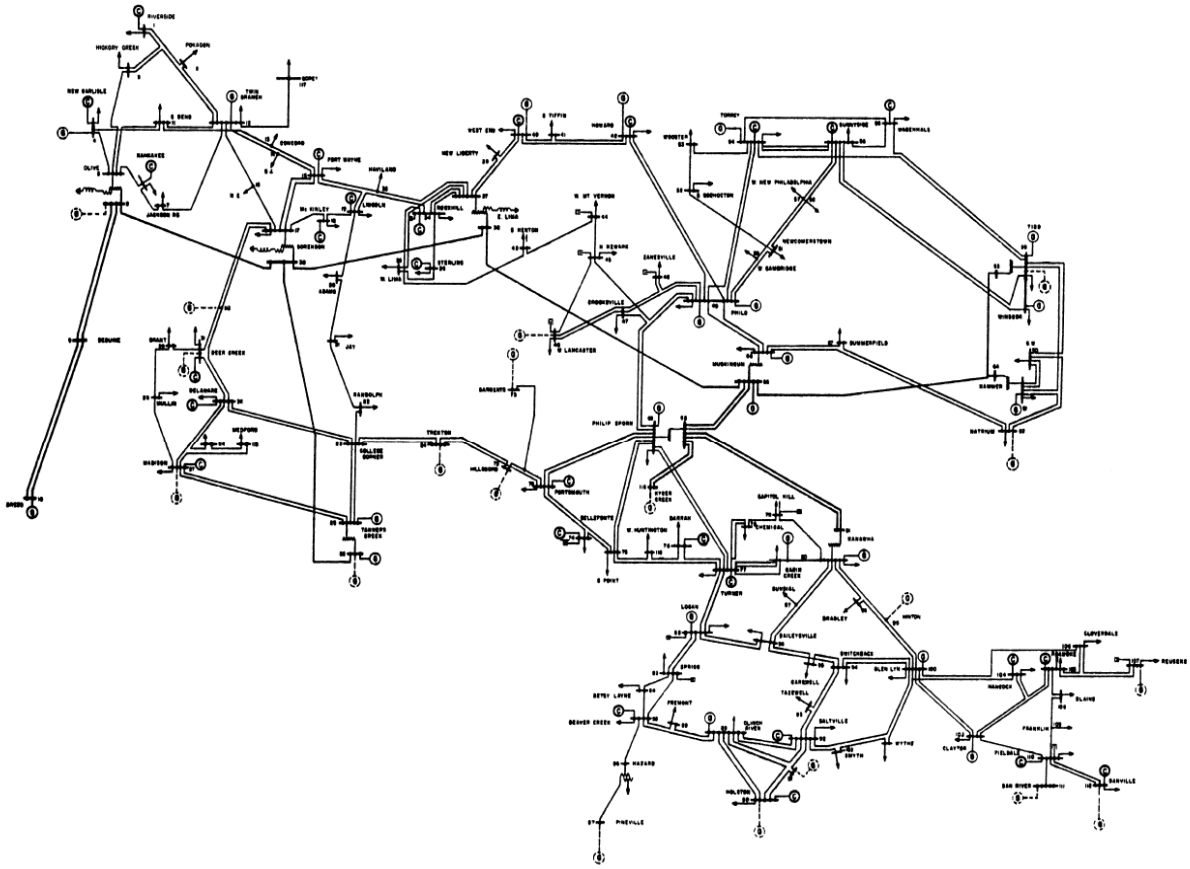

Figure 2.14. IEEE 118-bus test system [84]

Table 2.7. System Characteristics of the IEEE 118-bus test system

System Characteristics	Value
Buses	118
Generators	58
Loads	99
Transmission lines	179
Total load real power	4242 MW
Total load reactive power	1438 MVAR

2.4.2 Power System Stability Software

PSS®E 31.2 is well-known in the power industry for its use in power system stability studies due to its fast power flow calculation and its fast time domain simulation of power systems with small simulation time steps. This can be useful for large systems due to the reduction of the number of differential equations. Differential equations are

Table 2.8. Islanded buses after line tripping for the IEEE 118-bus system

Tripped line	Islanded buses
008-009	9 & 10
009-010	10
012-117	117
068-116	116
071-073	73
085-086	86 & 87
086-087	87
110-111	111
110-112	112

associated only with the dynamics of the components of the system (such as the generator, exciter, governor, relay and FACTS). Another advantage consists of the use of automation with python code. Many cases can then be simulated with DGs connected at different buses and with different sizes (Chapters 3, 4 and 5). As discussed in Section 2.1.2, PV curves are drawn using the NDSM method due to its ability to find the point of collapse relatively quickly. The dynamic library provided by the software includes many useful models to obtain a detailed modeled system. NEVA is a software that performs small-signal stability studies and that can be launched from PSS®E when a dynamic file is defined.

Chapter 3: Impact of Large Penetration of DG on the Long-Term Voltage Stability

3.1 Introduction

In 2003, three major blackouts occurred in North America and Europe that led to extensive research on the reliability of current systems and some recommendations to avoid future voltage collapse. In [85], the authors discuss the causes of the blackouts that they qualify as "among the worst power system failures in the last few decades". A few recommendations have been proposed to increase the overall reliability of the power system, including the use of new emerging technologies such as:

- On-line security assessment
- New relay technologies
- Real-time monitoring of the grid
- FACTS and HVDC
- DG technologies

The main focus of this section is to study the impact of DG on the long-term and the short-term voltage stability of the system and how this emerging technology can be used to improve the reliability of the system. It is predicted that by 2010 European DG penetration levels will average between 10% and 23% [86]. Utilities may have to set a maximum DG penetration level in order to maintain the control on the grid. The penetration level of DG connected at one bus is in percentage of the load connected at that bus in order to avoid high generation at a load bus. The total penetration level (*PL*) of DG is dependent on the total peak load demand and is calculated by

$$PL = \frac{\sum P_{DG}}{\sum P_L} \tag{3.1}$$

3.2 Long-Term Voltage Stability

The different methods of obtaining the point of collapse where the power system becomes unstable and can collapse are discussed in Section 2.1. System operators request reliable measurements of the actual situation of the system as well as an easy way to read

those measurements. PV curves are then very useful to indicate where the current load demand is located from the point of collapse, as well as the bus voltage if this load is increased or decreased. The Voltage Security Margin (VSM) is defined as the MW-distance between the point of voltage collapse of the system and the operating load level. Figure 3.1 shows an example of a PV curve where a bus voltage of the system is monitored with slowly increasing load demand. λ_0 and λ_{max} correspond to the base case loading and the maximum loadability point respectively. A load increase leads to a smaller VSM which indicates a deterioration of the stability of the system. Utilities try to increase the VSM using several means such as improving the transmission system by adding more transmission lines and by providing reactive compensation.

In the long-term frame, load tap changers (LTC) keep voltages constant and therefore, voltage-dependent loads are considered as constant power, assuming that the LTCs do not reach their limits [87]. Therefore, loads are modeled as constant power. If the load demand is larger than λ_{max}, a voltage collapse can occur due to the lack of generation to meet that increase in load. Contingencies reduce the VSM by reducing the reactive power supplied to the load which would reduce the maximum loadability point. An increase in demand would then increase the chances of a voltage collapse. Figure 3.1 shows three different scenarios, and the first one is the base case. The two other cases show the state of the system of the occurrence of a contingency (*Contingency 1* and *Contingency 2* respectively). The maximum loadability point $\lambda_{max\,1}$ associated with Contingency 1 is still larger than the base case λ_0, and therefore, the system can still operate but with a smaller VSM. As for Contingency 2, where $\lambda_{max\,2}$ is smaller than λ_0, a voltage collapse can occur. System operators would perform certain actions to maintain a positive VSM by extending the maximum loadability point to ensure that it is larger than the load demand. As a last resort to avoid total collapse of the system, the option of load tripping is taken into account to decrease the demand point and maintain the bus voltages.

3.3 Impact of DG on the Voltage Security Margin

A large penetration of DG can be viewed as a reduction in load demand that will decrease generation from large power plants. It is then thought that, regardless of the

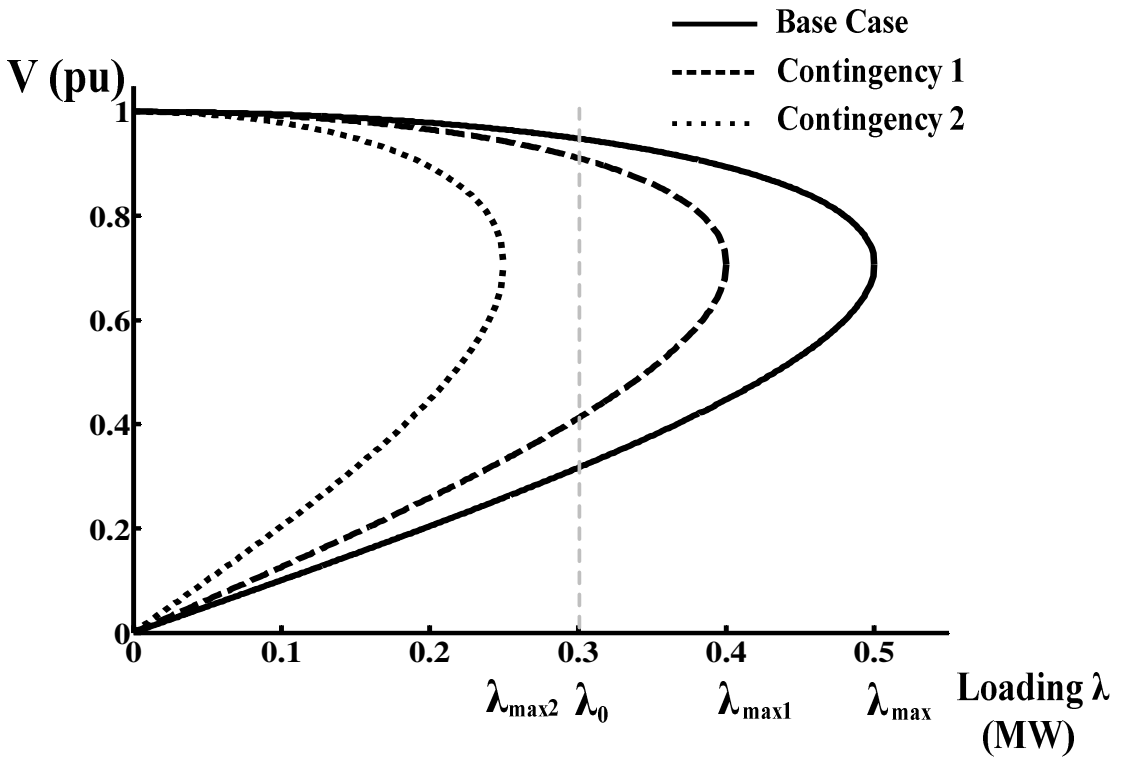

Figure 3.1. PV curves of different scenarios

location, the voltage stability is improved because the stress on the transmission lines is reduced.

Figure 3.2 shows the different PV curves of the base case scenario, as well as the Contingency 2 scenario with and without DG. It is assumed that DG will improve the voltage stability of the system because having a DG connected is like reducing the load power, which means the VSM is increased. DG penetration can even help avoid a voltage collapse, as can be seen in the case where the VSM following the Contingency 2 changes sign and becomes stable. The difference between the two VSMs ($\lambda_{\max}$ and $\lambda_{\max}^{DG}$) is called "DG assistance".

A Bus Voltage Improvement index (BVI_i) is developed as a mean to assess the contribution of DG to the voltage security margin. The index is defined by the difference between the new VSM with aggregated DG and the base VSM relative to the amount of aggregated DG integrated:

$$BVI_i = \frac{\lambda_{\max i}^{DG} - \lambda_{\max}}{P_{DGi}} \tag{3.2}$$

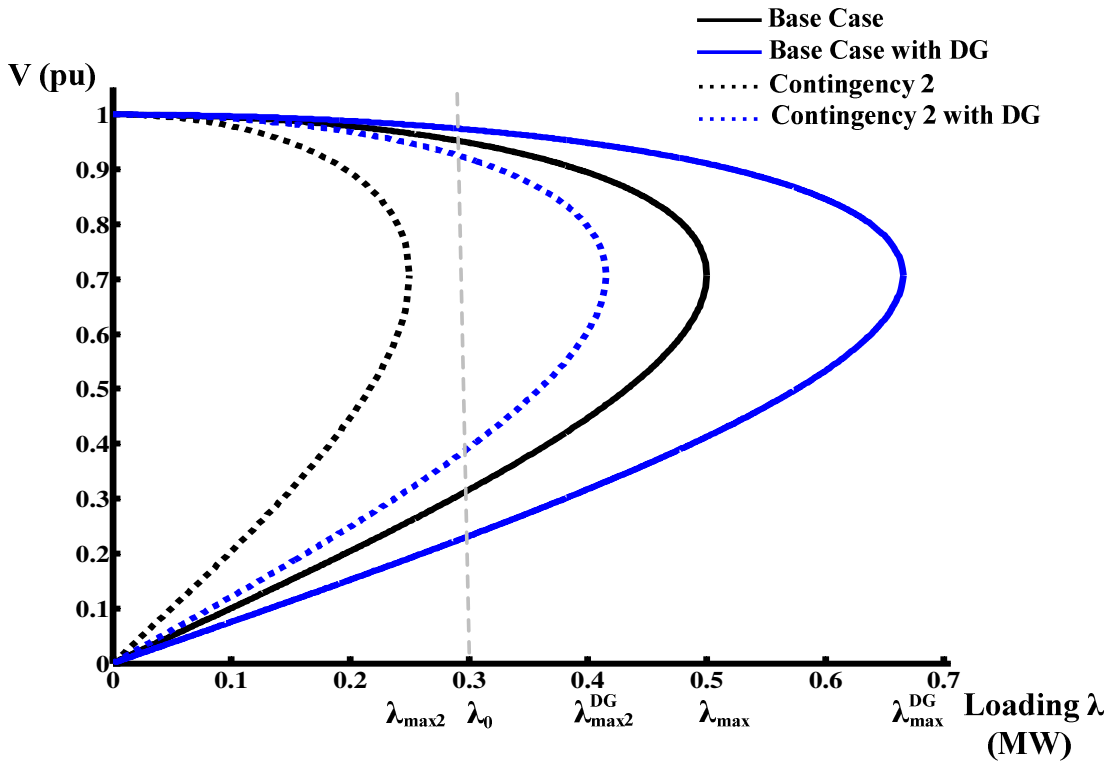

Figure 3.2. PV-curves of the base case scenario and a severe contingency scenario with and without DG

With $\lambda_{\max i}^{DG}$ and $\lambda_{\max}$ representing the VSM of the system with and without DG penetration respectively and assuming that the reference load is zero and P_{DGi} representing the active power produced by the aggregated DG at bus i. The BVI_i index can either be positive, zero or negative and indicates then how the VSM is improved, unchanged or reduced. The location of DG can then be decided based upon this index as it consists of connecting DG at a singular bus and analyzing the system.

A similar index can be defined for a subset Ω of buses with DG connected simultaneously:

$$BVI_{\Omega} = \frac{\lambda_{\max \Omega}^{DG} - \lambda_{\max}}{\sum_{\Omega} P_{DGi}} \tag{3.3}$$

Eq. (3.3) can be related to Eq. (3.2) by having a weight factor γ_i that depends on the size of the DG connected at each bus i over the total DG connected in the subset.

The BVI_{Ω} index can then be calculated by the following method which is considered as an approximation of Eq. (3.3):

$$BVI_{\Omega} = \sum_{\Omega} \gamma_i BVI_i \tag{3.4}$$

With

$$\gamma_i = \frac{P_{DGi}}{\sum_{\Omega} P_{DGi}} \tag{3.5}$$

An operator can then calculate all the BVI_i indices of the system and can associate any combinations without having to perform further analysis.

3.4 Long-Term Voltage Stability Simulation

The impact of DG on the long-term voltage stability is studied using the three test cases presented in Section 2.4.1. BVI_i indices are calculated for each system and their applications are discussed. In order to have better PV curves, generators and loads are reduced to 30 % of their power for the base case. The DG penetration levels are increased from 5 % to 20 % in steps of 5 % in order not to have an excess in generation when the loads are at their lowest levels.

3.4.1 The IEEE Reliability Test System 1996

Voltage instability can occur following a large contingency where the load demand cannot be met by the generation. Large contingencies consist of tripping a transmission line following a three-phase fault. For voltage stability, the PV curve is drawn after the system reaches a steady-state stability which means after the line is tripped. In Table 3.1, the contingencies are ranked in descending order based on their VSM. The first row represents the base case and is considered as a reference. Some contingencies did not affect the voltage stability as their VSMs are very close to the base case (ranking 1 to 6). Contingency "Line 16-19" is considered the most critical since the VSM is the lowest and is almost half the base case VSM. Similar approaches can be taken for machine tripping or when several contingencies occur.

The earlier prediction of improving voltage stability when DG is connected regardless of the location is contradicted as BVI_{16} is zero and BVI_{15} and BVI_{18} are negative. The

voltage stability is not affected when DG is connected at bus 16 and is worsened when DG is connected at buses 15 and 18.

Table 3.1. Ranking of contingencies according to their VSM for the IEEE RTS-96 24 bus system

Ranking	Contingency	VSM
0	Base case	2843.75
1	Line 01-05	2843.75
2	Line 02-04	2837.5
3	Line 05-10	2837.5
4	Line 08-10	2837.5
5	Line 02-06	2831.25
6	Line 04-09	2831.25
7	Line 01-02	2812.5
8	Line 08-09	2812.5
9	Line 18-21	2806.25
10	Line 01-03	2775
11	Line 17-18	2775
12	Line 03-09	2768.75
13	Line 15-16	2768.75
14	Line 12-23	2737.5
15	Line 13-23	2650
16	Line 12-13	2643.75
17	Line 06-10	2575
18	Line 11-14	2568.75
19	Line 11-13	2525
20	Line 15-24	2512.5
21	Line 17-22	2512.5
22	Line 16-17	2356.25
23	Line 21-22	2287.5
24	Line 14-16	2275
25	Line 20-23	2256.25
26	Line 15-21	2231.25
27	Line 19-20	2062.5
28	Line 16-19	1756.25

The BVI_i index can help determine the weak areas where compensation is needed. Large loads are located in the South of the system and it can be seen that BVI_i indices are high. DGs near large central generators can slightly improve, do no affect or can even worsen the system stability (Buses 13 to 20).

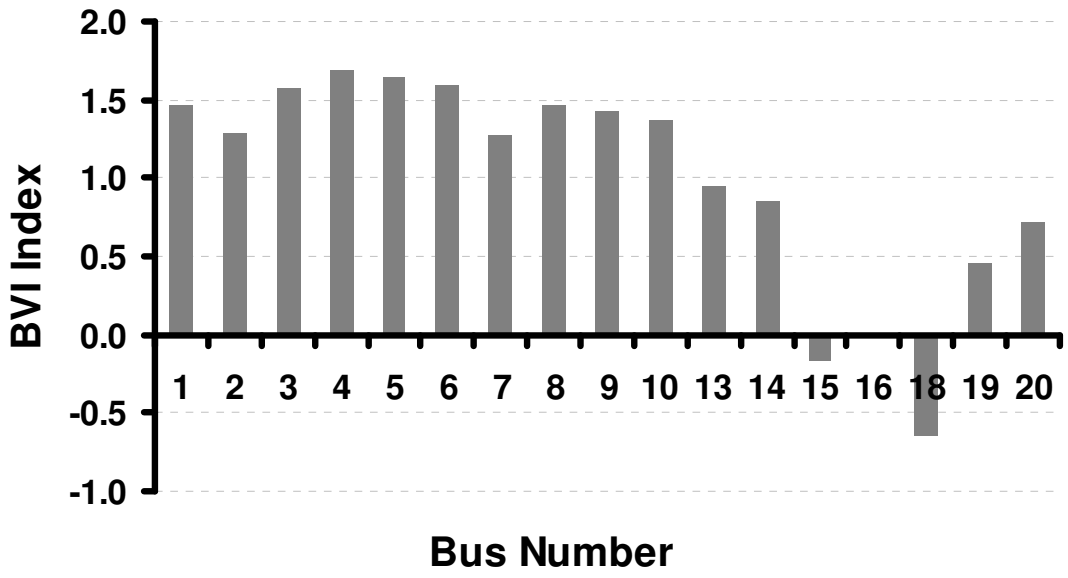

Figure 3.3. BVI indices for all load buses for the IEEE RTS-96 24 bus system

As mentioned in Section 2.2.2, utilities allow DG to operate within a power factor range while maintaining the PF constant. Due to economical factors, DG owners have the incentive to operate at unity power factor. The utility does not pay DG owners for supplying or absorbing reactive power [12]. Voltage stability is affected when DGs operate at different power factors. Table 3.2 shows the total BVI_{Ω} with DGs connected at all buses using both methods discussed in Section 3.3 and with three different power factors (unity, 0.9 lagging and 0.9 leading). The values in black are found using the exact method (Eq.(3.3)) and the values in grey are obtained by the approximation method defined in Eq.(3.4). It can be seen that the values are very close with an accuracy of almost 95% in most cases. The concept of linearity is applied for the IEEE RTS-96 24-bus system.

The exact values are depicted in Figure 3.4 to clearly see the effect of operating DG with different power factors. When all DG operate at a lagging power factor, the VSM is improved because DGs supply the local reactive power loads which reduce the stress on the transmission level and therefore more loads can be supplied. When DGs absorb reactive power, the VSM is worsened compared to their operation at unity power factor.

Therefore, an induction generator without its proper compensation would not significantly help improve the VSM. The BVI_{Ω} index remains constant with increasing the DG penetration level. This is because the index is relative to the amount of DG which

then shows another concept of linearity. The effect of different DG penetration levels other than the ones defined here can be determined using Figure 3.4.

The concepts viewed will be also discussed in the following sections with the other two test cases (IEEE 39-bus New England system and the IEEE 118 bus system).

Table 3.2. Comparison of calculation methods of BVI for IEEE RTS-96 24 bus system

Power Factor	5% DG	10% DG	15% DG	20% DG
Unity	0.750 0.763	0.789 0.768	0.762 0.746	0.761 0.742
0.9 Lagging	1.140 1.197	1.184 1.206	1.168 1.197	1.169 1.203
0.9 Leading	0.329 0.351	0.351 0.351	0.367 0.354	0.367 0.354

3.4.2 The IEEE 39-Bus New England Test System

Similar simulations are performed on the IEEE 39-bus New England test system which is considered as a medium case. In this system, no islands are formed following line tripping due to a contingency. Therefore, all contingencies involving non-transformer branches are considered and ranked in Table 3.3 based on their VSM. The system can operate following any of these contingencies because all the VSM are positive and therefore an equilibrium point can be found. Blackouts usually occur after a succession of contingencies which alters the sign of the VSM. "Line 21-22" is the worst contingency due to its lowest VSM.

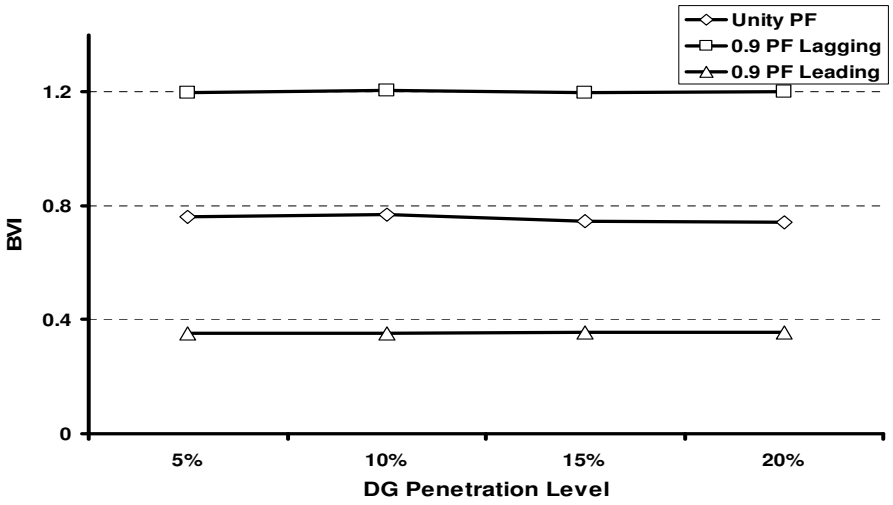

Figure 3.4. BVI for three power factors with different DG penetration level for the IEEE RTS-96 24 bus system

The individual BVI_i indices for the IEEE 39-bus New England test system are depicted in Figure 3.5 with a 10% DG penetration level. The individual BVI_i index refers to calculating the index with only one DG connected at bus *i*. Adding a DG at bus 12

Table 3.3. Ranking of contingencies according to their VSM for the IEEE 39-bus New England system

Ranking	Contingency	VSM
0	Base case	11531.3
1	Line 22-23	11493.8
2	Line 03-18	11475.4
3	Line 17-27	11443.8
4	Line 16-24	11381.3
5	Line 25-26	11337.5
6	Line 26-28	11312.5
7	Line 14-15	11293.8
8	Line 07-08	11281.3
9	Line 17-18	11168.8
10	Line 26-29	11131.3
11	Line 04-05	11106.3
12	Line 02-25	11050.1
13	Line 04-14	11000.3
14	Line 01-39	10837.5
15	Line 05-08	10800.5
16	Line 26-27	10800.5
17	Line 01-02	10793.8
18	Line 10-11	10706.3
19	Line 03-04	10693.8
20	Line 10-13	10568.8
21	Line 16-17	10493.8
22	Line 06-11	10481.3
23	Line 09-39	10406.3
24	Line 05-06	10368.8
25	Line 13-14	10343.8
26	Line 08-09	10318.8
27	Line 06-07	10218.8
28	Line 23-24	10212.5
29	Line 02-03	10143.8
30	Line 16-21	10112.5
31	Line 16-19	9175.8
32	Line 15-16	9068.75
33	Line 28-29	8587.5
34	Line 21-22	7606.25

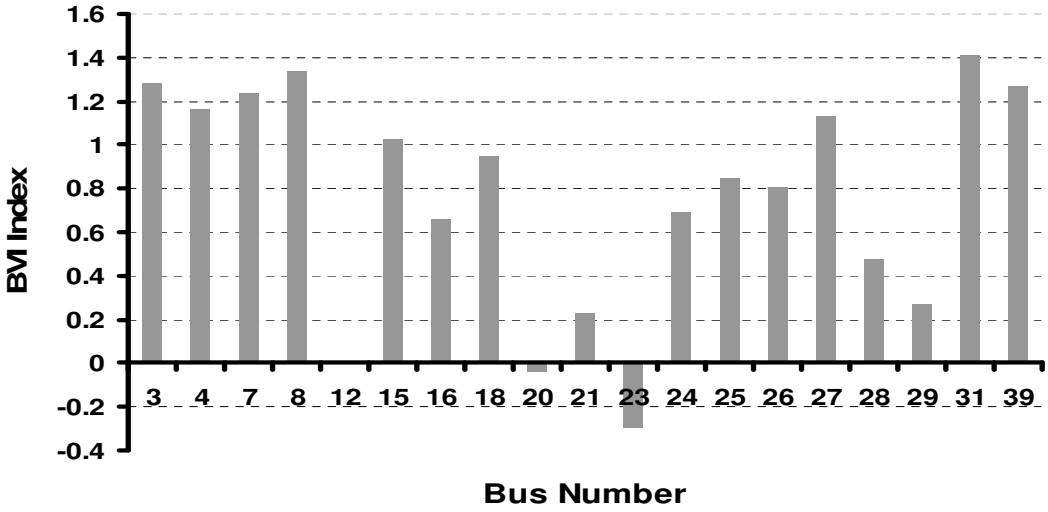

Figure 3.5. BVI indices for all load buses for the IEEE 39-bus New England system

does not affect the VSM of the system which means that no contribution on the voltage stability is added with having this DG. DGs connected at buses 20 and 23 worsen the VSM of the system and therefore should be avoided. It can be seen that adding DG in the Southeast of the New England test case where large generators are present, does not affect or even worsens the stability of the system. The BVI_i indices of DG connected in the West of the system are extremely high due to the large concentration of loads in this area. The same conclusion is found in this system as the previous one. Therefore, size and location of DG affect the voltage stability of the system.

The concept of linearity is tested for this system by comparing both the exact (in black) and the approximated (in grey) methods in Table 3.4. The relative errors do not exceed 5 % in most cases and therefore, an approximation of the BVI_Ω index of the whole IEEE 39-bus New England test system is validated. It should be noted that if the area in concern is smaller (i.e. only the North of the system), the approximation of the BVI_Ω index of that region is more accurate. The three power factor levels are presented in Table 3.4 and the same observation can be made as in Section 3.4.1. DGs with a lagging power factor improve the VSM more than when operating at unity power factor, while DGs with a leading power factor worsen the VSM compared to the unity power factor case. By comparing the values in Table 3.2 and Table 3.4, it can be seen that the BVI_Ω index, for both cases, is almost equal to 0.8 at unity power factor, 1.2 at lagging power and 0.4 at leading power factor.

The results using the exact method are depicted in Figure 3.6 and the second effect of linearity that was discussed in the previous section is confirmed. The BVI_Q index remains constant when the DG penetration level is increased and therefore the contribution is proportional to the total output of the DGs. The impact of any other penetration level can be determined without any calculations.

The observations of the results found for the IEEE 39-bus New England test system confirm the one made for the IEEE RTS-96 24 bus system. It remains to be seen if the same conclusions can be drawn for the IEEE 118-bus system that is considered as a large system.

Table 3.4. Comparison of calculation methods of BVI for the IEEE 39-bus New England system

Power Factor	5% DG	10% DG	15% DG	20% DG
Unity	0.836 0.830	0.831 0.831	0.813 0.840	0.795 0.852
0.9 Lagging	1.188 1.167	1.145 1.169	1.143 1.167	1.130 1.173
0.9 Leading	0.517 0.492	0.520 0.500	0.468 0.502	0.446 0.515

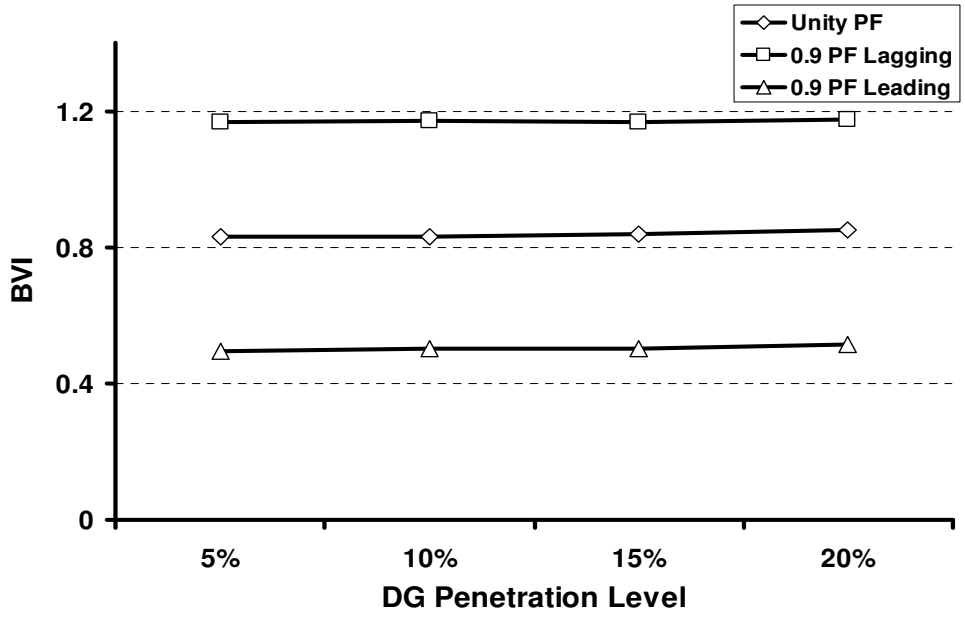

Figure 3.6. BVI for three power factors with different DG penetration level for the IEEE 39-bus New England system

3.4.3 The IEEE 118-Bus Test System

The IEEE 118-bus system is a complex system with 19 synchronous generators and 35 synchronous condensers. For this system, all contingencies leading to an island are omitted. Similarly, the contingencies for this system are ranked based on their VSM in Table 3.5. It can be seen that most contingencies do not affect the system; 111 out of 161 contingencies have the same VSM as the base case. This is due to the complex interconnection of the system with many branches and synchronous condensers. The following 40 contingencies are just few tens of MW less than base case. The most critical is "Line 79-80" with almost two thirds the value of the base case. The system can then be considered as quite robust as it can withstand all three-phase fault contingencies.

The individual BVI_i indices for the IEEE 118-bus system are depicted in Figure 3.7 with a 10% DG penetration level. It can be seen that the BVI_{116} index is superior to the other indices as it is almost equal to 0.95 and the others range from -0.01 to 0.02. In order to see the other indices, a close-up of Figure 3.7 is shown in Figure 3.8.

All BVI_i indices of buses located in the North are either negative or zero. Most of the BVI_i indices in the South are positive, and the one at 116 is extremely high. Although the generators and the loads of this system are dispersed, large generators are located in the North and a large concentration of loads is in the South of the system. Therefore, the same conclusion can be drawn as for the other two systems. The impact of the location of DG is based on the nature of the area (generation or large loads) and a study on determining the ideal location of DG (in this case at bus 116) should be implemented.

The results of the two methods (exact in black and approximated in grey) to obtain the total BVI_Ω index of the system are shown in Table 3.6. The concept of linearity is confirmed as the approximated method is a very good prediction of the exact method (less than 5%). Therefore, the approximated method can be used to determine the impact of connecting DGs at any set of buses. In the previous two cases, it was seen that having DGs operate at a lagging power factor is more beneficial than at unity power factor and leading power factor. For this test case, regardless of the power factor, the contribution of DGs is the same. In all three cases, the BVI_Ω index is almost equal to 1.

Table 3.5. Ranking of contingencies according to their VSM for the IEEE 118-bus system

Ranking	Contingency	VSM
0	Base case, Line 001-002, Line 001-003, Line 002-012, Line 003-005, Line 003-012, Line 004-005, Line 004-011, Line 005-006, Line 005-011, Line 006-007, Line 007-012, Line 008-030, Line 011-012, Line 011-013, Line 012-014, Line 012-016, Line 013-015, Line 014-015, Line 015-017, Line 015-019, Line 015-033, Line 016-017, Line 017-018, Line 017-031, Line 017-113, Line 018-019, Line 019-020, Line 019-034, Line 020-021, Line 023-032, Line 024-072, Line 027-028, Line 027-032, Line 027-115, Line 028-029, Line 029-031, Line 031-032, Line 032-113, Line 032-114, Line 033-037, Line 034-036, Line 034-037, Line 035-036, Line 035-037, Line 037-039, Line 037-040, Line 039-040, Line 040-041, Line 045-049, Line 046-048, Line 048-049, Line 049-050, Line 049-051, Line 049-054, Line 050-057, Line 051-052, Line 051-058, Line 052-053, Line 053-054, Line 054-055, Line 054-056, Line 054-059, Line 055-056, Line 055-059, Line 056-057, Line 056-058, Line 056-059, Line 059-060, Line 059-061, Line 060-061, Line 060-062, Line 061-062, Line 062-066, Line 062-067, Line 066-067, Line 070-071, Line 071-072, Line 074-075, Line 076-077, Line 076-118, Line 077-080, Line 077-082, Line 078-079, Line 080-096, Line 080-097, Line 080-098, Line 083-084, Line 084-085, Line 085-088, Line 090-091, Line 091-092, Line 092-093, Line 092-094, Line 092-100, Line 092-102, Line 093-094, Line 094-100, Line 095-096, Line 096-097, Line 098-100, Line 099-100, Line 100-101, Line 101-102, Line 103-104, Line 103-105, Line 105-106, Line 105-107, Line 105-108, Line 108-109, Line 109-110, Line 114-115	7481.25
1	Line 021-022, Line 022-023, Line 023-025, Line 034-043, Line 040-042, Line 041-042, Line 043-044, Line 045-046, Line 049-069, Line 063-064, Line 070-074, Line 070-075, Line 080-099, Line 083-085, Line 088-089, Line 094-095, Line 094-096, Line 104-105, Line 106-107, Line 103-110	7475
2	Line 024-070, Line 030-038, Line 044-045, Line 046-047, Line 075-118, Line 085-089, Line 100-103	7468.75
3	Line 026-030, Line 064-065, Line 082-096, Line 100-106	7462.5
4	Line 075-077	7456.25
6	Line 100-104, Line 069-075	7443.75
7	Line 049-066, Line 082-083	7437.5
9	Line 023-024, Line 047-049	7412.5
10	Line 025-027	7393.75
11	Line 089-092	7381.25
12	Line 069-077	7343.75
13	Line 038-065	7275
14	Line 069-070	7218.75
15	Line 068-081	6856.25
16	Line 047-069, Line 089-090	6793.75
18	Line 065-068	6318.75
19	Line 077-078	6100
20	Line 042-049	5456.25
21	Line 079-080	5300

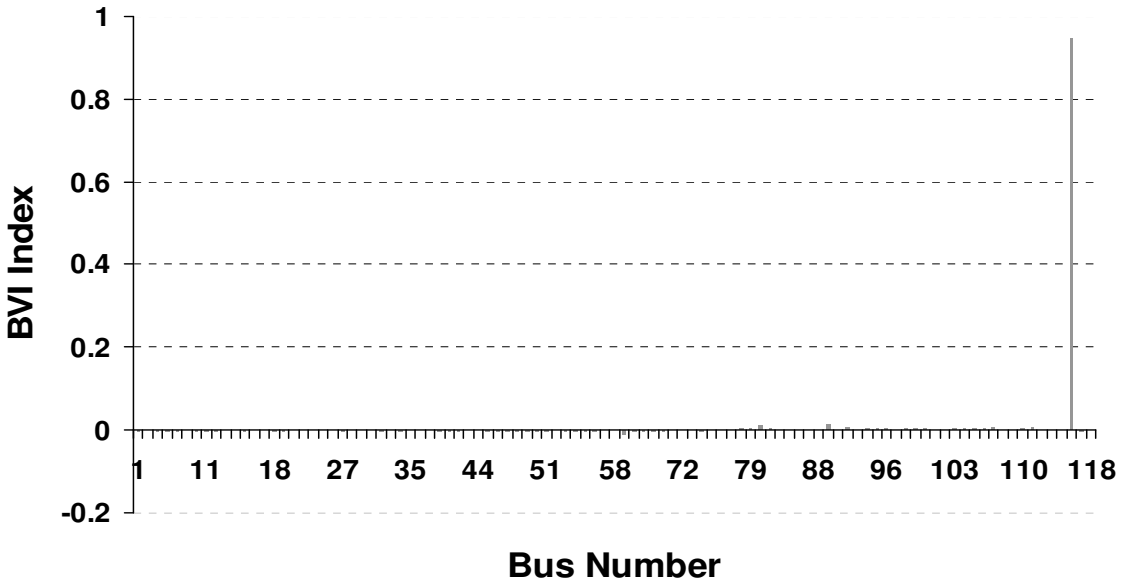

Figure 3.7. BVI indices for all load buses for the IEEE 118-bus system

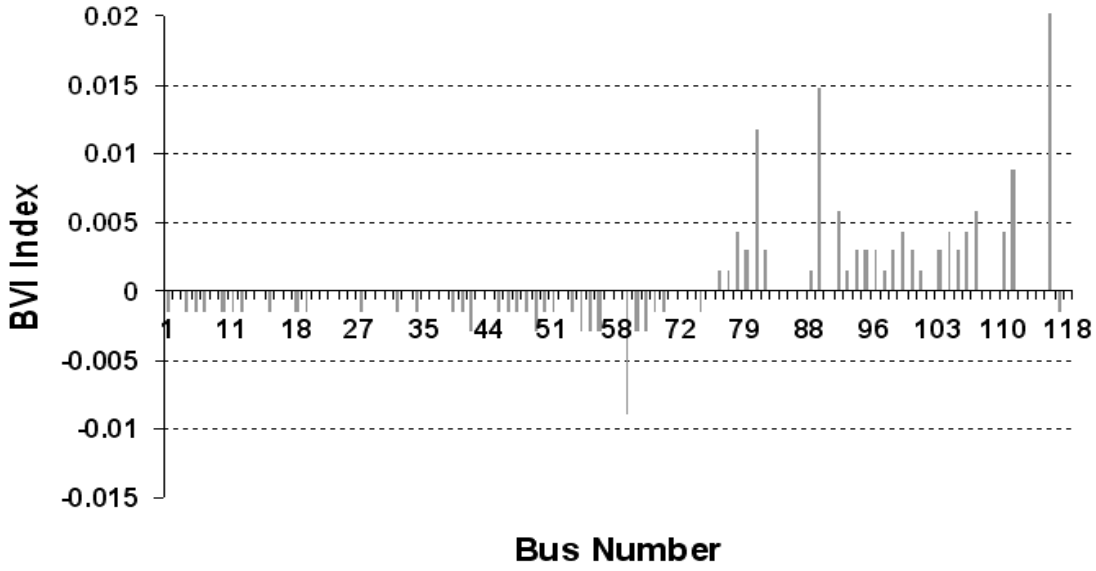

Figure 3.8. Close-up of BVI indices for all load buses for the IEEE 118-bus system

Table 3.6. Comparison of calculation methods of BVI for the IEEE 118-bus system

Power Factor	5% DG	10% DG	15% DG	20% DG
Unity	0.984 1.028	1.017 1.029	1.009 1.021	1.011 1.034
0.9 Lagging	0.996 1.028	1.008 1.029	1.010 1.028	1.011 1.034
0.9 Leading	0.981 1.025	1.013 1.028	1.011 1.030	1.009 1.034

Figure 3.9 confirms the observations made from Table 3.6 as the three lines representing the three power factor levels are superimposed. This is due to the contribution of bus 116 which remains unchanged with different power factors. This test case shows that when DGs operate at a lagging power factor, they do not necessarily improve the VSM of the system. The second concept of linearity is confirmed for this case as the BVI_{Ω} index remains constant with an increase in the DG penetration level. Therefore, the contribution of any penetration level can be found without further calculations hence, it saves computational time, especially for large systems that are similar to the IEEE 118-bus system.

3.5 Applications of DG Assistance: Load Duration Curve

The normalized load duration curve (LDC) illustrates the load variation within a certain period where the load is ordered according to its magnitude rather than chronologically. The load data is taken on an hourly basis for a full year period. The data for the LDC curve of the IEEE RTS-96 24 bus system, shown in Figure 3.10, is provided by [82]. The probability p of the load being larger than a certain load level d_0 is determined from the LDC:

$$p[d \geq d_0] = LDC(d_0) \tag{3.6}$$

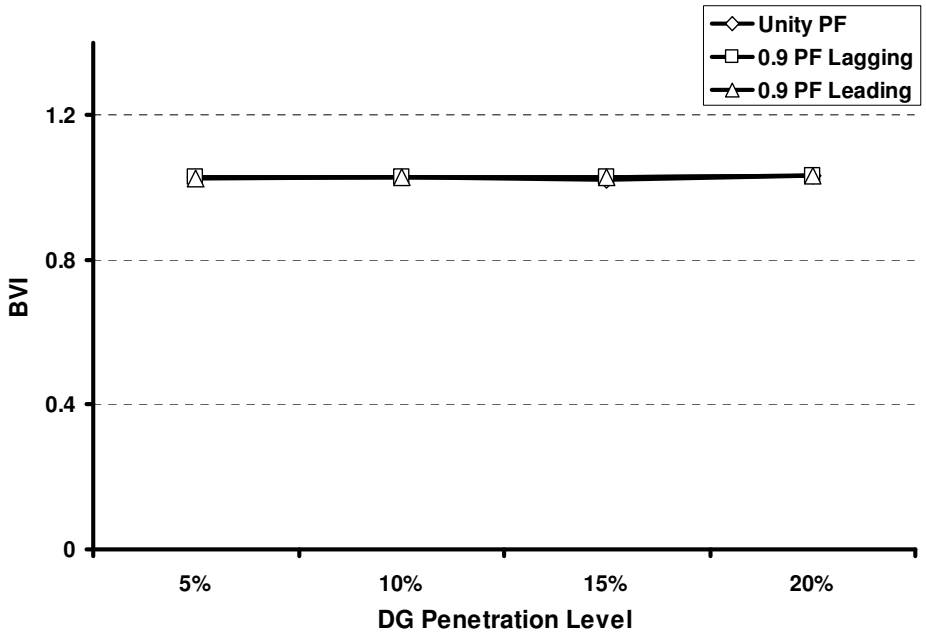

Figure 3.9. BVI for three power factors with different DG penetration level for the IEEE 118-bus system

It should be noticed that the smallest probability is at the load peak. The interval where the load can fall can be determined by:

$$\alpha(d_0, d_1) = p[d_1 \geq d \geq d_0] = LDC(d_0) - LDC(d_1) \tag{3.7}$$

For instance, the probability of obtaining a load higher than 2,000 MW is:

$$p[d \geq 2{,}000] = LDC(2{,}000) = 0.287$$

The probability that the load falls between 2,000 MW and 2,200 MW is:

$$\alpha(2000, 2200) = LDC(2000) - LDC(2200) = 0.287 - 0.171 = 0.116$$

The probability α is 11.6 % which is quite small because the two values taken are close to the peak load. The probability is also small at the other extremity when the load is near its lowest value (1000 MW).

Using the LDC, the effect of "DG assistance" is considered by determining the probability of avoiding voltage collapse following a large contingency. The post-contingency VSM with and without DG are obtained to define the interval where the load is located. Eq. (3.7) is used to find the probability of having the load fall into this interval. This can be used to determine the probability of avoiding voltage collapse due to the presence of DG. The three curves, depicted in Figure 3.11, correspond to the probability of loads falling into "DG assistance" following a contingency with having 10 % DG

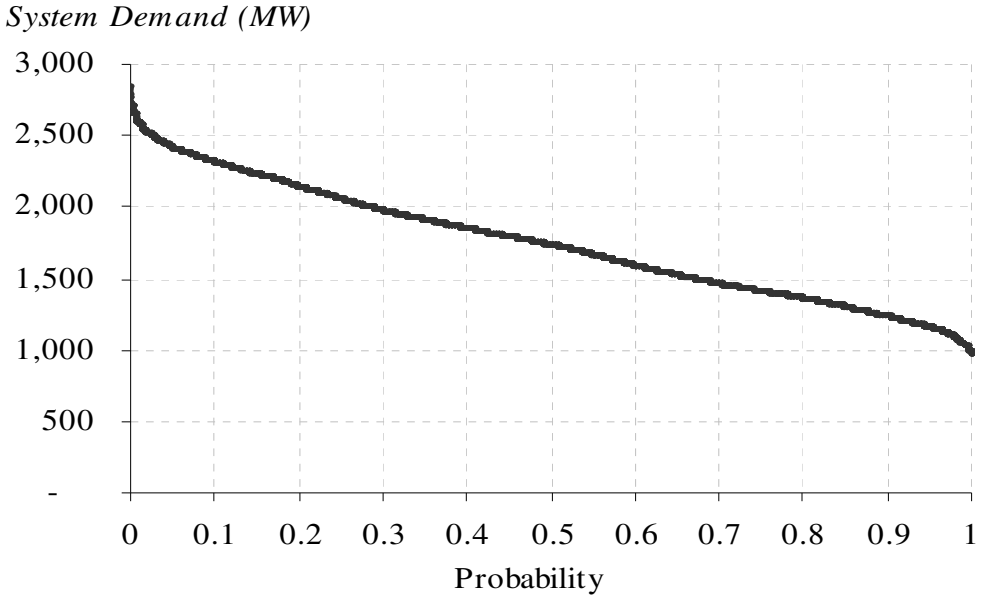

Figure 3.10. Load duration curve of the IEEE RTS-96 24 bus system

penetration level and operating at the three different power factors. For a unity power factor ($BVI_{\Omega} = 0.8$), if DG remains connected after a contingency that reduced the VSM to 45%, there is a 21% higher chance that the system will not collapse. It can be seen that with a higher BVI_{Ω} index, the probability of falling into "DG assistance" is more significant. DG can provide support for large contingencies which reduce the VSM between 40 % and 75 %. When less than 35 %, a voltage collapse is inevitable even with the presence of DG.

Taking the same load data and using the peak load of the IEEE 39-bus New England test system, the same curves are obtained. Therefore, in order to see the impact of different LDCs, the load data is collected for the year 2008 from multiple utilities such as IESO (Independent Electricity System Operator - Ontario), ISO New England, NYISO (New York), AEMO (Australian Energy Market Operator), RTE (Gestionnaire du Réseau de Transport d'Electricité – France) and National Grid (United Kingdom) [88-93]. Figure 3.12, Figure 3.13, Figure 3.14, Figure 3.15, Figure 3.16 and Figure 3.17 show the different probabilities that DG can help prevent a voltage collapse using different LDCs. There are similarities with the curves shown in Figure 3.11 but with shifted peaks between 50 % and 70 %. It is interesting to see that the probabilities given by the Ontario LDC and the Australian LDC are very similar to the IEEE RTS-96 bus system LDC. The LDCs of New England and New York are almost identical and the same observation can

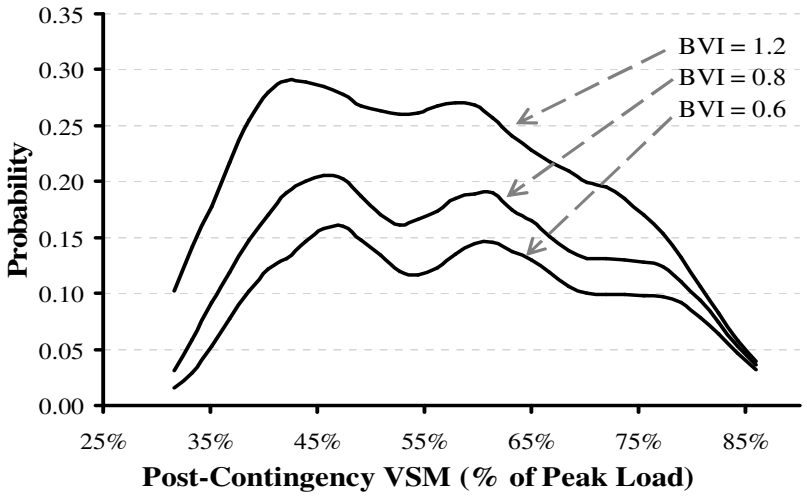

Figure 3.11. Probabilities that aggregated DG will provide support on contingencies for the IEEE RTS-96 24 bus system

be made about the LDCs of France and UK. With certain LDCs, the probabilities can reach 45 %. "DG assistance" is therefore very useful to avoid collapse of the system following a severe contingency.

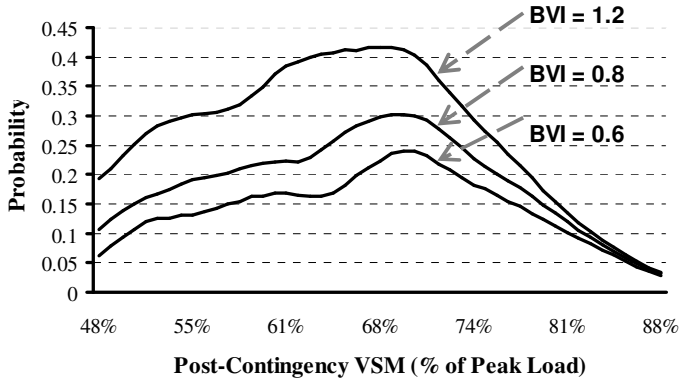

Figure 3.12. Probabilities that aggregated DG will provide support on contingencies using the Ontario LDC for the year 2008

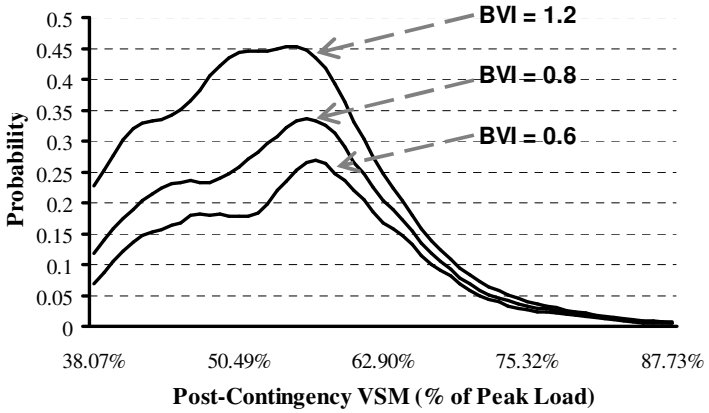

Figure 3.13. Probabilities that aggregated DG will provide support on contingencies using the New England LDC for the year 2008

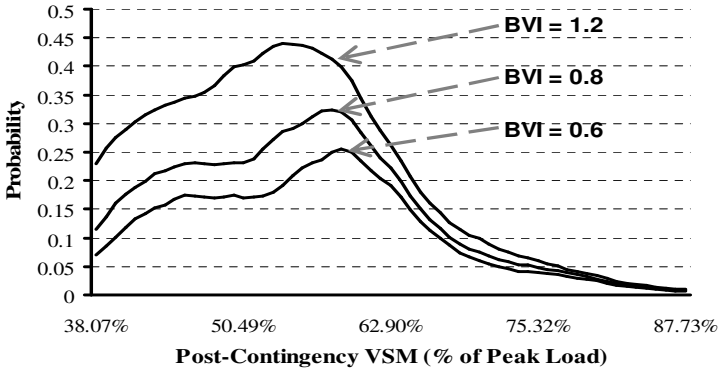

Figure 3.14. Probabilities that aggregated DG will provide support on contingencies using the New York LDC for the year 2008

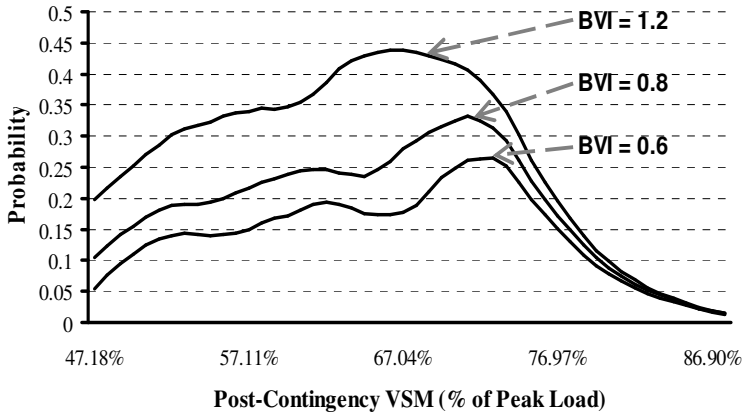

Figure 3.15. Probabilities that aggregated DG will provide support on contingencies using the Australian LDC for the year 2008

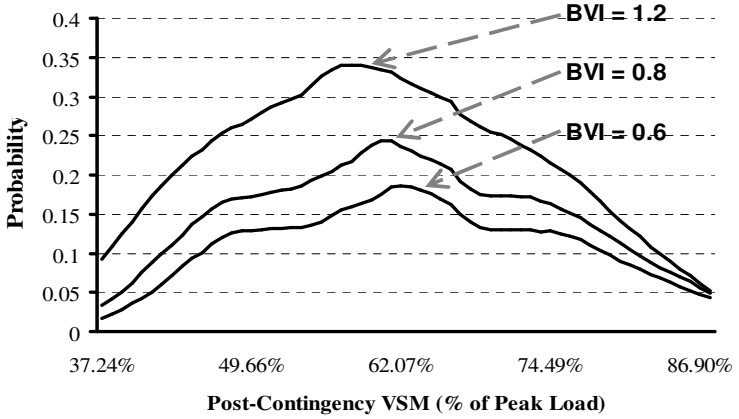

Figure 3.16. Probabilities that aggregated DG will provide support on contingencies using the French LDC for the year 2008

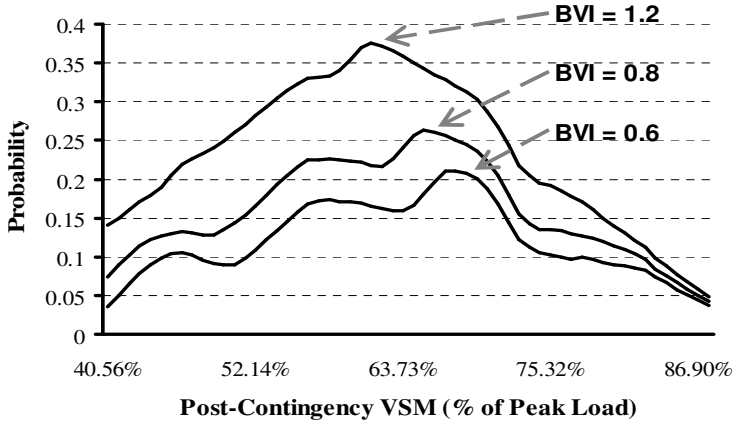

Figure 3.17. Probabilities that aggregated DG will provide support on contingencies using the UK LDC for the year 2008

3.6 Conclusion

The location and the size of DGs have an impact on the long-term voltage stability. When DGs are connected near large centralized generators, the voltage security margin is worse. On the other hand, the highest positive impact is when DGs are located in areas with large loads.

The first concept of linearity consists of estimating the contribution of DGs when connected at all loads simultaneously (BVI_{Ω}) by adding all the individual contributions (BVI_i) multiplied by a weighing factor. This concept is applicable for the three test systems where errors did not exceed 5 %. An operator can then determine the contribution of DGs connected at multiple loads without a performing PV analysis.

In most cases, when DGs operate at a lagging power factor, the VSM is improved compared to the VSM of DGs with unity power factor, whereas when the power factor is leading the VSM is worse. This is not applicable for the IEEE 118 bus system due to the presence of many synchronous condensers. The reactive power of DGs has little effect on the system. The total contribution of DG (BVI_{Ω}) is increased linearly with the DG penetration level. The contribution of any penetration level can then be determined using the BVI_{Ω} index.

Using the load duration curve, the probability of the system falling into "DG assistance" following a large contingency can be found. Using different LDCs, high probabilities occur when severe contingencies reduce the VSM between 40 % and 60 %.

Chapter 4: Impact of Large Penetration of DG on the Short-Term Voltage Stability

4.1 Introduction

Few researches have been performed regarding short-term voltage stability compared with the long-term stability and therefore there are only a small amount of documented incidents related to short-term stability. One of the problems of the North American blackout in 2003 is believed to be related to short-term voltage stability. Contingencies such as a three-phase fault can trigger a fast voltage collapse due to fast recovery loads that try to restore power consumption after a voltage dip. The components that can help increase the chances of short-term voltage instability consist of [18,94]:

- Low inertia compressor motors
- Electronically controlled loads
- HVDC ties linking weak areas
- Uncompensated DG consuming reactive power
- Large amounts of capacitor banks for reactive power compensation

Many measures can be taken to counter the short-term voltage instability by using [95]:

- Fast-acting generator excitation controls
- Fast load shedding
- Voltage source converter reactive power support devices (STATCOM, SMES)

DG can be considered as a new means to help improve the short-term voltage stability.

4.2 Impact of DG on the Short-Term Voltage Stability

The contribution of DG on the short-term voltage stability depends on many factors such as the size, the location and the technology of the DG. A short-term voltage stability index ($SVSI_{base}$) is defined as the difference between the pre-fault voltage load bus and the minimum fault voltage multiplied by the load apparent power for all load buses N.

This index emphasizes on the voltage stress on load buses during a fault with considering the size of the load:

$$SVSI_{base} = \sum_{i=1}^{N} \Delta V_i \left(S_{L,i} \right) \tag{4.1}$$

With

$$\Delta V = V_0 - V_{\min}$$

$SVSI_{base}$ can be used as a contingency ranking index where the highest value of the index can be associated with the most severe contingency. The equation of $SVSI_{base}$ (Eq. (4.1)) is reformulated to include the impact of DG on the short-term voltage stability:

$$SVSI_{DG} = \sum_{i=1}^{N} \Delta V_i \left(S_{L,i} - S_{DG,i} \right) \tag{4.2}$$

The apparent power S_{DG} of a DG is defined as:

$$S_{DG} = \sqrt{P_{DG}^2 + Q_{DG}^2} \tag{4.3}$$

With

$$P_{DG} = p\, P_L$$
$$Q_{DG} = \frac{P_{DG}}{PF} \sin\left(\cos^{-1}\left(PF \right) \right)$$

P_{DG} and Q_{DG} represent the real and reactive power of the aggregated DGs connected at a load bus. p is the penetration level of DG defined in percentage and multiplied by the load power P_L. Q_{DG} is found by the power factor PF set by the PF controller and the active power of the DG. Depending on the power factor (lagging or leading), DG either produces or absorbs reactive power (Q_{DG} is positive or negative).

The contribution of DG is defined as the difference between the two indices $SVSI_{base}$ and $SVSI_{DG}$:

$$SVSI_{diff} = SVSI_{base} - SVSI_{DG} \tag{4.4}$$

$SVSI_{tot}$ is defined as the contribution of DGs connected at all load buses. It will then be verified if:

$$SVSI_{tot} \approx \sum_{j=1}^{N} SVSI_{diff\ j} \tag{4.5}$$

4.3 Short-Term Voltage Stability Simulation

The impact of DGs on the short-term voltage stability is studied using the three test cases defined in Section 2.4.1. A three-phase fault is applied at a branch of the system and then cleared after a certain number of cycles. The loads are modeled as constant current for short-term stability [96]. Different clearing times are chosen for each case depending on the CCT of the selected fault. A large clearing time can be chosen when the CCT is high to show that the concept can be applied for any clearing time.

4.3.1 The IEEE Reliability Test System 1996

The indices defined in the previous section are applied on the IEEE RTS-96 24 bus system. Faults on transformer branches and on lines that cause islanding are omitted. Contingencies can be ranked according to the $SVSI_{base}$ index where the highest indicate the most severe contingency due to the large voltage dips that can damage some equipment. Table 4.1 shows the ranking of the contingencies after a three-phase fault is applied and is cleared after 6 cycles. The small number of cycles is chosen in order to include all contingencies.

The most severe contingency is "Line 16-19" with an $SVSI_{base}$ index significantly higher than the others and therefore the system operator should find methods to improve the short-term voltage stability at these weak buses by adding reactive support.

The contingency "Line 14-16" is chosen with a fault clearing of 12 cycles to study the impact of DGs on the system. The $SVSI_{base}$ for the contingency "Line 14-16"is found to be approximately 1206 V-MVA. Table 4.2 shows all the $SVSI_{DG}$ of aggregated power electronic interfaced DG with unity power factor and connected to each load bus. A 5% penetration level is considered. All $SVSI_{DG}$ are lower than $SVSI_{base}$ and therefore, connecting DGs at any load bus during the contingency improves the short-term voltage stability of the system. The real power of DGs at bus 18 is higher than those at bus 14, but the $SVSI_{diff}$ at bus 18 is lower than at bus 14. This indicates that the size of the aggregated DG is not the only factor that affects the short-term voltage stability; the location plays an important role as well.

The contribution of each aggregated power electronic interfaced DG ($SVSI_{diff}$) is shown in Figure 4.1 with three different power factors (unity, 0.9 lagging and 0.9

leading). It is noticed that in most cases when DG is operating with a leading power factor, the short-term voltage stability is improved. When generators operate at a leading power factor, the terminal voltages are reduced which leads to a reduction in the overall power flow. Therefore, following a fault, voltage drops are less severe.

Table 4.1. Contingency ranking based on the $SVSI_{base}$ for the IEEE RTS-96 24 bus system

Ranking	Contingency	$SVSI_{base}$ (V-MVA)
1	Line 04-09	592.7397
2	Line 05-10	702.3796
3	Line 08-09	711.5116
4	Line 08-10	711.5116
5	Line 06-10	715.2778
6	Line 03-09	739.5764
7	Line 02-04	932.2058
8	Line 02-06	932.2058
9	Line 01-02	943.554
10	Line 01-03	943.554
11	Line 01-05	943.554
12	Line 14-16	992.8176
13	Line 12-13	1135.297
14	Line 12-23	1135.297
15	Line 17-18	1152.84
16	Line 17-22	1152.84
17	Line 20-23	1164.605
18	Line 21-22	1203.93
19	Line 19-20	1205.946
20	Line 11-13	1209.086
21	Line 11-14	1209.086
22	Line 18-21	1225.674
23	Line 13-23	1266.857
24	Line 15-16	1416.824
25	Line 15-21	1416.824
26	Line 15-24	1416.824
27	Line 16-17	1617.809
28	Line 16-19	7787.148

By adding all the $SVSI_{diff}$ in Table 4.2, an approximation of the impact of aggregated power electronic interfaced DG connected at all load buses can be obtained. Table 4.3

shows the values obtained by adding all the $SVSI_{diff}$ and calculating the total impact with aggregated DGs connected at all load buses ($SVSI_{tot}$).

Table 4.2. $SVSI_{DG}$ of power electronic interfaced DG with unity power factor connected at a load bus for the IEEE RTS-96 bus system

Load Bus Number	P_{DG} (MW)	$SVSI_{DG}$ (V-MVA)	$SVSI_{diff}$ (V-MVA)
1	5.40	1203.67	2.543
2	4.85	1204.00	2.206
3	9	1201.87	4.336
4	3.7	1204.33	1.883
5	3.55	1204.40	1.813
6	6.8	1202.32	3.891
7	6.25	1203.69	2.519
8	8.55	1202.14	4.070
9	8.75	1201.62	4.594
10	9.75	1200.79	5.417
13	13.25	1200.08	6.134
14	9.7	1198.13	8.080
15	15.85	1200.37	5.835
16	5	1204.23	1.978
18	16.65	1200.73	5.478
19	9.05	1202.81	3.399
20	6.4	1203.90	2.312

An error of less than 3 % is obtained by comparing the two values and therefore the approximation can be considered as valid. Table 4.4 shows the comparison of the two methods to obtain the total contribution of power electronic interfaced DGs connected at all buses. The largest error is around 6 % which can be considered as a good estimation

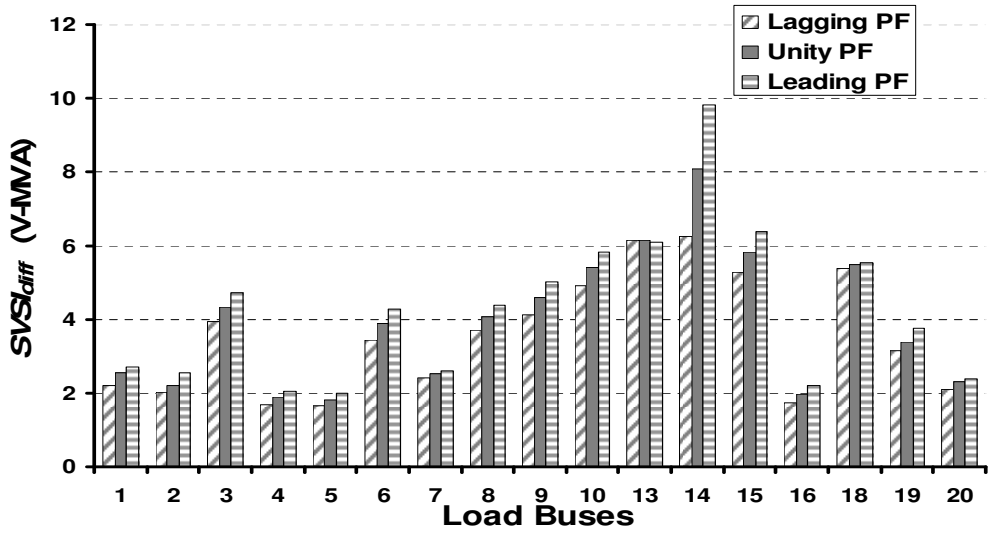

Figure 4.1. $SVSI_{diff}$ of power electronic interfaced DG at each load bus and with different power factors

for large DG penetration. A system operator can then approximate the contribution of any set of multiple aggregated power electronic interfaced DGs for the IEEE RTS-96 bus system.

Table 4.3. Comparison between $SVSI_{tot}$ and the sum of all $SVSI_{diff}$ of 5 % penetration of power electronic interfaced DG for the IEEE RTS-96 24 bus system

P_{DG} (MW)	$SVSI_{tot}$	$\sum_{j=1}^{N} SVSI_{diff\ j}$
142.50	64.87	66.49

Table 4.4. Comparison between $SVSI_{tot}$ and the sum of all $SVSI_{diff}$ of 10 %, 15 % and 20 % penetrations of power electronic interfaced DG for the IEEE RTS-96 24 bus system

Penetration level	**10 %**	**15 %**	**20 %**
P_{DG} **(MW)**	285.00	427.50	570.00
$SVSI_{tot}$ **(V-MVA)**	125.89	186.50	248.67
$\sum_{j=1}^{N} SVSI_{diff\ j}$ **(V-MVA)**	132.90	198.72	263.77

Connecting synchronous generator based DGs has a higher effect on voltage dips because the machines tend to inject reactive power in response to a voltage dip. Figure 4.2 shows the impact of connecting a synchronous machine based DG with different power factors. Compared to the power electronic interfaced DG, the $SVSI_{diff}$ is almost ten times higher. The highest $SVSI_{diff}$ in Figure 4.1 corresponds to the lowest one in Figure 4.2. Operating at different power factors has a very small effect as $SVSI_{diff}$ indices are almost equal for the three cases (leading, lagging and unity power factors).

Due to the presence of synchronous machine based DGs, the prediction of the contribution of DGs connected at all load buses is not accurate enough (Table 4.5). This is due to the non-linear behavior of such technologies. This method is not applicable to these types of DGs.

Induction machine based DGs can only operate at one power factor depending on the compensation connected at its extremity. It is then assumed that these DGs are fully compensated. In other words, they operate at unity power factor. Table 4.6 shows the

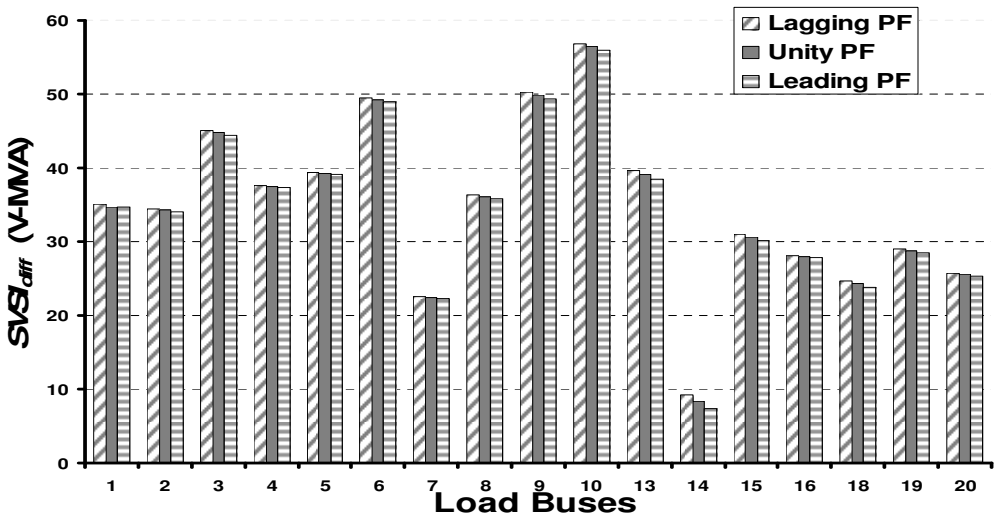

Figure 4.2. $SVSI_{diff}$ of synchronous machine interfaced DG at each load bus and with different power factors

Table 4.5. Comparison between $SVSI_{tot}$ and the sum of all $SVSI_{diff}$ of synchronous machine interfaced DG for the IEEE RTS-96 24 bus system

Penetration level	**5 %**	**10 %**	**15 %**	**20 %**
$\mathbf{P_{DG}}$ **(MW)**	142.50	285.00	427.50	570.00
$\boldsymbol{SVSI_{tot}}$ **(V-MVA)**	431.91	519.87	563.85	606.73
$\sum_{j=1}^{N} SVSI_{diff\ j}$ **(V-MVA)**	588.96	605.52	673.39	737.74

values of the total contribution of induction machine based DGs using both methods. The contribution is higher than the one with power electronic interfaced DG but lower than the one with synchronous machine based DG. It is interesting to see that at a low penetration level (5 %), the relative error is quite high (28 %) but it decreases with an increase of penetration level. The relative error becomes almost 5 % (which is acceptable) at a penetration level of 20 %. This method can then be used to approximate the contribution of induction machine based DGs at high penetration levels only.

Table 4.6. Comparison between $SVSI_{tot}$ and the sum of all $SVSI_{diff}$ of induction machine interfaced DG for the IEEE RTS-96 24 bus system

Penetration level	**5 %**	**10 %**	**15 %**	**20 %**
$\mathbf{P_{DG}}$ **(MW)**	142.50	285.00	427.50	570.00
$\boldsymbol{SVSI_{tot}}$ **(V-MVA)**	184.99	252.60	316.68	378.01
$\sum_{j=1}^{N} SVSI_{diff\ j}$ **(V-MVA)**	132.28	209.35	283.95	356.05

Figure 4.3 and Figure 4.4 show the voltage at buses 14 and 13 respectively with and without DG connected at all load buses during the fault that is applied on the line 14-16. At bus 14, regardless of the DG technology, the voltage drops to zero until the fault is cleared. The second voltage dip shows the impact of the technology of the DG. The synchronous based voltage DG reduces the voltage dip more than any other technology. Power electronic interfaced DG also reduces the voltage dip, whereas induction generator based DG increases the voltage dip compared to the one without DG. The oscillation of the voltage after the clearance of the fault is improved by installing DG, where synchronous machine based DG has the most impact and power electronic based has the least. At bus 13, the contribution of DG on the first voltage dip is clear where all DG technologies improve the short-term voltage stability. Synchronous generator based DG has the largest impact, followed by the induction machine and finally the power electronic based DG. The observations on the second voltage dip and the voltage oscillations are similar to the one on bus 14. It can be seen that due to the dynamics of the synchronous generator, synchronous machine based DGs are the most favorable to withstand contingencies and help improve the stability of the system.

4.3.2 The IEEE 39-Bus New England Test System

The concept of linearity (Eq. (4.5)) is tested using the IEEE 39-bus New England test system (medium power system). The number of loads and generators are higher than the previous test case and therefore, the presence of non-linearity is more significant. Table 4.8 shows the contingency ranking based on the $SVSI_{base}$ index for the short-term voltage stability. Several contingencies associated with a certain bus have identical indices.

The most severe contingencies occur at the lines connected to bus 16 which is located at the center of the system. The system operator should improve the short-term voltage stability at critical buses (i.e. buses 3, 4 and 16) by adding reactive power support devices or as will be shown in this section, by connecting aggregated DG. A bus is qualified as critical, in this case, when the $SVSI_{base}$ indices of the contingencies on the lines connected at these buses are high.

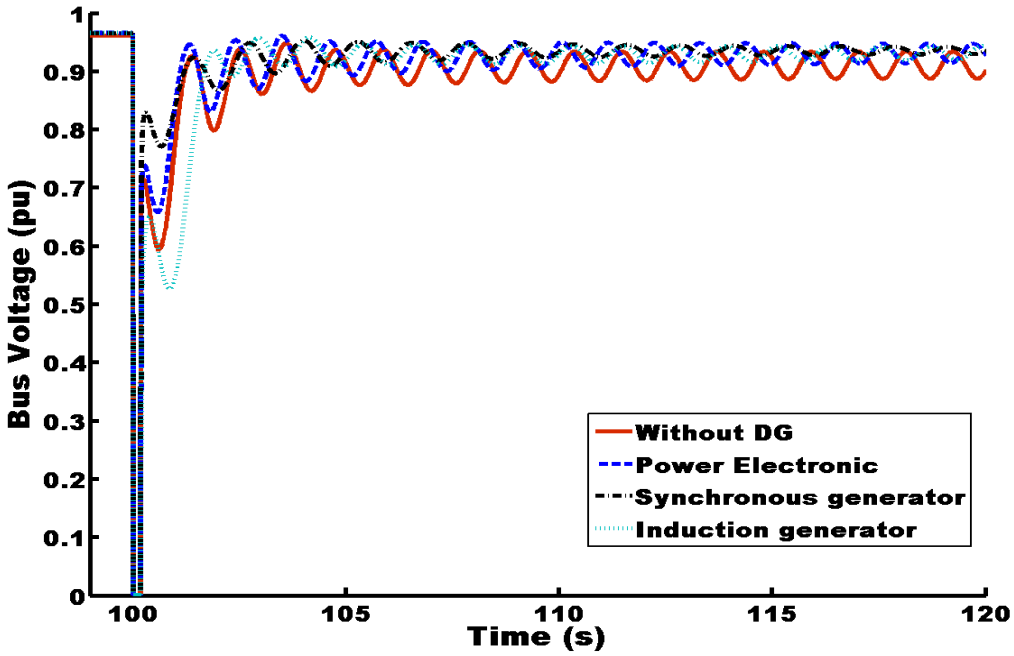

Figure 4.3. Voltage at bus 14 during the fault with different DG technologies

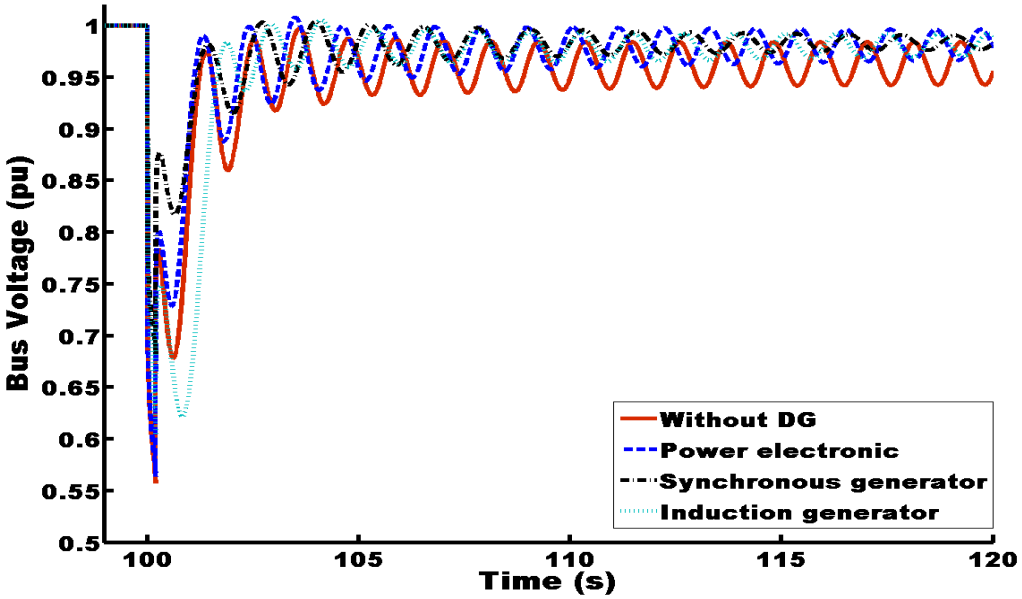

Figure 4.4. Voltage at bus 13 during the fault with different DG technologies

A critical contingency is chosen to clearly demonstrate the effect of adding DG to the system. A three-phase fault occurs at "Line 03-04" and is cleared by tripping the line after 3 cycles. All the voltages at the load buses are monitored during different scenarios where each scenario consists of connecting aggregated DG at a certain load bus. Table 4.8 shows the contribution of power electronic based DGs connected at all load buses using the direct method (by connecting all DGs simultaneously) and the

approximated method (adding all the individual $SVSI_{diff}$). The relative errors are slightly higher than the one found for the IEEE RTS-96 24 bus system but are still considered as acceptable (largest error is almost 6 %). The concept of linearity is then applicable for the IEEE 39-bus New England system with power electronic interfaced DGs.

Table 4.7. Contingency ranking based on the $SVSI_{base}$ for the IEEE 39-bus New England system

Ranking	Contingency	$SVSI_{base}$ (V-MVA)
1	Line 28-29	2007.513
2	Line 01-02, Line 01-39	2161.995
3	Line 09-39	2181.515
4	Line 07-08	2736.721
5	Line 23-24	2763.109
6	Line 08-09	2813.572
7	Line 26-27	2829.471
8	Line 22-23	2850.208
9	Line 10-11, Line 10-13	2864.323
10	Line 13-14	2867.750
11	Line 26-28	2933.162
12	Line 26-29	2939.233
13	Line 21-22	3024.800
14	Line 06-07, Line 06-11	3054.046
15	Line 05-06, Line 05-08	3062.214
16	Line 14-15	3149.779
17	Line 25-26	3231.186
18	Line 04-05, Line 04-14	3266.679
19	Line 15-16	3313.922
20	Line 02-03, Line 02-25	3541.017
21	Line 03-04, Line 03-18	3553.819
22	Line 17-18, Line 17-27	3671.384
23	Line 16-17, Line 16-21, Line 16-24	3919.653
24	Line 16-19	4093.021

Connecting synchronous machine based DGs increases the non-linearity effect of the system which complicates the prediction of the contributions of these DGs. Table 4.9 shows the difference between the contributions found using the direct method and the approximated method. This difference is reduced when there is a high penetration level of aggregated DG (relative errors of 2.2 % and 4.5 % for a penetration level of 15 % and

Table 4.8. Comparison between $SVSI_{tot}$ and the sum of all $SVSI_{diff}$ of power electronic interfaced DG for the IEEE 39-bus New England system

Penetration level	**5 %**	**10 %**	**15 %**	**20 %**
$\mathbf{P_{DG}}$ **(MW)**	302.06	604.11	906.17	1208.23
$\boldsymbol{SVSI_{tot}}$ **(V-MVA)**	152.85	302.26	457.06	619.29
$\sum_{j=1}^{N} SVSI_{diff\ j}$ **(V-MVA)**	160.29	321.91	476.33	607.05

20 % respectively).Comparing with Table 4.8, the total contributions $SVSI_{tot}$ of synchronous machine based DGs are slightly higher than to the contributions of power electronic interfaced DGs. In fact, at high penetration levels, the total contributions of both technologies are approximately equivalent. The total contribution of 10 % and 15 % DG penetration levels, in Table 4.9 is surprisingly smaller than the total contribution at a 5 % penetration level. This can be due to the impact of increasing DGs at certain load buses that reduce the short-term voltage stability.

Table 4.9. Comparison between $SVSI_{tot}$ and the sum of all $SVSI_{diff}$ of synchronous machine based DG for the IEEE 39-bus New England system

Penetration level	**5 %**	**10 %**	**15 %**	**20 %**
$\mathbf{P_{DG}}$ **(MW)**	302.06	604.11	906.17	1208.23
$\boldsymbol{SVSI_{tot}}$ **(V-MVA)**	544.31	418.17	510.32	632.42
$\sum_{j=1}^{N} SVSI_{diff\ j}$ **(V-MVA)**	334.96	360.49	499.08	660.98

With induction machine based DG, the total contributions $SVSI_{tot}$ of induction machine based DGs of 15 % and 20 % DG penetration levels are inferior to the contributions at 5 % and 10 %. A high penetration of induction generator based DGs at some load buses have a negative impact on the short-term voltage stability due to the lack of sufficient reactive support. This can be seen when the total contribution, using the approximated method, is negative at a 20 % penetration level. Having several induction generators at some buses can reduce the stability or even cause instability of the system. At low levels, the difference between the contributions using both methods is relatively small.

Table 4.10. Comparison between $SVSI_{tot}$ and the sum of all $SVSI_{diff}$ of induction machine based DG for the IEEE 39-bus New England system

Penetration level	**5 %**	**10 %**	**15 %**	**20 %**
$\mathbf{P_{DG}}$ **(MW)**	302.06	604.11	906.17	1208.23
$\boldsymbol{SVSI_{tot}}$ **(V-MVA)**	366.40	537.22	232.58	155.08
$\sum_{j=1}^{N} SVSI_{diff\ j}$ **(V-MVA)**	329.53	508.70	354.12	-809.72

4.3.3 The IEEE 118-Bus Test System

As mentioned previously, the IEEE 118-bus system has 19 synchronous generators, 35 synchronous condensers and 99 loads (as well as 99 DGs). This large system is highly non-linear due to the presence of several machines and static compensators. Due to the large number of contingencies, only the first and the last ten are represented in Table 4.11. Buses 59 and 69 are considered the most critical due to the ranking of the contingencies associated with these buses.

Table 4.11. Contingency ranking based on the $SVSI_{base}$ for the IEEE 118-bus system

Ranking	**Contingency**	$\boldsymbol{SVSI_{base}}$ **(V-MVA)**
1	Line 028-029	314.060
2	Line 014-015	333.732
3	Line 114-115	340.051
4	Line 035-037	341.950
5	Line 035-036	345.169
6	Line 071-072	346.345
7	Line 044-045	350.135
8	Line 021-022	350.480
9	Line 039-040	359.013
10	Line 009-010	365.842
157	Line 069-077	1127.449
158	Line 069-075	1127.910
159	Line 069-070	1128.089
160	Line 059-060	1142.775
161	Line 059-061	1144.011
162	Line 049-066	1154.905
163	Line 049-051	1193.525
164	Line 049-069	1194.994
165	Line 049-050	1312.653
166	Line 049-054	1313.551

The two methods (direct method and approximated method) to obtain the total contribution of DG are tested on the IEEE-118 bus case. Following several simulations, only one case was found with a small relative error between the two methods at low penetration level of power electronic interfaced DG. The relative error of contingency "Line 016-017" is almost equal to 3 % with a DG penetration level of 5 %. For higher penetration levels, the error increases until reaching 831 % (Table 4.12). The large difference of the total contributions found using the direct and the approximated methods is due to the impact of connecting several DGs simultaneously. When aggregated DG is connected at several load buses and with the presence of many compensators, the impact of these DGs is reduced. It is then thought that a small relative error for the low penetration level for this case is obtained as a coincidence. Therefore, the concept of linearity is not applicable in this case due to the large number of non-linear equations. This method can only be applied to small and medium systems where the number of generators is limited. Using the direct method, the total contribution of power electronic interfaced DG at a 20 % penetration level is inferior to the total contribution at 15 %. This is due to the fast increase of DGs that negatively affect the short-term voltage stability. Using the approximated method, it can be seen that the total contribution is augmented with the increase in penetration level. The rate of increase is declining due to the high presence of DGs that have a negative impact on the stability of the system. The sizing of the DGs plays an important role in the short-term voltage stability.

Table 4.12. Comparison between $SVSI_{tot}$ and the sum of all $SVSI_{diff}$ of power electronic interfaced DG for the IEEE 118-bus system

Penetration level	**5 %**	**10 %**	**15 %**	**20 %**
$\mathbf{P_{DG}}$ **(MW)**	212.10	424.20	636.30	848.40
$\boldsymbol{SVSI_{tot}}$ **(V-MVA)**	82.74	89.99	127.16	121.34
$\sum_{j=1}^{N} SVSI_{diff\ j}$ **(V-MVA)**	80.18	596.75	938.09	1130.54

By adding synchronous machine based DGs, the non-linearity effect in the system is increased and the difference between the direct and the approximated methods becomes more significant (Table 4.13). The total contribution, using the exact method, is almost constant except at a DG penetration level of 15 % where it reaches its minimum. Similar

observations can be made as the power electronic interface DG for the approximated method; the contribution is increasing with a decline in the rate of increase, which indicates that the sizing of DG has an impact on the short-term voltage stability.

The total contribution of induction machine based DGs, found using the exact method, is superior to the contribution of power electronic interfaced DG with one exception at a DG penetration level of 10 %. At this penetration level, the total contribution reaches its lowest. Using the approximated method, the contribution of DG augments with increasing of penetration levels.

Table 4.13. Comparison between $SVSI_{tot}$ and the sum of all $SVSI_{diff}$ of synchronous machine based DG for the IEEE 118-bus system

Penetration level	**5 %**	**10 %**	**15 %**	**20 %**
$\mathbf{P_{DG}}$ **(MW)**	212.10	424.20	636.30	848.40
$\boldsymbol{SVSI_{tot}}$ **(V-MVA)**	293.12	310.15	262.63	321.67
$\sum_{j=1}^{N} SVSI_{diff\ j}$ **(V-MVA)**	1476.31	1877.07	2167.22	2386.89

Table 4.14. Comparison between $SVSI_{tot}$ and the sum of all $SVSI_{diff}$ of induction machine based DG for the IEEE 118-bus system

Penetration level	**5 %**	**10 %**	**15 %**	**20 %**
$\mathbf{P_{DG}}$ **(MW)**	212.10	424.20	636.30	848.40
$\boldsymbol{SVSI_{tot}}$ **(V-MVA)**	140.41	70.85	173.28	186.95
$\sum_{j=1}^{N} SVSI_{diff\ j}$ **(V-MVA)**	390.40	947.45	1328.45	1501.08

4.4 Conclusion

The short-term voltage stability is not well-known and few studies have been made. Avoiding large voltage dips is requested in order not to trip power system equipment. In most cases, DG, depending on its technology, helps reduce voltage dips and therefore, system operators can consider DG as a mean to increase the stability of the system.

Using a short-term voltage stability index, contingencies can be ranked according to the severity of the voltage dips at the load buses. The index is modified to illustrate the effect of adding DG to the system. The contribution of power electronic interfaced DG connected at all load buses can be predicted by adding the individual contributions for

small and medium systems only. For large systems with numerous machines, such as the IEEE 118 bus system, this approximation is not applicable.

The approximated method for machine based DG provides erroneous results as the gap between the total contributions given by both methods is immense. The large difference between the total contributions using both methods is due to the decrease of the effect of adding a machine based DG in the vicinity of another DG due to the interaction between these machines. Nevertheless, the approximated method offers an idea of how the contributions of DG when connected at a single load bus affect the stability of the system. The total contribution, found using the direct method, does not necessarily improve with increasing DG penetration levels. Therefore, both the location and the sizing of the DG affect the short-term voltage stability.

Chapter 5: Impact of Large Penetration of DG on Transient Stability

5.1 Introduction

Since the 1965 Northeast blackout, no major blackouts were associated with transient instability that occurs due to a slow-clearance of transmission faults. Nowadays, transmission system protection acts fast enough to maintain all generators in synchronism. Nevertheless, a failure in the protection system can occur, and when a synchronous generator is out of synchronism, it is disconnected automatically to prevent any damage to the machine. Following the 1965 event, most power system operators concentrated on improving the transient stability to avoid a system collapse [1,15, 97]. In [15], the factors affecting the transient stability of the synchronous generators consist of:

- The output power of the generator in terms of its nominal capacity
- The fault location and type and the reaction of the generator to that fault
- The duration of the fault
- The characteristics of the transmission system (post-fault reactance)
- The generator characteristics (mainly the reactance, the inertia and the internal voltage magnitude)

5.2 Transient Stability for Large Systems

The equal-area criterion method is only useful for systems with a single synchronous generator connected to the infinity grid and for a two synchronous generator system. For a multi-generator system, the swing equations are solved using numerical integration methods such as the Euler method, Runge-Kutta methods and implicit integration methods. For large systems, a simulation tool is required in order to study the power system dynamic response [1,15]. Multiple time domain simulations are required to obtain an approximation of the CCT. If the clearing time is larger than the CCT, the machine accelerates until the protective relay acts and trips the generator.

In [37], two transient stability indices are defined to show the impact of different DG technologies and different penetrations (Figure 5.1). The maximum rotor speed deviation

is used to determine the severity of the fault. The second index consists of the oscillation duration. In other words, the time difference between the initial fault time and the time when the rotor speed deviation is within a defined bandwidth.

The index to determine the transient stability of the system is defined as the sum of the maximum rotor speed deviations of centralized synchronous generators ($MRSD_{base}$). $MRSD_{base}$ is defined in p.u. as the ratio between the maximum deviation and the synchronous speed of the machine. A fault with a higher $MRSD_{base}$ index indicates a more severe contingency. The impact of connecting aggregated DG at a load bus j is measured by the difference between the maximum rotor speed deviations with and without DG:

$$MRSD_{diff\ j} = \sum_{i=1}^{Ng} MRSD_{base\,i} - MSRD_{DG\,i} \tag{5.1}$$

Where N_g represents the number of centralized central generator, $MRSD_{basei}$ and $MSRD_{DGi}$ represent the maximum rotor speed deviation of the synchronous generator i without any DG and with DG connected at load bus j respectively. It should be noted that a positive index indicates that the transient stability is improved. $MRSD_{tot}$ represents the contribution of DG, connected at all load buses, on the maximum rotor speed deviation and the oscillation duration respectively.

5.3 Transient Stability Simulation

The test cases, presented in Section 2.4.1, are used to analyze the impact of a large penetration of DG on the transient stability of the system. Similar to the previous chapter, the contingency consists of a three-phase fault at a branch of the system that is cleared by tripping the line. The loads are modeled as constant current for the transient stability.

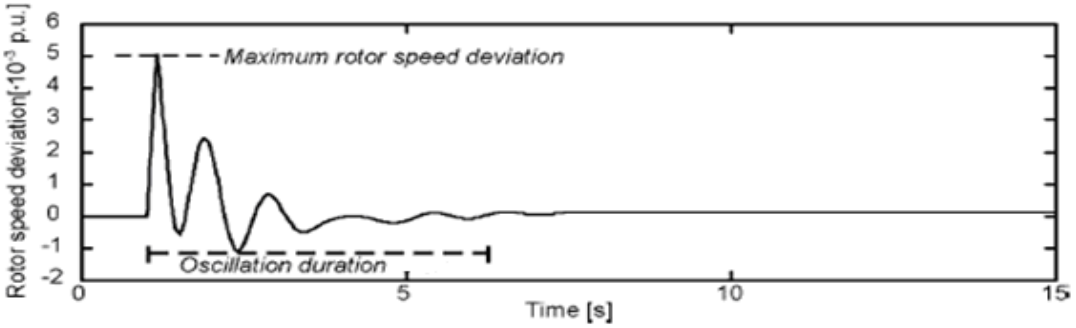

Figure 5.1. Transient stability indices using synchronous generators rotor speed deviation [37]

5.3.1 The IEEE Reliability Test System 1996

The transient stability of the small power system (the IEEE RTS-96 24 bus system) is studied using the indices defined in the previous section. The $MRSD_{base}$ index indicates how the synchronous generators react during the fault. A contingency that causes a high $MRSD_{base}$ index is considered as critical.

A three-phase fault is applied on each branch and is cleared after 3 cycles. Table 4.1 shows the contingency ranking according to the $MRSD_{base}$ index. In this case, contingency "Line 21-22" is considered as the most critical due to its highest $MRSD_{base}$ index. Slow clearance of such contingency can lead to a collapse of the system. The index of the worst contingency is almost 100 times the value of the first contingency ("Line 04-09"). A gradual increase is observed with each contingency until the last two where the values of the indices increase rapidly. The system operator should find ways to improve those last two contingencies as they could cause major damage to the system.

Similar to Section 4.3.2, the contingency "Line 14-16" is selected with a fault clearing time of 12 cycles. The contribution of power electronic based DG on each load bus with different penetration levels is shown in Figure 5.2. Except for a few load buses, the contribution of power electronic interfaced DG has a positive impact on the rotor speed deviation. Increasing the penetration levels leads to an increase in the effect DG has on the transient stability. When the index is positive, the transient stability is improved when the size of DG is increased. Whereas, when the index is negative, the transient stability is worsened. The stability of the system deteriorates only when power electronic based DG is located near large centralized generators. Depending on the location of DG, operating with any power factor can either improve or worsens the DG contribution.

As previously stated, power electronic interfaced DG can either supply or absorb reactive power. Figure 5.3 shows the impact of operating DG at different power factors. Depending on the location of DG, the contribution of DG can either be improved or worsened when operating at a lagging power factor. Similar remarks can be made with DG operating at a leading power factor. When DG is connected at all load buses, the transient stability is improved when operating at a lagging power factor and worsened at a leading power factor.

The contribution of power electronic interfaced DG when connected at all load buses simultaneously is depicted in Figure 5.4. It can be seen that the contribution increases linearly with the increase in penetration level. A linear approximation was added to show that given two indices from two different penetration levels, the contribution of power electronic interfaced DG can be predicted for this system.

Table 5.1. Contingency ranking based on the $MRSD_{base}$ for the IEEE RTS-96 24 bus system

Ranking	**Contingency**	$MRSD_{base}$ **(p.u.)**
1	Line 04-09	0.015137
2	Line 05-10	0.017060
3	Line 08-10	0.019155
4	Line 08-09	0.020143
5	Line 03-09	0.024186
6	Line 02-06	0.033855
7	Line 02-04	0.034745
8	Line 01-03	0.034811
9	Line 01-05	0.035235
10	Line 01-02	0.037210
11	Line 12-13	0.039848
12	Line 11-13	0.044810
13	Line 11-14	0.050368
14	Line 12-23	0.051534
15	Line 20-23	0.056075
16	Line 13-23	0.056474
17	Line 17-18	0.079795
18	Line 19-20	0.086059
19	Line 15-16	0.087339
20	Line 06-10	0.092838
21	Line 18-21	0.092964
22	Line 17-22	0.103463
23	Line 14-16	0.120913
24	Line 16-17	0.145637
25	Line 15-24	0.147056
26	Line 15-21	0.203123
27	Line 16-19	0.662284
28	Line 21-22	1.144668

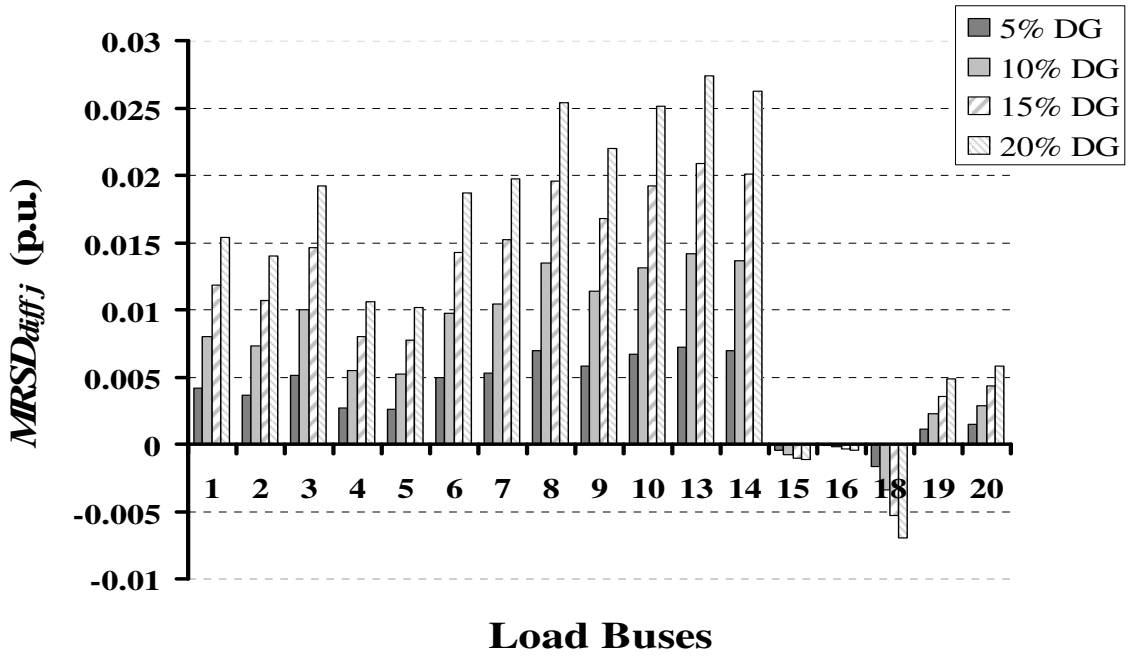

Figure 5.2. $MRSD_{diff}$ of power electronic interfaced DG at each load bus and with different penetration levels for the IEEE RTS-96 24 bus system

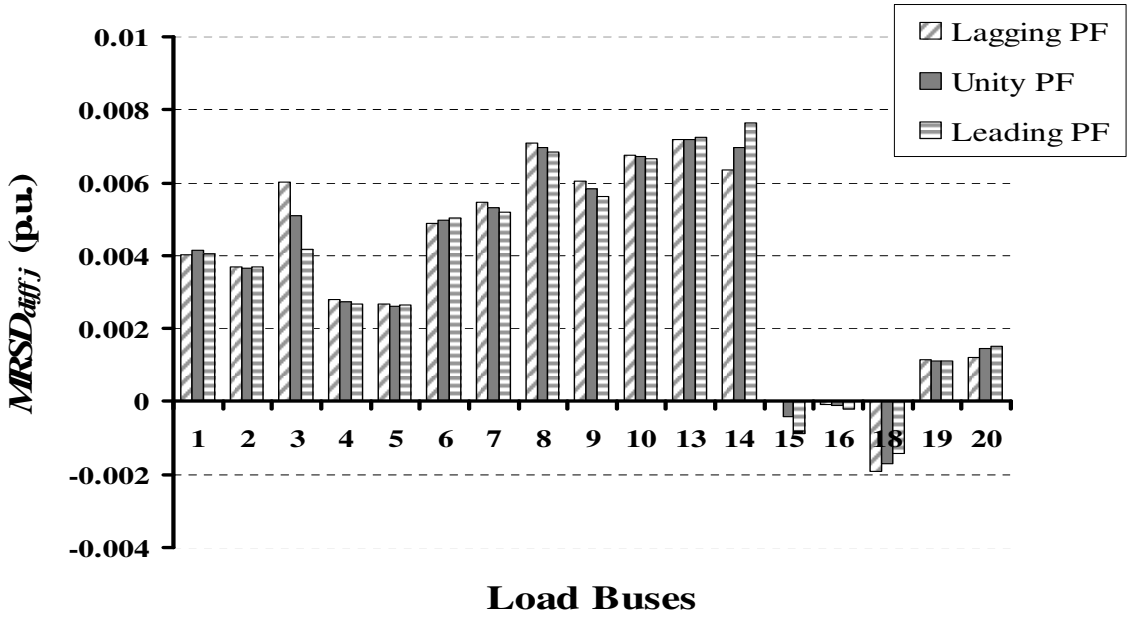

Figure 5.3. $MRSD_{diff}$ of power electronic interfaced DG at each load bus and with different power factors for the IEEE RTS-96 24 bus system

Table 5.2. $MRSD_{tot}$ of power electronic interfaced DG at different power factors for the IEEE RTS-96 24 bus system

Power factor	Unity	Lagging	Leading
$MRSD_{tot}$ **(p.u.)**	0.059632	0.060015	0.059264

The contributions of synchronous machine based DG are depicted in Figure 5.5 at different penetration levels. With synchronous generators located near large loads, the contributions of these DGs are mainly negative, which implies that they worsen the stability of the system. Near large centralized generators, the DG contributions improve the transient stability. When the DG penetration level is increased, the DG contributions are increased near large loads and decreased near centralized generators.

When aggregated synchronous generator based DG is connected at a single load bus, its contribution does not vary when the DG operates at different power factors. Therefore, only the total contribution of DGs (when aggregated DGs are connected at all load buses) is emphasized in Table 5.3. Although the differences between the contributions are minor, the transient stability is slightly improved when DGs operate at a lagging power factor and worsened when DGs operate at a leading power factor compared with unity power factor.

The total contribution of synchronous machine based DG is depicted in Figure 5.6 at different penetration levels. The contribution augments with increasing DG penetration levels. A second-order polynomial approximation is used to show that any contribution at a DG penetration level in the range of 5 % to 20 % can be predicted using that curve.

The contribution of induction machine based DG at each load bus is very similar to the one with synchronous machine based DG (Figure 5.7). The main difference is that the

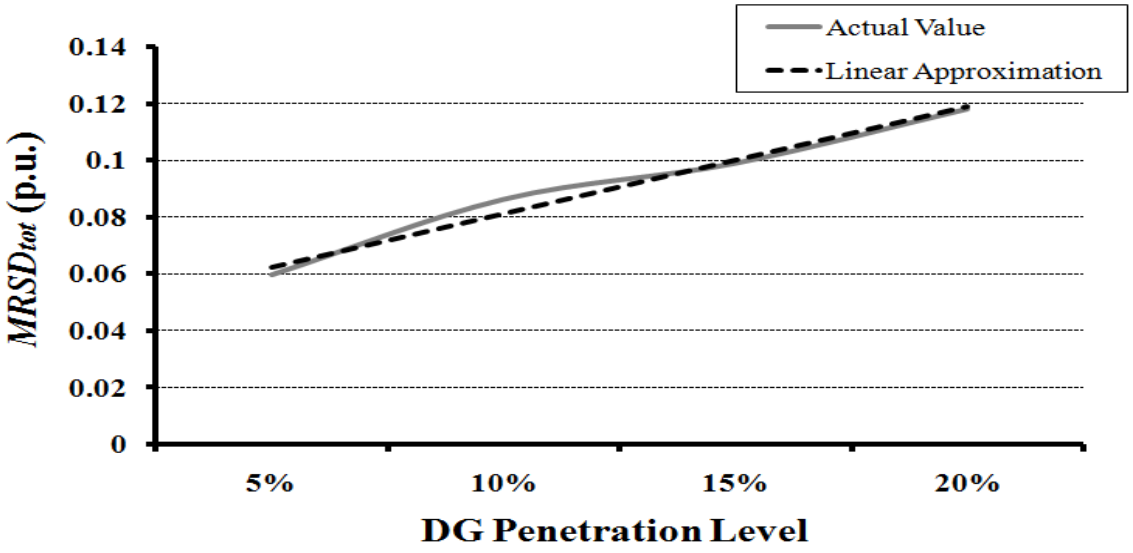

Figure 5.4. $MRSD_{tot}$ of power electronic interfaced DG at different penetration levels for the IEEE RTS-96 24 bus system

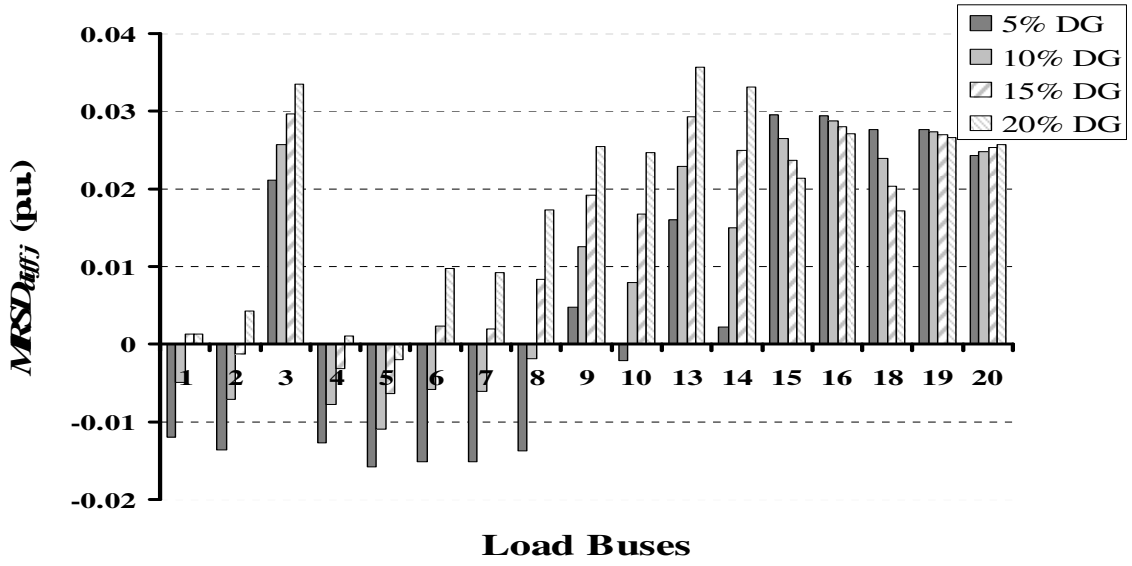

Figure 5.5. $MRSD_{diff}$ of synchronous machine based DG at each load bus and with different penetration levels for the IEEE RTS-96 24 bus system

Table 5.3. $MRSD_{tot}$ of synchronous machine based DG at different power factors for the IEEE RTS-96 24 bus system

Power factor	Unity	Lagging	Leading
***MRSD*$_{tot}$ (p.u.)**	0.149506	0.149597	0.149393

contribution of induction generators is less significant. At low penetration levels, the $MRSD_{diff}$ indices are negative in most cases, except for those near large centralized generators (buses 15 to 20). These indices become positive at higher levels and therefore the transient stability is improved.

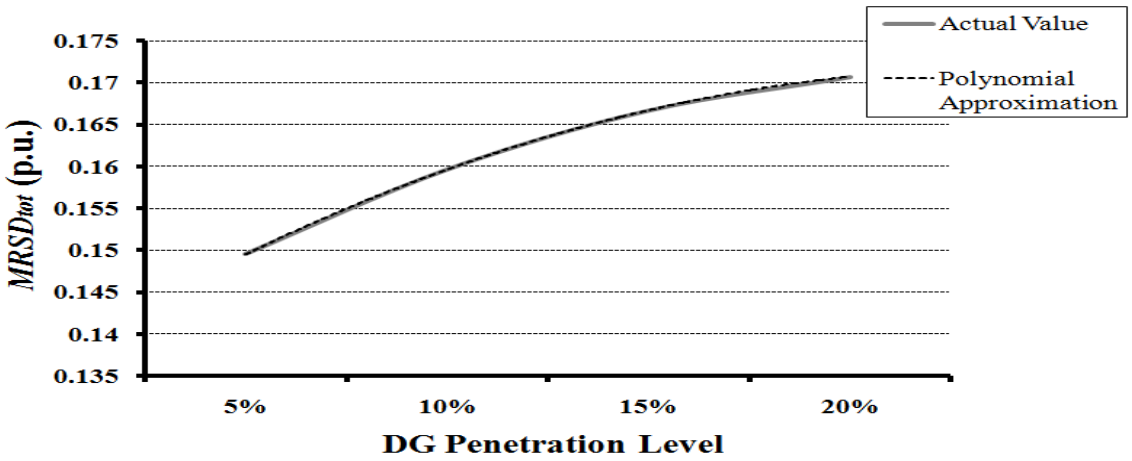

Figure 5.6. $MRSD_{tot}$ of synchronous machine based DG at different penetration levels for the IEEE RTS-96 24 bus system

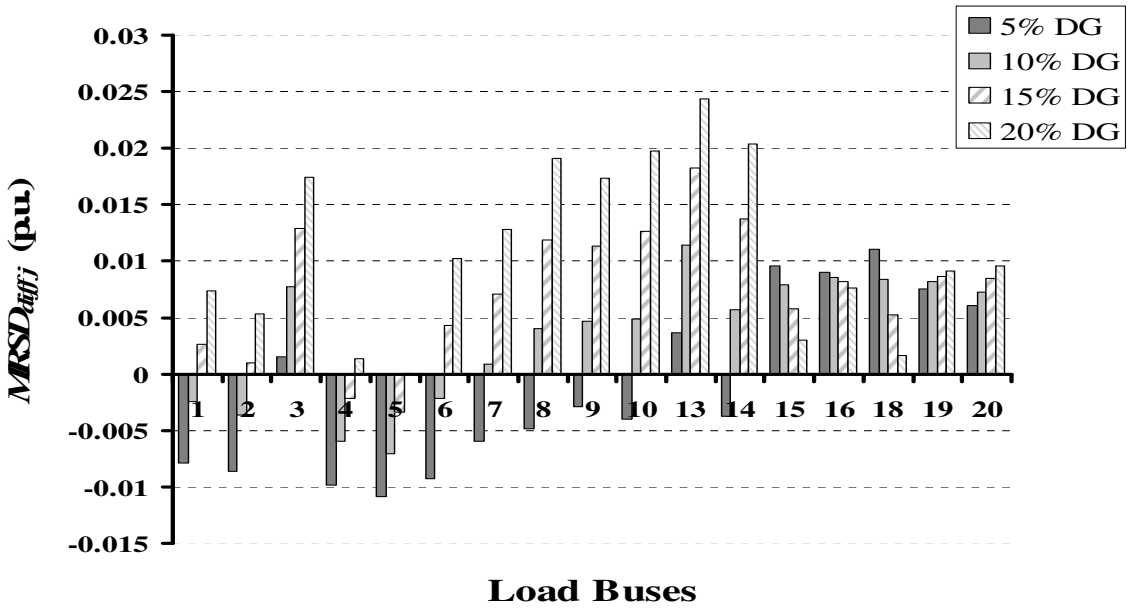

Figure 5.7. $MRSD_{diff}$ of induction machine based DG at each load bus and with different penetration levels for the IEEE RTS-96 24 bus system

The total contribution of induction machine based DG is depicted in Figure 5.8 at different penetration levels. The contribution is improved with the increase of DG penetration levels and can be predicted using a second-order polynomial approximation. The total contributions are significantly inferior to those of synchronous machine based DG and slightly inferior to the contributions of power electronic interfaced DG.

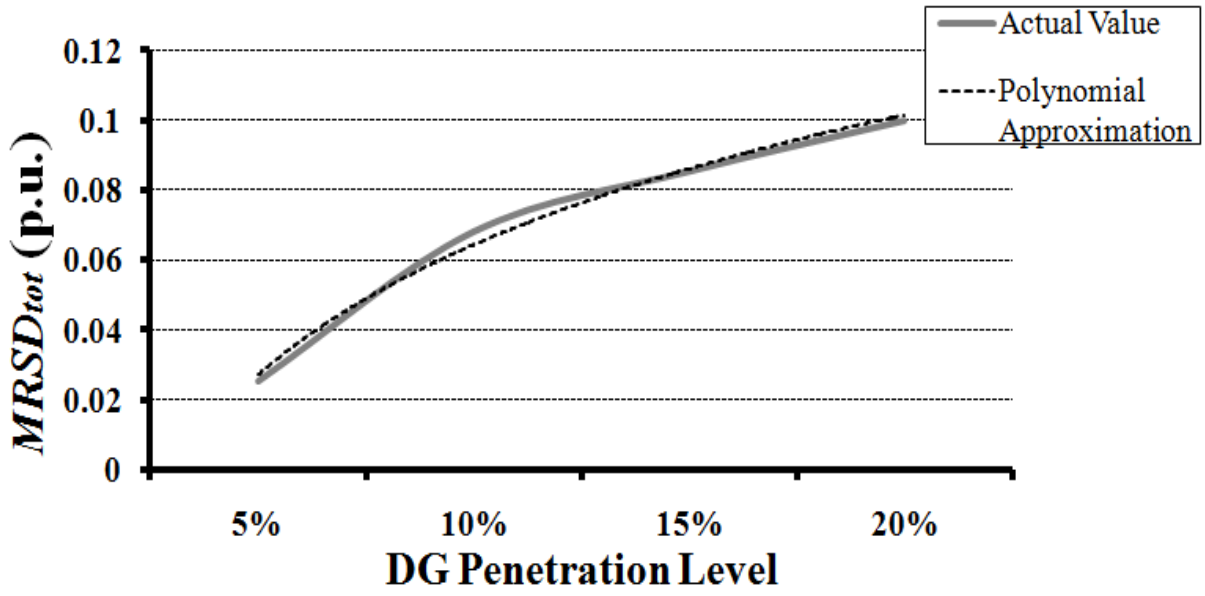

Figure 5.8. . $MRSD_{tot}$ of induction machine based DG at different penetration levels for the IEEE RTS-96 24 bus system

5.3.2 The IEEE 39-Bus New England Test System

The indices defined in Section 5.2 are tested on the "medium-size" system (the IEEE 39-bus New England system). Table 5.4 shows the contingency ranking based on the $MRSD_{base}$ index to determine the critical contingencies. A three-phase fault is applied on each branch and is then cleared by tripping that branch after 3 cycles. Apart from the last four contingencies, the indices range between 0.13 p.u. and 0.39 p.u. A jump in the values of the indices is observed, which indicates that the last four contingencies are considered as severe and "Line 16-17" is the most critical.

The contingency "Line 03-04" is chosen with a clearing time of 3 cycles. The individual contributions of power electronic interfaced DG, shown in Figure 5.9, indicates that the optimized location is at bus 39. The index at that bus is much higher than indices at other buses. The DG is located near a centralized synchronous generator that is placed in an area with large loads. The lowest indices occur when DGs are located in the region where large generators are located (buses 12, 23 and 31). Unlike the contributions in the previous system, some contributions are worsened when the size of DG is increased.

Nevertheless, the total contribution of power electronic interfaced DG increases linearly with an increase in the penetration level (Figure 5.10). Contributions of power electronic interfaced DG at other penetration levels can be predicted using the curve in Figure 5.10.

The individual contribution of synchronous machine based DG is depicted in Figure 5.11. The highest index is found at bus 26 at a 10 % penetration level. Other high indices are associated with DGs located in the Northern area of the system and at a 5 % penetration level. The other indices are significantly small (less than 0.001 p.u.) and therefore their impact is minimal. The individual contributions of power electronic interfaced DG can decrease with the increase in DG penetration level.

The total contribution of synchronous machine based DG is shown in Figure 5.12. The contribution decreases gradually with an increase in the DG penetration level. The curve can be estimated using a second-order polynomial approximation. At 20 % penetration level, the curve seems to stabilize. The size of DG plays an important role when the contribution reaches its maximum at low penetration levels.

Figure 5.13 shows the individual contribution of induction machine based DG for the IEEE 39-bus New England system. At bus 39, the index reaches its maximum value at a 5 % penetration level and its minimum value at a 10 % penetration level. At 15 %, the contribution becomes positive again before returning to negative at 20 %.

Table 5.4. Contingency ranking based on the $MRSD_{base}$ for the IEEE 39-bus New England system

Ranking	Contingency	$MRSD_{base}$ (p.u.)
1	Line 28-29	0.125172
2	Line 01-39	0.132257
3	Line 01-02	0.134861
4	Line 09-39	0.13788
5	Line 07-08	0.204837
6	Line 26-28	0.209736
7	Line 26-29	0.210286
8	Line 26-27	0.212044
9	Line 08-09	0.213003
10	Line 13-14	0.235733
11	Line 10-13	0.244678
12	Line 05-06	0.247046
13	Line 04-14	0.247868
14	Line 04-05	0.248104
15	Line 10-11	0.248525
16	Line 05-08	0.249637
17	Line 14-15	0.253871
18	Line 06-07	0.259313
19	Line 06-11	0.261009
20	Line 03-18	0.263767
21	Line 03-04	0.265244
22	Line 15-16	0.271833
23	Line 25-26	0.277710
24	Line 17-18	0.287413
25	Line 02-25	0.287570
26	Line 02-03	0.292258
27	Line 17-27	0.298192
28	Line 22-23	0.315878
29	Line 16-24	0.376279
30	Line 16-21	0.391012
31	Line 16-19	1.857310
32	Line 21-22	4.823656
33	Line 23-24	6.060924
34	Line 16-17	8.424061

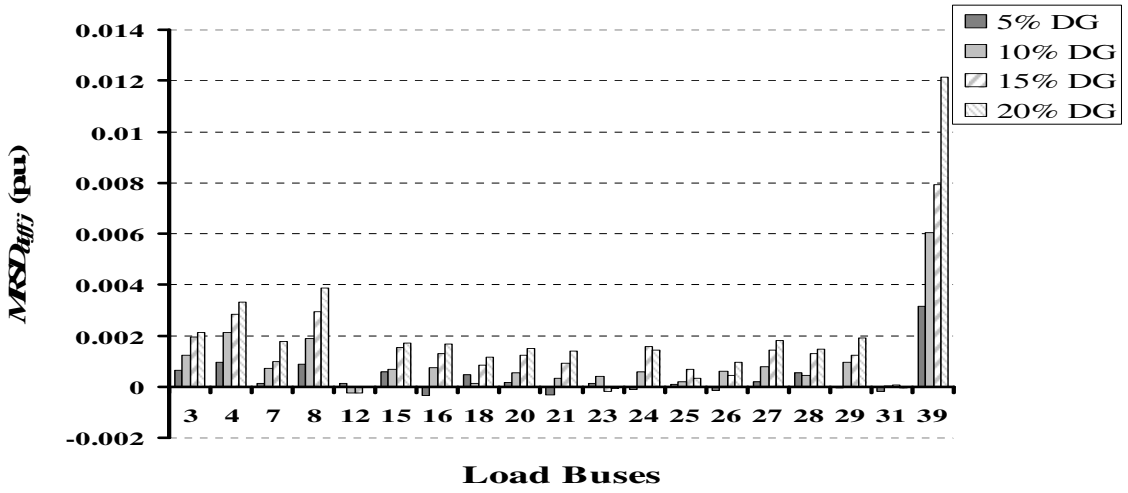

Figure 5.9. $MRSD_{diff}$ of power electronic interfaced DG at each load bus and with different penetration levels for the IEEE 39-bus New England system

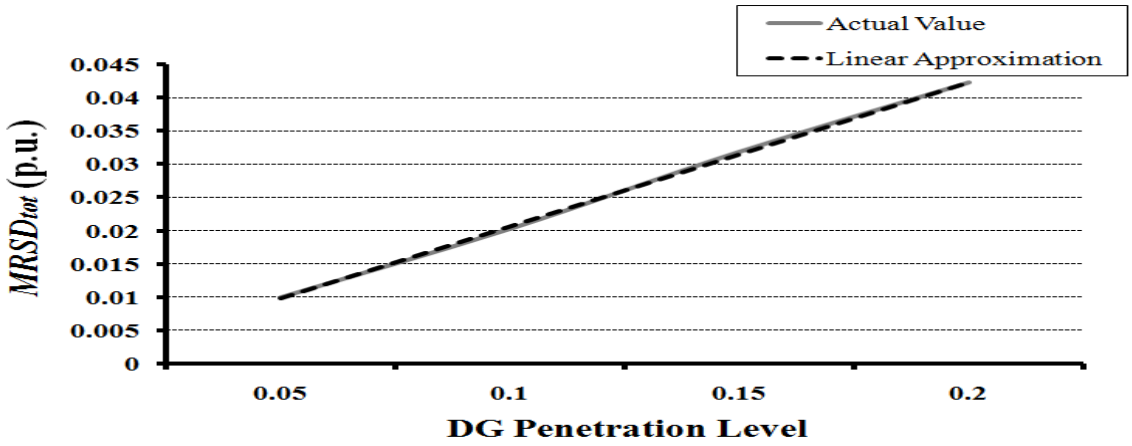

Figure 5.10. $MRSD_{tot}$ of power electronic interfaced DG at different penetration levels for the IEEE 39-bus New England system

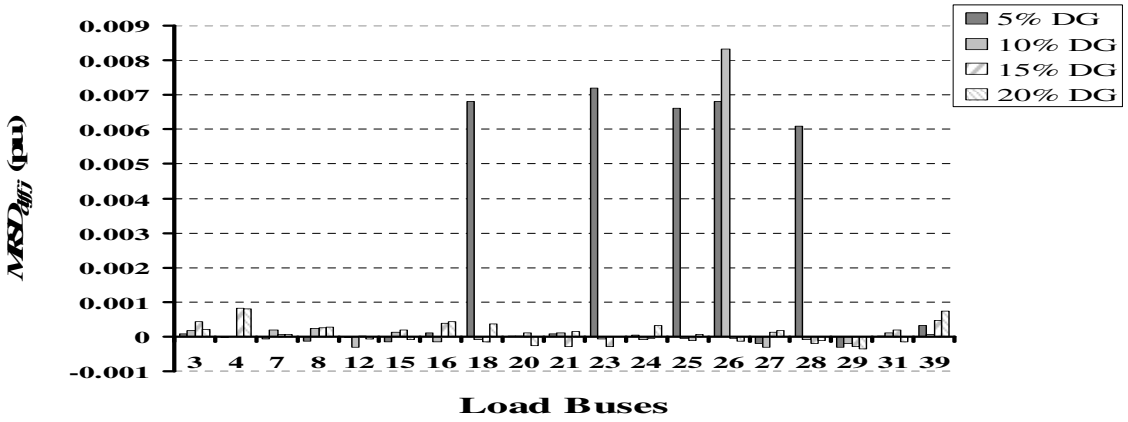

Figure 5.11. $MRSD_{diff}$ of synchronous machine based DG at each load bus and with different penetration levels for the IEEE 39-bus New England system

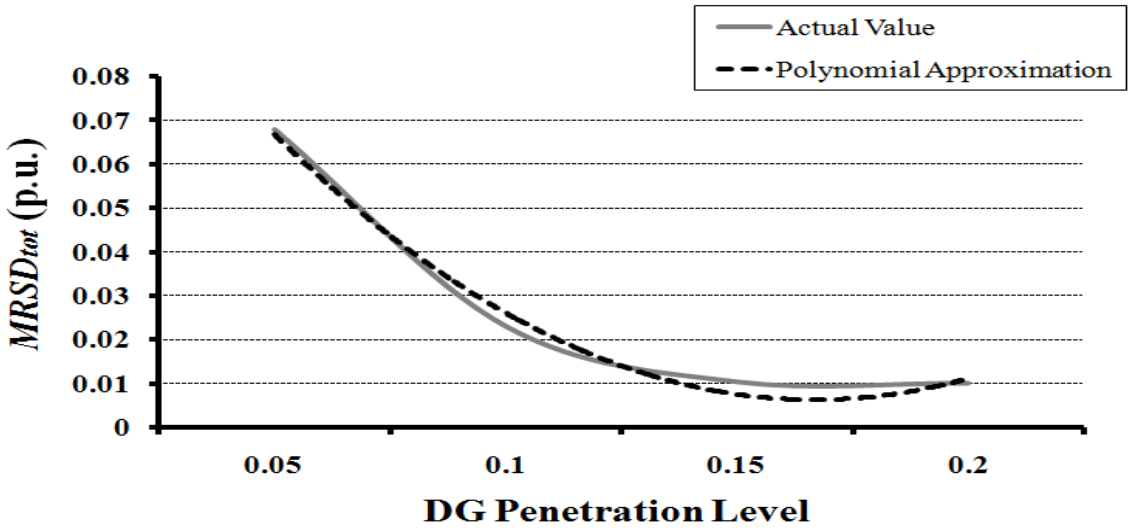

Figure 5.12. $MRSD_{tot}$ of synchronous machine based DG at different penetration levels for the IEEE 39-bus New England system

The other indices are mainly positive and increase with an increase in DG penetration level. The few indices where contributions negatively affect the transient stability are located near large centralized synchronous generators.

The total contributions of induction machine based DG are shown in Figure 5.14. Unlike the contributions of synchronous machine based DG, these contributions improve with increasing DG penetration levels. Therefore, large penetration levels of induction machine based DG help improve the transient stability of the system. A second-order polynomial approximation curve is drawn to show that the total contribution curve can be estimated.

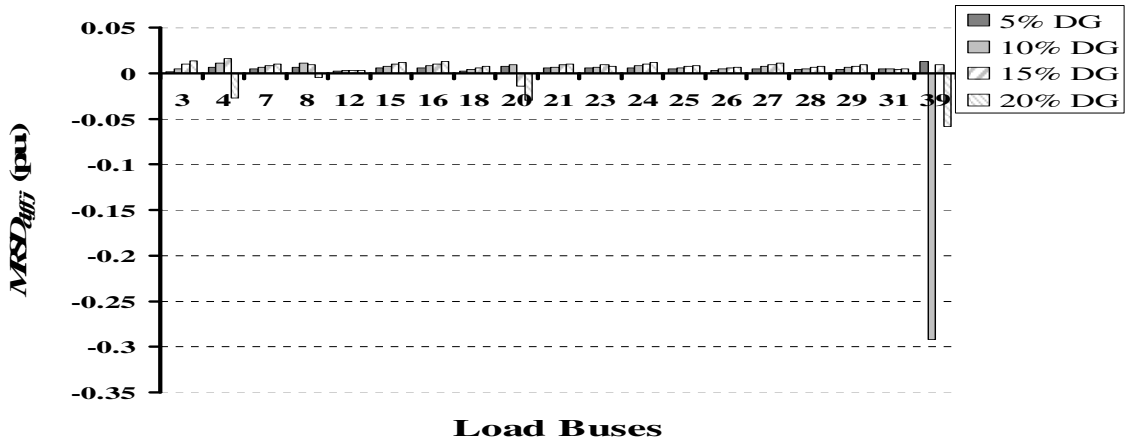

Figure 5.13. $MRSD_{diff}$ of induction machine based DG at each load bus and with different penetration levels for the IEEE 39-bus New England system

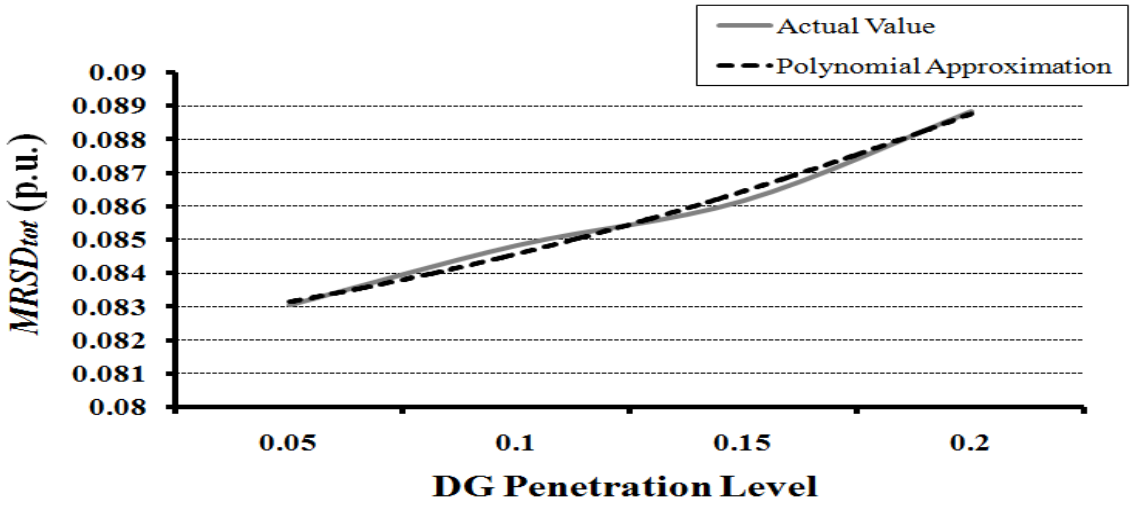

Figure 5.14. $MRSD_{tot}$ of induction machine based DG at different penetration levels for the IEEE 39-bus New England system

5.3.3 The IEEE 118-Bus Test System

The transient stability of the "large" system (the IEEE 118-bus system) is studied using the indices defined in Section 5.2. Table 4.11 illustrates the contingency ranking of the system. Due to the large number of contingencies, only the first and last 10 are shown in the table. The three-phase fault is cleared after 6 cycles by tripping the line. The difference between the indices of the 10^{th} and the 157^{th} contingencies are very little (approximately 0.04 p.u.). The indices of the last three contingencies are to a large extent higher than other indices. Therefore, these contingencies are considered as the most critical.

In Figure 5.15, 15 indices of power electronic interfaced DG are randomly chosen due to the large number of indices. The contributions are unpredictable, with the largest index present at bus 59 at a 10 % penetration level. At the same penetration level, the index is at its lowest at bus 29. In most cases, contributions of power electronic interfaced DG at low penetration levels improve the transient stability of the system. The sizing of DG should be optimized to help prevent transient instability during a three-phase fault.

The total contribution of power electronic interfaced DG is depicted in Figure 5.16. Unlike individual contributions, the highest value is at a 20 % DG penetration level. Even with the presence of large numbers of centralized synchronous generators, the total contribution increases linearly with increasing penetration levels.

Table 5.5. Contingency ranking based on the $MRSD_{base}$ for the IEEE 118-bus system

Ranking	Contingency	$MRSD_{base}$ (p.u.)
1	Line 005-006	0.155066
2	Line 004-011	0.155509
3	Line 015-033	0.158333
4	Line 017-113	0.158420
5	Line 015-017	0.158540
6	Line 004-005	0.158590
7	Line 016-017	0.159517
8	Line 012-016	0.159877
9	Line 014-015	0.160023
10	Line 001-003	0.160376
157	Line 056-057	0.199753
158	Line 071-073	0.200854
159	Line 056-058	0.201111
160	Line 059-061	0.203687
161	Line 086-087	0.208069
162	Line 062-066	0.215539
163	Line 110-111	0.234349
164	Line 009-010	0.399731
165	Line 008-009	0.401101
166	Line 026-030	0.641806

Figure 5.17 shows the individual contribution of the synchronous machine based DG at the same load buses chosen for power electronic interfaced DG. Similarly, high penetration levels do not lead to a higher contribution. Most indices are positive, showing that the synchronous machine based DG improve the transient stability of the system and can be optimized by finding the highest contribution at a certain penetration level.

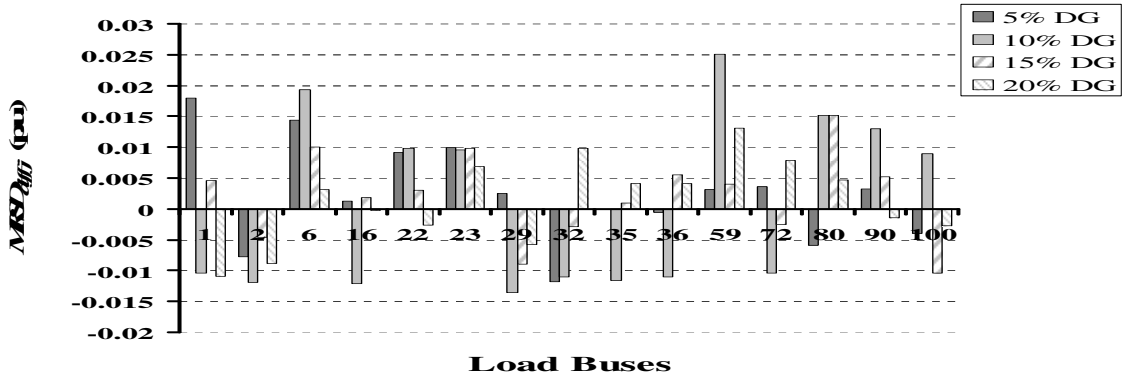

Figure 5.15. $MRSD_{diff}$ of power electronic interfaced DG at each load bus and with different penetration levels for the IEEE 118-bus system

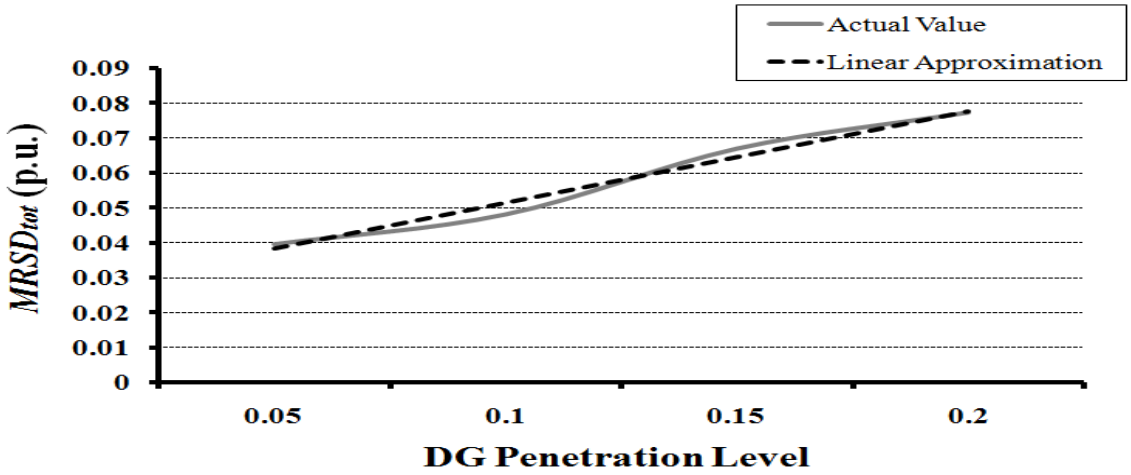

Figure 5.16. $MRSD_{tot}$ of power electronic interfaced DG at different penetration levels for the IEEE 118-bus system

The total contribution of synchronous machine based DG is shown in Figure 5.18. The contribution appears to reach its maximum at 10 % and 20 % DG penetration level. Unlike other systems, the presence of several centralized synchronous generators makes the total contributions of synchronous machine based DG unpredictable. A second-order polynomial approximation gives erroneous estimations and therefore, is not included.

The individual contribution of induction machine based DG is also unpredictable where the highest indices can be reached at different penetration levels (Figure 5.19). The total contribution, depicted in Figure 5.20, reaches its peak at 5 % and 15 %. Similar to the total contribution of synchronous machine based DG, this contribution cannot be estimated using a second-order approximation.

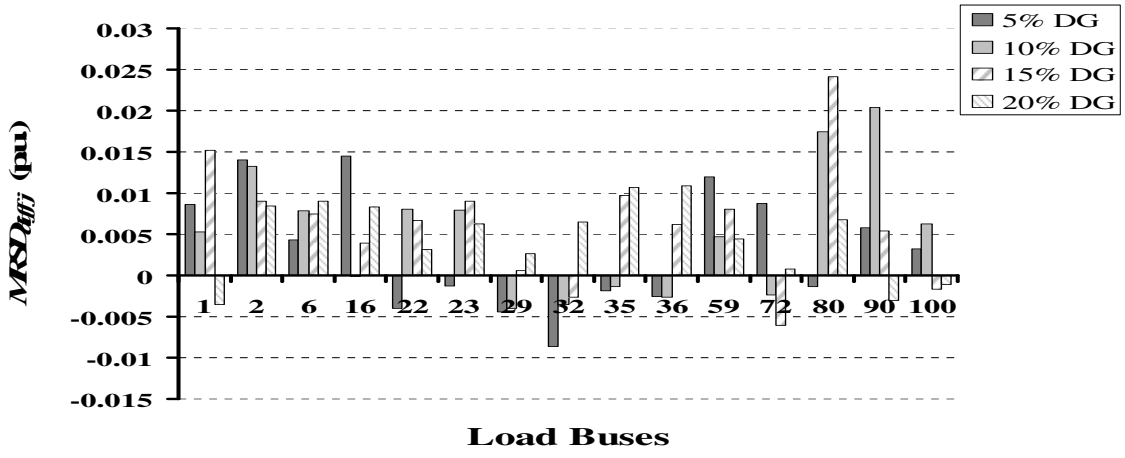

Figure 5.17. $MRSD_{diff}$ of synchronous machine based DG at each load bus and with different penetration levels for the IEEE 118-bus system

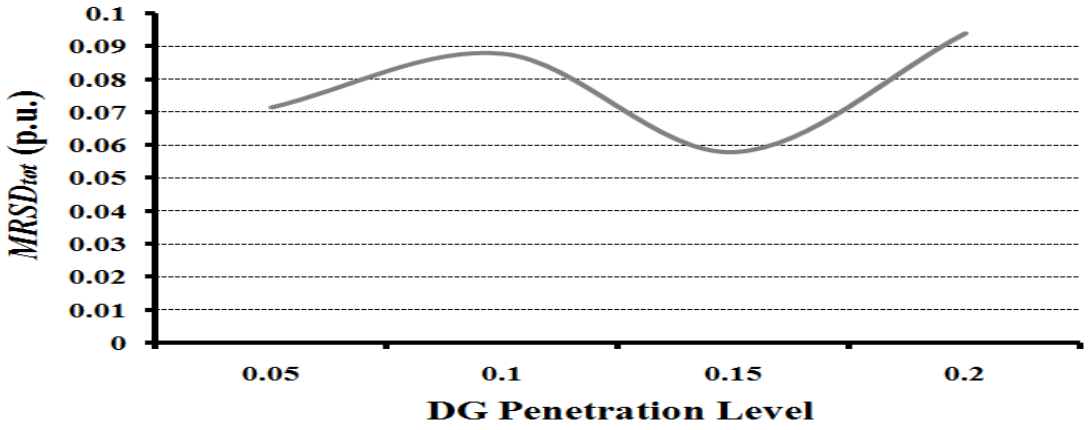

Figure 5.18. $MRSD_{tot}$ of synchronous machine based DG at different penetration levels for the IEEE 118-bus system

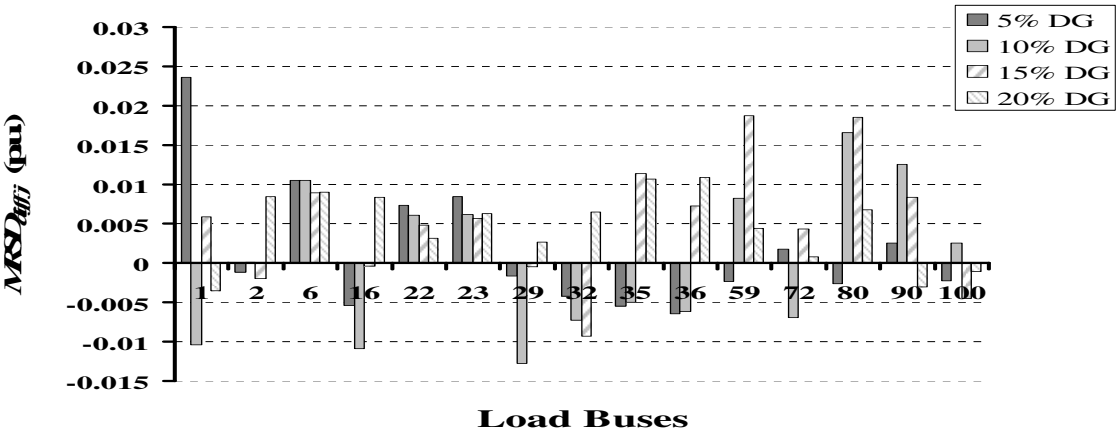

Figure 5.19. $MRSD_{tot}$ of induction machine based DG at different penetration levels for the IEEE 118-bus system

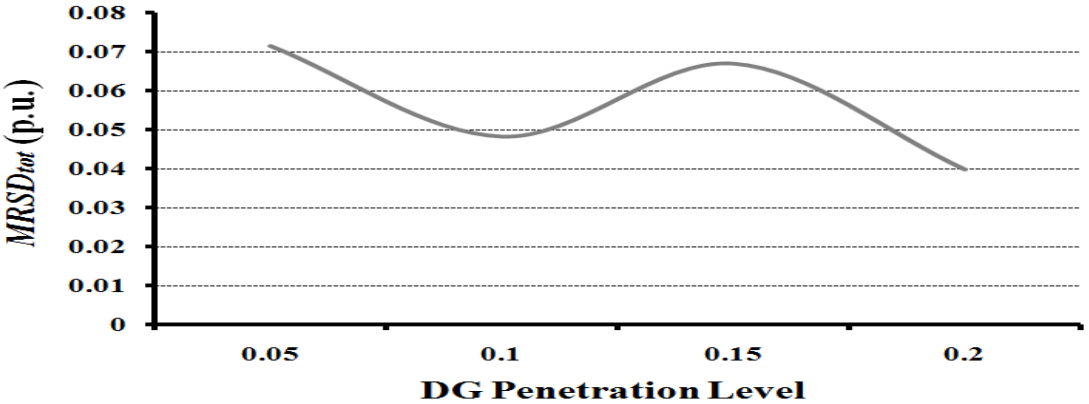

Figure 5.20. $MRSD_{tot}$ of induction machine based DG at different penetration levels for the IEEE 118-bus system

5.4 Conclusion

A fast method to assess the transient stability of the system is derived based on monitoring the rotor speed deviation of centralized synchronous generators following a large disturbance. An index consisting of obtaining the maximum rotor speed deviation of all synchronous generators is used to classify the contingencies which consist of applying a three-phase fault on each branch of the system (except transformers and tripping of branches that cause islanding). The fault is then cleared by tripping the faulted branch. The critical contingencies have the highest $MRSD_{base}$ indices.

The changes of these indices, given the presence/absence and the penetration levels of DGs, are observed in order to monitor the contribution of DGs to the transient stability of the power system. The contribution of power electronic interfaced DG improves the transient stability and augments with an increase in DG penetration levels when located at an area with large loads. Near large generators, the individual contribution can worsen the stability and can further decrease with a larger size of DG. When DG operates at different power factors, the difference between the contributions is minimal. Therefore, for the benchmarks under study, operating at different power factors has no significant impact on the rotor speed deviations. The total contribution of power electronic interfaced DG increases linearly with the size of DG and can therefore be predicted at any penetration level.

The contribution of machine based DG depends on the location and the size of DG. Near large centralized generators, the impact of DG improves the stability of the system whereas near large loads, it increases the total rotor deviations. In a large system, such as the IEEE 118-bus system, the contribution cannot be predicted due to the large number of centralized synchronous generators. The total contribution of machine based DG can be predicted for small and medium systems using a second-order polynomial approximation. The location, the size and the technology of DG affect to a great extent the transient stability of the system.

Chapter 6: Conclusions and Future Work

6.1 Summary

This thesis focuses on the impact of DG on the stability of the power system. With a large penetration, the integration of DG has major effects on the long-term and short-term voltage stability, as well as on the transient stability. In this work, the DG is not allowed to disconnect to either the voltage or frequency fluctuations. Indices are defined for each type of stability in order to study the contribution of DG.

For long-term studies, PV curves are generated and are used to define the voltage security margin (distance to voltage collapse). DGs are then added at load buses and their contributions are monitored using defined indices. All DG technologies are modeled as constant power operating at different power factors.

Time-domain simulations are performed to analyze the impact of DG on the short-term stability. DGs are modeled in detail based on their technology. The voltage stability index is derived by monitoring the load bus voltages following a large disturbance (three-phase fault) and is used to classify the contingencies. The index is modified to include the impact of DG on the short-term voltage stability.

For transient stability, the maximum rotor speed deviations of centralized synchronous generators are monitored. The index consists then of the sum of maximum speed deviations and is used to rank contingencies as well as to emphasize the impact of adding aggregated DG.

Three power system test cases are employed to study the contributions of DG: a small-size system (the IEEE RTS-96 24-bus system), a medium-size system (the IEEE 39-bus New England system) and a large-size system (the IEEE 118 bus system). The software used is PSS®E

6.2 Conclusions

Regarding stability, the following conclusions are drawn from the results of this work:

1. For long-term studies, the total contribution of DG, when DG is connected at all load buses, can be estimated as the sum of the individual contributions

consisting of connecting DGs at one bus at a time. The placement of DGs in the system affects to a great extent the long-term voltage stability. DGs near large loads greatly improve the voltage security margin whereas if placed near large generation, DG can worsen the voltage stability of the system. For most cases, when DG operates at a lagging power factor, the voltage stability is improved. Only four penetration levels have been considered but the total contribution increases linearly and can therefore be predicted at any other penetration level. An application of the defined index consists of determining whether a large disturbance could cause the system would to fall into "DG assistance" which consists of the probability of avoiding voltage collapse with the presence of DG.

2. Contingency ranking is performed using the short-term voltage stability index to determine the critical contingencies. The total contribution of power electronic interfaced DG can be predicted using individual contributions (where DG is connected at one load bus) for small-size and medium-size power systems (the IEEE RTS-96 24 bus system and the IEEE 39-bus New England system). For large systems (the IEEE 118-bus system), the total contributions cannot be predicted due to the large number of non-linear elements. Similarly, the total contributions of machine based DG cannot be estimated. Synchronous machine based DG decreases the voltage dips more than other technologies. The contribution of induction machine based DG depends on the location and the size of the DG. The contribution of power electronic interfaced DG operating at a leading power factor further improves the short-term voltage stability compared with unity power factor. Whereas, when operating at a lagging power factor, the stability is worsened.
3. For transient stability, severe contingencies can be identified using the maximum rotor speed deviations indices. The contributions of power electronic interfaced DG depend on the DG placement and size. Near large loads, the stability is improved compared to the base case and is enhanced with an increase in DG penetration level. When placed near large centralized generators, the contribution of power electronic interfaced DG worsens the

stability of the system. The total contribution increases linearly with increasing penetration levels and therefore can be predicted at any DG penetration. The contribution of machine based DG enhances the stability of the system near large generators and increases the rotor deviations near large loads. The total contribution is predictable using a second-order polynomial approximation for the small and the medium systems. For large systems, the total contributions cannot be predicted due to the large number of centralized generators that are well dispersed in the system.

Another conclusion made regarding the stability of the power system relates to the power factor setting of the DG. The present approach is to operate DG at unity power factor for economical reasons. However, the study reveals the following:

1. It is more beneficial to have DGs operating at a lagging power factor for long-term voltage stability because it improves the voltage security margin by increasing the distance to voltage collapse.
2. When DG operates at a leading power factor, the short-term voltage stability is generally improved because the voltage dips are reduced.
3. Utilities should therefore try to convince owners to let the utilities control the DGs in order to improve the stability of the system.

6.3 Future Works

The work presented in this thesis can be further expanded to include the following issues:

1. The short-term voltage stability index can be modified to better estimate the total contribution of rotating machine based DG by taking into account the non-linear elements introduced into the DG models by taking into account higher order phenomena.
2. For transient stability, it is important to also consider the oscillation duration of rotor speed deviations. The lack of damping torque introduced by synchronous generators could cause rotor speeds to oscillate continuously. This phenomenon may cause the system to become unstable if the oscillation is propagated to other generators which can then be tripped.

3. In this thesis, only three-phase faults were considered for short-term stability analysis. Other types of large disturbances could also be used to test the indices proposed in this work, such as machine tripping and load transients.
4. The analysis of large DG penetration could be enhanced by taking into account the small-signal stability and the frequency and defining corresponding indices. An index can then be defined by combining the indices of all types of stability associated with a weighing factor to determine the optimal sizing of DG that can be installed at a specific location.

List of References

[1] J.D. Glover and M.S. Sarma, *Power System Analysis and Design*, Brooks/Cole, 2001.

[2] CIRED, "Dispersed Generation," Nice, France: Preliminary report of CIRED working group WG04, 1999.

[3] G. Pepermans, J. Driesen, D. Haeseldonckx, R. Belmans, and W. D'haeseleer, "Distributed generation: definition, benefits and issues," *Energy Policy*, vol. 33, Apr. 2005, pp. 787-798.

[4] CIGRE Working Group 37.23, "Impact of increasing contribution of dispersed generation on the power system," *CIGRE Technical Brochure no. 137*, 1999.

[5] Electric Power Research Institute, "Distributed Generation," www.epri.com, 1998.

[6] D. Sharma and R. Bartels, "Distributed electricity generation in competitive energy markets: a case study in Australia," *The International Association for Energy Economics*, The Energy Journal Special issue: Distributed Resources: Toward a New Paradigm of the Electricity Business, 1998, pp. 17-40.

[7] A. Chambers, B. Schnoor, and S. Hamilton, *Distributed generation: A Nontechnical Guide*, PennWell Books, 2001.

[8] Gas Research Institute, "Distributed Power Generation: A Strategy for a Competitive Energy Industry," *Gas Research Institute*, Chicago, USA: 1998.

[9] P. Dondi, D. Bayoumi, C. Haederli, D. Julian, and M. Suter, "Network integration of distributed power generation," *Journal of Power Sources*, vol. 106, Apr. 2002, pp. 1-9.

[10] P. Fraser, O.F.E.C.A. Development, A.I.D. l'énergie, and I.E. Agency, *Distributed generation in liberalised electricity markets*, OECD/IEA, 2002.

[11] T. Ackermann, G. Andersson, and L. Soder, "Distributed generation: a definition," *Electric Power Systems Research*, vol. 57, Apr. 2001, pp. 195-204.

[12] N. Jenkins, R. Allan, I.O.E. Engineers, P. Crossley, D. Kirschen, and G. Strbac, *Embedded generation*, IET, 2000.

[13] M. Rabinowitz, "Power systems of the future. 4," *IEEE Power Eng. Review*, vol. 20, 2000, pp. 4-9.

[14] P. Kundur, J. Paserba, V. Ajjarapu, G. Andersson, A. Bose, C. Canizares, N. Hatziargyriou, D. Hill, A. Stankovic, C. Taylor, T. Van Cutsem, and V. Vittal, "Definition and classification of power system stability IEEE/CIGRE joint task force on stability terms and definitions," *IEEE Trans. Power Syst.*, vol. 19, 2004, pp. 1387-1401.

[15] P. Kundur, N.J. Balu, and M.G. Lauby, *Power system stability and control*, McGraw-Hill Professional, 1994.

[16] T.V. Cutsem and C. Vournas, *Voltage stability of electric power systems*, Springer, 1998.

[17] C.W. Taylor, N.J. Balu, and D. Maratukulam, *Power System Voltage Stability*,

McGraw-Hill, 1994.

[18] E. Potamianakis and C. Vournas, "Short-term voltage instability: effects on synchronous and induction machines," *IEEE Trans. Power Syst.*, vol. 21, 2006, pp. 791-798.

[19] T. Van Cutsem, "Voltage instability: phenomena, countermeasures, and analysis methods," *IEEE Proc.*, vol. 88, 2000, pp. 208-227.

[20] B. Gao, G. Morison, and P. Kundur, "Towards the development of a systematic approach for voltage stability assessment of large-scale power systems," *IEEE Trans. Power Syst.*, vol. 11, 1996, pp. 1314-1324.

[21] G. Morison, B. Gao, and P. Kundur, "Voltage stability analysis using static and dynamic approaches," *IEEE Trans. Power Syst.*, vol. 8, 1993, pp. 1159-1171.

[22] P. Lof, T. Smed, G. Andersson, and D. Hill, "Fast calculation of a voltage stability index," *IEEE Trans. Power Syst.*, vol. 7, 1992, pp. 54-64.

[23] V. Ajjarapu and C. Christy, "The continuation power flow: a tool for steady state voltage stability analysis," *IEEE Trans. Power Syst.*, vol. 7, 1992, pp. 416-423.

[24] M. Pavella and P.G. Murthy, *Transient stability of power systems*, Wiley, 1994.

[25] J. Machowski, J. Bialek, and D.J. Bumby, *Power System Dynamics: Stability and Control*, Wiley, 2008.

[26] P. Kundur and Lei Wang, "Small signal stability analysis: experiences, achievements, and challenges," *2002 Proc. PowerCon Int. Conf. Power Syst. Technology*, pp. 6-12 vol.1.

[27] Y. Makarov, Zhao Yang Dong, and D. Hill, "A general method for small signal stability analysis," *IEEE Trans. Power Syst.*, vol. 13, 1998, pp. 979-985.

[28] S. Gomes, N. Martins, and C. Portela, "Computing small-signal stability boundaries for large-scale power systems," *IEEE Trans. Power Syst.*, vol. 18, 2003, pp. 747-752.

[29] H. Hedayati, S. Nabaviniaki, and A. Akbarimajd, "A Method for Placement of DG Units in Distribution Networks," *IEEE Trans. Power Del.*, vol. 23, 2008, pp. 1620-1628.

[30] Yue Yuan, Kejun Qian, and Chengke Zhou, "The optimal location and penetration level of distributed generation," *UPEC 2007 42nd Int. Universities Power Eng. Conf.*, 2007, pp. 917-923.

[31] W. Freitas, J. Vieira, A. Morelato, and W. Xu, "Influence of excitation system control modes on the allowable penetration level of distributed synchronous generators," *IEEE Trans. Energy Convers.*, vol. 20, 2005, pp. 474-480.

[32] W. Freitas, J. Vieira, A. Morelato, L. da Silva, V. da Costa, and F. Lemos, "Comparative analysis between synchronous and induction machines for distributed generation applications," *IEEE Trans. Power Syst.*, vol. 21, 2006, pp. 301-311.

[33] W. Freitas, L. DaSilva, and A. Morelato, "Small-Disturbance Voltage Stability of Distribution Systems With Induction Generators," *IEEE Trans. Power Syst.*, vol. 20, 2005, pp. 1653-1654.

[34] V. Thong, J. Driesen, and R. Belmans, "Transmission system operation concerns with high penetration level of distributed generation," *UPEC 2007 42nd Int.*

Universities Power Eng. Conf., 2007, pp. 867-871.

[35] R. Londero, C. Affonso, and M. Nunes, "Impact of distributed generation in steady state, voltage and transient stability — Real case," *2009 IEEE Bucharest PowerTech*, pp. 1-6.

[36] I. Xyngi, A. Ishchenko, M. Popov, and L. van der Sluis, "Transient Stability Analysis of a Distribution Network With Distributed Generators," *IEEE Trans. Power Syst.*, vol. 24, 2009, pp. 1102-1104.

[37] J. Slootweg and W. Kling, "Impacts of distributed generation on power system transient stability," *2002 IEEE Power Eng. Soc. Summer Meeting*, pp. 862-867 vol.2.

[38] E. Collins and Jian Jiang, "Voltage Sags and the Response of a Synchronous Distributed Generator: A Case Study," *IEEE Trans. Power Del.*, vol. 23, 2008, pp. 442-448.

[39] Hsiao-Dong Chiang, A. Flueck, K. Shah, and N. Balu, "CPFLOW: a practical tool for tracing power system steady-state stationary behavior due to load and generation variations," *IEEE Trans. Power Syst.*, vol. 10, 1995, pp. 623-634.

[40] PSS™E 31.0, *VOLUME I: PROGRAM OPERATION MANUAL*, Siemens Power Transmission & Distribution, Inc. Power Technologies International, 2007.

[41] A. Lerm, C. Canizares, and A. Silveira e Silva, "Multiparameter bifurcation analysis of the south Brazilian power system," *IEEE Trans. Power Syst.*, vol. 18, 2003, pp. 737-746.

[42] M. Begovic, A. Pregelj, A. Rohatgi, and C. Honsberg, "Green power: status and perspectives," *IEEE Proc.*, vol. 89, 2001, pp. 1734-1743.

[43] S.W. Hadley and W. Short, "Electricity sector analysis in the clean energy futures study," *Energy Policy*, vol. 29, Nov. 2001, pp. 1285-1298.

[44] C. Soares, *Microturbines*, Elsevier, 2007.

[45] T. Kaarsberg and J. Roop, "Combined heat and power: how much carbon and energy can manufacturers save?," *IEEE Aerosp. Electron. Syst. Mag.*, vol. 14, 1999, pp. 7-12.

[46] H. Gil and G. Joos, "Customer-Owned Back-Up Generators for Energy Management by Distribution Utilities," *IEEE Trans. Power Syst.*, vol. 22, 2007, pp. 1044-1050.

[47] R. Dettmer, "Wind of change [gas turbine based CHP]," *IEE Review*, vol. 46, 2000, pp. 21-24.

[48] A. Saha, S. Chowdhury, and P. Crossley, "Modeling and Performance Analysis of a Microturbine as a Distributed Energy Resource," *IEEE Trans. Energy Convers.*, vol. 24, 2009, pp. 529-538.

[49] R. O'Hayre, W. Colella, S. Cha, and F.B. Prinz, *Fuel Cell Fundamentals*, Wiley, 2009.

[50] M. Laughton, "Fuel cells," *Engineering Science and Education Journal*, vol. 11, 2002, pp. 7-16.

[51] B. Cook, "Introduction to fuel cells and hydrogen technology," *Engineering Science and Education Journal*, vol. 11, 2002, pp. 205-216.

[52] R.A. Messenger and J. Ventre, *Photovoltaic Systems Engineering*, CRC, 1999.

[53] T. Burton, D. Sharpe, N. Jenkins, and E. Bossanyi, *Wind Energy Handbook*, Wiley, 2001.

[54] L. Monition, M.L. Nir, and J. Roux, *Micro Hydroelectric Power Stations*, John Wiley & Sons Inc, 1985.

[55] F. Schwartz and M. Shahidehpour, "Small Hydro as Green Power," *2006 IEEE EIC Climate Change Technology*, pp. 1-6.

[56] C. Abbey and G. Joos, "Energy Storage and Management in Wind Turbine Generator Systems," *2006 12th Int. Power Electronics and Motion Control Conf.*, pp. 2051-2056.

[57] R. Schainker, "Executive overview: energy storage options for a sustainable energy future," *2004 IEEE Power Eng. Soc. General Meeting*, pp. 2309-2314 Vol.2.

[58] T. Sels, C. Dragu, T. Van Craenenbroeck, and R. Belmans, "Overview of new energy storage systems for an improved power quality and load managing on distribution level," *Electricity Distribution, 2001. Part 1: Contributions. CIRED. 16th International Conference and Exhibition on (IEE Conf. Publ No. 482)*, 2001, p. 5 pp. vol.4.

[59] Yaosuo Xue, Liuchen Chang, and J. Meng, "Dispatchable Distributed Generation Network - A New Concept to Advance DG Technologies," *2007 IEEE Power Eng. Soc. General Meeting*, pp. 1-5.

[60] F. Blaabjerg, Zhe Chen, and S. Kjaer, "Power electronics as efficient interface in dispersed power generation systems," *IEEE Trans. Power Electron.*, vol. 19, 2004, pp. 1184-1194.

[61] G. Joos, B. Ooi, D. McGillis, F. Galiana, and R. Marceau, "The potential of distributed generation to provide ancillary services," *2000 IEEE Power Eng. Soc. Summer Meeting*, pp. 1762-1767 vol. 3.

[62] J. Enslin, "Interconnection of distributed power to the distribution network," *2004 IEEE PES Power Syst. Conf.and Exposition*, pp. 726-731 vol.2.

[63] *IEEE Standard for Interconnecting Distributed Resources with Electric Power Systems*, IEEE Standard 1547, 2003.

[64] P. Barker and B. Johnson, "Power system modeling requirements for rotating machine interfaced distributed resources," *2002 IEEE Power Eng. Soc. Summer Meeting*, 2002, pp. 161-166 vol.1.

[65] P. Barker and R. De Mello, "Determining the impact of distributed generation on power systems. I. Radial distribution systems," *2000 IEEE Power Eng. Soc. Winter Meeting*, pp. 1645-1656 vol. 3.

[66] PSS™E 31.0, *VOLUME II: PROGRAM APPLICATION GUIDE*, Siemens Power Transmission & Distribution, Inc. Power Technologies International, 2007.

[67] J. Hurley, L. Bize, and C. Mummert, "The adverse effects of excitation system VAr and power factor controllers," *IEEE Trans. Energy Convers.*, vol. 14, 1999, pp. 1636-1645.

[68] J. Morren, S. de Haan, and J. Ferreira, "Model reduction and control of electronic interfaces of voltage dip proof DG units," *2004 IEEE Power Eng. Soc. General*

Meeting, pp. 2168-2173 Vol.2.

[69] M. Reza, A.O. Dominguez, P.H. Schavemaker, and W.L. Kling, "Maintaining the power balance in an lsquoempty networkrsquo," *European Trans. Elect. Power*, vol. 16, 2006, pp. 479-493.

[70] K. Kauhaniemi and L. Kumpulainen, "Impact of distributed generation on the protection of distribution networks," *2004 8th IEE Int. Conf. Develop. in Power Syst. Protection*, pp. 315-318 Vol.1.

[71] T. Ackermann, *Wind Power in Power Systems*, Wiley, 2005.

[72] S. Chiang, K. Chang, and C. Yen, "Residential photovoltaic energy storage system," *IEEE Trans. Ind. Electron.*, vol. 45, 1998, pp. 385-394.

[73] "35 kV and Below Interconnection Requirements for Power Generators," Feb. 2008.

[74] "Alberta Distributed Generation: Interconnection Guide," Jul. 2002.

[75] "California Interconnection Guidebook: A Guide to Interconnecting Customer-owned Electric Generation Equipment to the Electric Utility Distribution System Using California's Electric Rule 21," Sep. 2003.

[76] "Exigence Relatives au Raccordement de la Production Décentralisée Utilisant des Onduleurs de Faible Puissance au Réseau de Distribution Basse Tension d'Hydro-Québec," Jul. 2005.

[77] "Generation Interconnection Requirements at Voltages 34.5 kV and Below," Mar. 2005.

[78] "Interconnection Guideline For Connecting Distributed Resources to the Manitoba Hydro Distribution System," Jan. 2003.

[79] "New York State Standardized Interconnection Requirements and Application Process for New Distributed Generators 2 MW or Less Connected in Parallel with Utility Distribution Systems," Feb. 2009.

[80] "Grid Connection Requirements," *Market Rules for the Ontario Electricity Market*, Independent Electricity System Operator (IESO), 2006.

[81] P.M. Anderson and A.A. Fouad, *Power System Control and Stability*, Wiley-IEEE Press, 2002.

[82] C. Grigg, P. Wong, P. Albrecht, R. Allan, M. Bhavaraju, R. Billinton, Q. Chen, C. Fong, S. Haddad, S. Kuruganty, W. Li, R. Mukerji, D. Patton, N. Rau, D. Reppen, A. Schneider, M. Shahidehpour, and C. Singh, "The IEEE Reliability Test System-1996. A report prepared by the Reliability Test System Task Force of the Application of Probability Methods Subcommittee," *IEEE Trans. Power Syst.*, vol. 14, 1999, pp. 1010-1020.

[83] M.A. Pai, *Energy function analysis for power system stability*, Springer, 1989.

[84] R. Christie, "Power System Test Archive," Aug. 1999.

[85] G. Andersson, P. Donalek, R. Farmer, N. Hatziargyriou, I. Kamwa, P. Kundur, N. Martins, J. Paserba, P. Pourbeik, J. Sanchez-Gasca, R. Schulz, A. Stankovic, C. Taylor, and V. Vittal, "Causes of the 2003 major grid blackouts in North America and Europe, and recommended means to improve system dynamic performance," *Power Systems, IEEE Transactions on*, vol. 20, 2005, pp. 1922-1928.

[86] C. Foote, G. Burt, I. Elders, and G. Ault, "Developing distributed generation

penetration scenarios," *2005 Int. Conf. Future Power Syst.*, pp. 6 pp.-6.

[87] C. Canizares, *Voltage Stability Assessment: Concepts, Practices and Tools*, IEEE Power Engineering Society, 2002.

[88] "IESO Power to Ontario. On Demand.," *Independent Electricity System Operator (IESO)*.

[89] "ISO New England," *ISO New England Inc.*

[90] "NYISO: New York Independent System Operator," *NYISO*.

[91] "AEMO - Australian Energy Market Operator," *AEMO*.

[92] "RTE Gestionnaire du Réseau de Transport d'Electricité," *RTE - Transmission System Operator in France*.

[93] "National Grid," *National Grid: Electricity Homepage*.

[94] C. Vournas and E. Potamianakis, "Investigation of short-term voltage stability problems and countermeasures," *2004 IEEE PES Power Syst. Conf.and Exposition*, pp. 385-391 vol.1.

[95] J. Diaz de Leon and C. Taylor, "Understanding and solving short-term voltage stability problems," *2002 IEEE Power Eng. Soc. Summer Meeting*, 2002, pp. 745-752 vol.2.

[96] "Load representation for dynamic performance analysis [of power systems]," *IEEE Trans. Power Syst.*, vol. 8, 1993, pp. 472-482.

[97] C. Mozina, "A shot in the dark," *IEEE Ind. Appl. Mag.*, vol. 14, 2008, pp. 45-52.

Appendix A: Power Systems Data

A.1 The IEEE Reliability Test System 1996

Table A.1. Bus data of the IEEE RTS-96 24 bus system

Bus Number	Volts (p.u.)	P_L (MW)	Q_L (MVAR)	P_G (MW)	Q_G (MVAR)
1	1.035	108	22	172	17.3218
2	1.035	97	20	172	0
3	-	180	37	-	-
4	-	74	15	-	-
5	-	71	14	-	-
6	-	136	28	-	-
7	1.025	125	25	240	57.3808
8	-	171	35	-	-
9	-	175	36	-	-
10	-	195	40	-	-
11	-	-	-	-	-
12	-	-	-	-	-
13	1.02	265	54	249.4567	139.7562
14	0.98	194	39	0	13.7
15	1.014	317	64	155	80
16	1.017	100	20	400	200
17	-	-	-	-	-
18	1.05	333	68	400	137.512
19	-	181	37	-	-
20	-	128	26	-	-
21	1.05	-	-	300	96
22	1.05	-	-	660	-1.5124
23	1.05	-	-	189.257	89.4242
24	-	-	-	-	-

Table A.2. Branch data of the IEEE RTS-96 24 bus system

From Bus	To Bus	R (p.u.)	X (p.u.)	B (p.u.)	Tap Ratio
1	2	0.0030	0.0140	0.4610	-
1	3	0.0550	0.2110	0.0570	-
1	5	0.0220	0.0850	0.0230	-
2	4	0.0330	0.1270	0.0340	-
2	6	0.0500	0.1920	0.0520	-
3	9	0.0310	0.1190	0.0320	-
3	24	0.0020	0.0840	-	1.015
4	9	0.0270	0.1040	0.0280	-
5	10	0.0230	0.0880	0.0240	-
6	10	0.0140	0.0610	2.4590	-
7	8	0.0160	0.0610	0.0170	-
8	9	0.0430	0.1650	0.0450	-
8	10	0.0430	0.1650	0.0450	-
9	11	0.0020	0.0840	-	1.03
9	12	0.0020	0.0840	-	1.03
10	11	0.0020	0.0840	-	1.015
10	12	0.0020	0.0840	-	1.015
11	13	0.0060	0.0480	0.1000	-
11	14	0.0050	0.0420	0.0880	-
12	13	0.0060	0.0480	0.1000	-
12	23	0.0120	0.0970	0.2030	-
13	23	0.0110	0.0870	0.1820	-
14	16	0.0050	0.0590	0.0820	-
15	16	0.0020	0.0170	0.0360	-
15	21	0.0030	0.0245	0.2060	-
15	24	0.0070	0.0520	0.1090	-
16	17	0.0030	0.0260	0.0550	-
16	19	0.0030	0.0230	0.0490	-
17	18	0.0020	0.0140	0.0300	-
17	22	0.0140	0.1050	0.2210	-
18	21	0.0015	0.0130	0.1100	-
19	20	0.0025	0.0200	0.1660	-
20	23	0.0015	0.0110	0.0920	-
21	22	0.0090	0.0680	0.1420	-

A.2 The IEEE 39-Bus New England Test System

Table A.3. Bus data of the IEEE 39-bus New England system

Bus Number	Volts (p.u.)	P_L (MW)	Q_L (MVAR)	P_G (MW)	Q_G (MVAR)
1	-	-	-	-	-
2	-	-	-	-	-
3	-	321.9056	2.3993	-	-
4	-	461.1859	169.7164	-	-
5	-	-	-	-	-
6	-	-	-	-	-
7	-	212.5000	76.3473	-	-
8	-	476.5785	160.6855	-	-
9	-	-	-	-	-
10	-	-	-	-	-
11	-	-	-	-	-
12	-	5.6998	66.8774	-	-
13	-	-	-	-	-
14	-	-	-	-	-
15	-	302.9448	144.8455	-	-
16	-	322.7319	31.6846	-	-
17	-	-	-	-	-
18	-	157.8441	29.9704	-	-
19	-	-	-	-	-
20	-	610.3152	100.0995	-	-
21	-	269.6314	113.1665	-	-
22	-	-	-	-	-
23	-	251.7204	86.0426	-	-
24	-	307.2028	-91.5834	-	-
25	-	236.7802	49.8930	-	-
26	-	146.9664	17.9743	-	-
27	-	287.4464	77.2320	-	-
28	-	209.1217	28.0182	-	-
29	-	280.4685	26.6123	-	-
30	1.0475	-	-	250	106.0626
31	0.9820	8.8718	4.4359	471.1658	109.5267
32	0.9831	-	-	650	-85.4185
33	0.9972	-	-	632	-41.2911
34	1.0123	-	-	508	146.1808
35	1.0493	-	-	650	133.4882
36	1.0635	-	-	560	141.1959
37	1.0278	-	-	540	-90.5243
38	1.0265	-	-	830	-148.3910
39	1.0300	1171.2340	265.2250	1000	15.9550

Table A.4. Branch data of the IEEE 39-bus New England system

From Bus	To Bus	R (p.u.)	X (p.u.)	B (p.u.)	Tap Ratio
1	2	0.0035	0.0411	0.6987	-
1	39	0.0010	0.0250	0.7500	-
2	3	0.0013	0.0151	0.2572	-
2	25	0.0070	0.0086	0.1460	-
2	30	0.0000	0.0181	-	1.025
3	4	0.0013	0.0213	0.2214	-
3	18	0.0011	0.0133	0.2138	-
4	5	0.0008	0.0128	0.1342	-
4	14	0.0008	0.0129	0.1382	-
5	6	0.0002	0.0026	0.0434	-
5	8	0.0008	0.0112	0.1476	-
6	7	0.0006	0.0092	0.1130	-
6	11	0.0007	0.0082	0.1389	-
6	31	0.0000	0.0250	-	1.07
7	8	0.0004	0.0046	0.0780	-
8	9	0.0023	0.0363	0.3804	-
9	39	0.0010	0.0250	1.2000	-
10	11	0.0004	0.0043	0.0729	-
10	13	0.0004	0.0043	0.0729	-
10	32	0.0000	0.0200	-	1.07
11	12	0.0000	0.0435	-	1.006
12	13	0.0000	0.0435	-	1.006
13	14	0.0009	0.0101	0.1723	-
14	15	0.0018	0.0217	0.3660	-
15	16	0.0009	0.0094	0.1710	-
16	17	0.0007	0.0089	0.1342	-
16	19	0.0016	0.0195	0.3040	-
16	21	0.0008	0.0135	0.2548	-
16	24	0.0003	0.0059	0.0680	-
17	18	0.0007	0.0082	0.1319	-
17	27	0.0013	0.0173	0.3216	-
19	20	0.0000	0.0138	-	1.06
19	33	0.0000	0.0142	-	1.07
20	34	0.0000	0.0180	-	1.009
21	22	0.0008	0.0140	0.2565	-
22	23	0.0006	0.0096	0.1846	-
22	35	0.0000	0.0143	-	1.025
23	24	0.0022	0.0350	0.3610	-
23	36	0.0000	0.0272	-	1
25	26	0.0032	0.0323	0.5130	-
25	37	0.0000	0.0232	-	1.025
26	27	0.0014	0.0147	0.2396	-
26	28	0.0043	0.0474	0.7802	-
26	29	0.0057	0.0625	1.0290	-
28	29	0.0014	0.0151	0.2490	-
29	38	0.0000	0.0156	-	1.025

A.3 The IEEE 118-Bus Test System

Table A.5. Bus data of the IEEE 118-bus system

Bus Number	Volts (p.u.)	P_L (MW)	Q_L (MVAR)	P_G (MW)	Q_G (MVAR)
1	0.955	51	27	0	-30.0354
2	-	20	9	-	-
3	-	39	10	-	-
4	0.998	30	12	0	-43.3367
5	-	-	-	-	-
6	0.99	52	22	0	-36.9629
7	-	19	2	-	-
8	1.015	-	-	0	155.7257
9	-	-	-	-	-
10	1.05	-	-	450	2.836957
11	-	70	23	-	-
12	0.99	47	10	85	90.794
13	-	34	16	-	-
14	-	14	1	-	-
15	0.97	90	30	0	36.9184
16	-	25	10	-	-
17	-	11	3	-	-
18	0.973	60	34	0	54.6463
19	0.962	45	25	0	-26.5339
20	-	18	3	-	-
21	-	14	8	-	-
22	-	10	5	-	-
23	-	7	3	-	-
24	0.992	-	-	0	-34.1573
25	1.05	-	-	220	137.5914
26	1.015	-	-	314	-73.0302
27	0.968	62	13	0	18.7108
28	-	17	7	-	-
29	-	24	4	-	-
30	-	-	-	-	-
31	0.967	43	27	7	35.1656
32	0.963	59	23	0	-64.3266
33	-	23	9	-	-
34	0.984	59	26	0	74.8169
35	-	33	9	-	-
36	0.98	31	17	0	27.7357
37	-	-	-	-	-
38	-	-	-	-	-
39	-	27	11	-	-
40	0.97	20	23	0	27.4492
41	-	37	10	-	-
42	0.985	37	23	0	11.1803
43	-	18	7	-	-
44	-	16	8	-	-
45	-	53	22	-	-

46	1.005	28	10	19	-3.2878
47	-	34	-	-	-
48	-	20	11	-	-
49	1.025	87	30	204	200.0466
50	-	17	4	-	-
51	-	17	8	-	-
52	-	18	5	-	-
53	-	23	11	-	-
54	0.955	113	32	48	-73.0263
55	0.952	63	22	0	-118.084
56	0.954	84	18	0	-177.018
57	-	12	3	-	-
58	-	12	3	-	-
59	0.985	277	113	155	407.5284
60	-	78	3	-	-
61	0.995	-	-	160	-27.8535
62	0.998	77	14	0	-202.543
63	-	-	-	-	-
64	-	-	-	-	-
65	1.005	-	-	391	-67.1025
66	1.05	39	18	392	208.0489
67	-	28	7	-	-
68	-	-	-	-	-
69	1.035	-	-	663.7812	86.1604
70	0.984	66	20	0	114.8425
71	-	-	-	-	-
72	0.98	-	-	0	-29.9559
73	0.991	-	-	0	9.1014
74	0.958	68	27	0	-299.012
75	-	47	11	-	-
76	0.943	68	36	0	-116.282
77	1.006	61	28	0	282.6617
78	-	71	26	-	-
79	-	39	32	-	-
80	1.04	130	26	477	217.3961
81	-	-	-	-	-
82	-	54	27	-	-
83	-	20	10	-	-
84	-	11	7	-	-
85	0.985	24	15	0	47.1462
86	-	21	10	-	-
87	1.015	-	-	4	16.1708
88	-	48	10	-	-
89	1.005	-	-	607	-6.9901
90	0.985	78	42	0	111.8854
91	0.98	-	-	0	-26.8084
92	0.99	65	10	0	31.5594
93	-	12	7	-	-
94	-	30	16	-	-
95	-	42	31	-	-

96	-	38	15	-	-
97	-	15	9	-	-
98	-	34	8	-	-
99	1.01	-	-	0	-95.1502
100	1.017	37	18	252	138.1113
101	-	22	15	-	-
102	-	5	3	-	-
103	1.01	23	16	40	132.2963
104	0.971	38	25	0	-35.555
105	0.965	31	26	0	-17.1991
106	-	43	16	-	-
107	0.952	28	12	0	4.4428
108	-	2	1	-	-
109	-	8	3	-	-
110	0.973	39	30	0	-18.9474
111	0.98	-	-	36	-4.2947
112	0.975	25	13	0	38.4424
113	0.993	-	-	0	63.4284
114	-	8	3	-	-
115	-	22	7	-	-
116	1.005	-	-	0	75.8353
117	-	20	8	-	-
118	-	33	15	-	-

Table A.6. Branch data of the IEEE 118-bus system

From Bus	To Bus	R (p.u.)	X (p.u.)	B (p.u.)	Tap Ratio
1	2	0.0303	0.0999	0.0254	-
1	3	0.0129	0.0424	0.0108	-
2	12	0.0187	0.0616	0.0157	-
3	5	0.0241	0.1080	0.0284	-
3	12	0.0484	0.1600	0.0406	-
4	5	0.0018	0.0080	0.0021	-
4	11	0.0209	0.0688	0.0175	-
5	6	0.0119	0.0540	0.0143	-
5	11	0.0203	0.0682	0.0174	-
6	7	0.0046	0.0208	0.0055	-
7	12	0.0086	0.0340	0.0087	-
8	9	0.0024	0.0305	1.1620	-
8	5	0.0000	0.0267	0.0000	0.985
8	30	0.0043	0.0504	0.5140	-
9	10	0.0026	0.0322	1.2300	-
11	12	0.0060	0.0196	0.0050	-
11	13	0.0223	0.0731	0.0188	-
12	14	0.0215	0.0707	0.0182	-
12	16	0.0212	0.0834	0.0214	-
12	117	0.0329	0.1400	0.0358	-
13	15	0.0744	0.2444	0.0627	-
14	15	0.0595	0.1950	0.0502	-
15	17	0.0132	0.0437	0.0444	-
15	19	0.0120	0.0394	0.0101	-
15	33	0.0380	0.1244	0.0319	-
16	17	0.0454	0.1801	0.0466	-
17	18	0.0123	0.0505	0.0130	-
17	31	0.0474	0.1563	0.0399	-
17	113	0.0091	0.0301	0.0077	-
18	19	0.0112	0.0493	0.0114	-
19	20	0.0252	0.1170	0.0298	-
19	34	0.0752	0.2470	0.0632	-
20	21	0.0183	0.0849	0.0216	-
21	22	0.0209	0.0970	0.0246	-
22	23	0.0342	0.1590	0.0404	-
23	24	0.0135	0.0492	0.0498	-
23	25	0.0156	0.0800	0.0864	-
23	32	0.0317	0.1153	0.1173	-
24	70	0.0022	0.4115	0.1020	-
24	72	0.0488	0.1960	0.0488	-
25	27	0.0318	0.1630	0.1764	-
26	25	0.0000	0.0382	0.0000	0.96
26	30	0.0080	0.0860	0.9080	-
27	28	0.0191	0.0855	0.0216	-
27	32	0.0229	0.0755	0.0193	-
27	115	0.0164	0.0741	0.0197	-
28	29	0.0237	0.0943	0.0238	-

29	31	0.0108	0.0331	0.0083	-
30	17	0.0000	0.0388	0.0000	0.96
30	38	0.0046	0.0540	0.4220	-
31	32	0.0298	0.0985	0.0251	-
32	113	0.0615	0.2030	0.0518	-
32	114	0.0135	0.0612	0.0163	-
33	37	0.0415	0.1420	0.0366	-
34	36	0.0087	0.0268	0.0057	-
34	37	0.0026	0.0094	0.0098	-
34	43	0.0413	0.1681	0.0423	-
35	36	0.0022	0.0102	0.0027	-
35	37	0.0110	0.0497	0.0132	-
37	39	0.0321	0.1060	0.0270	-
37	40	0.0593	0.1680	0.0420	-
38	37	0.0000	0.0375	0.0000	0.935
38	65	0.0090	0.0986	1.0460	-
39	40	0.0184	0.0605	0.0155	-
40	41	0.0145	0.0487	0.0122	-
40	42	0.0555	0.1830	0.0466	-
41	42	0.0410	0.1350	0.0344	-
42	49	0.0358	0.1615	0.1720	-
43	44	0.0608	0.2454	0.0607	-
44	45	0.0224	0.0901	0.0224	-
45	46	0.0400	0.1356	0.0332	-
45	49	0.0684	0.1860	0.0444	-
46	47	0.0380	0.1270	0.0316	-
46	48	0.0601	0.1890	0.0472	-
47	49	0.0191	0.0625	0.0160	-
47	69	0.0844	0.2778	0.0709	-
48	49	0.0179	0.0505	0.0126	-
49	50	0.0267	0.0752	0.0187	-
49	51	0.0486	0.1370	0.0342	-
49	54	0.0397	0.1450	0.1468	-
49	66	0.0090	0.0460	0.0496	-
49	69	0.0985	0.3240	0.0828	-
50	57	0.0474	0.1340	0.0332	-
51	52	0.0203	0.0588	0.0140	-
51	58	0.0255	0.0719	0.0179	-
52	53	0.0405	0.1635	0.0406	-
53	54	0.0263	0.1220	0.0310	-
54	55	0.0169	0.0707	0.0202	-
54	56	0.0028	0.0096	0.0073	-
54	59	0.0503	0.2293	0.0598	-
55	56	0.0049	0.0151	0.0037	-
55	59	0.0474	0.2158	0.0565	-
56	57	0.0343	0.0966	0.0242	-
56	58	0.0343	0.0966	0.0242	-
56	59	0.0407	0.1224	0.1105	-
59	60	0.0317	0.1450	0.0376	-
59	61	0.0328	0.1500	0.0388	-

60	61	0.0026	0.0135	0.0146	-
60	62	0.0123	0.0561	0.0147	-
61	62	0.0082	0.0376	0.0098	-
62	66	0.0482	0.2180	0.0578	-
62	67	0.0258	0.1170	0.0310	-
63	59	0.0000	0.0386	0.0000	0.96
63	64	0.0017	0.0200	0.2160	-
64	61	0.0000	0.0268	0.0000	0.985
64	65	0.0027	0.0302	0.3800	-
65	66	0.0000	0.0370	0.0000	0.935
65	68	0.0014	0.0160	0.6380	-
66	67	0.0224	0.1015	0.0268	-
68	69	0.0000	0.0370	0.0000	0.935
68	81	0.0018	0.0202	0.8080	-
68	116	0.0003	0.0041	0.1640	-
69	70	0.0300	0.1270	0.1220	-
69	75	0.0405	0.1220	0.1240	-
69	77	0.0309	0.1010	0.1038	-
70	71	0.0088	0.0355	0.0088	-
70	74	0.0401	0.1323	0.0337	-
70	75	0.0428	0.1410	0.0360	-
71	72	0.0446	0.1800	0.0444	-
71	73	0.0087	0.0454	0.0118	-
74	75	0.0123	0.0406	0.0103	-
75	77	0.0601	0.1999	0.0498	-
75	118	0.0145	0.0481	0.0120	-
76	77	0.0444	0.1480	0.0368	-
76	118	0.0164	0.0544	0.0136	-
77	78	0.0038	0.0124	0.0126	-
77	80	0.0108	0.0332	0.0700	-
77	82	0.0298	0.0853	0.0817	-
78	79	0.0055	0.0244	0.0065	-
79	80	0.0156	0.0704	0.0187	-
80	96	0.0356	0.1820	0.0494	-
80	97	0.0183	0.0934	0.0254	-
80	98	0.0238	0.1080	0.0286	-
80	99	0.0454	0.2060	0.0546	-
81	80	0.0000	0.0370	0.0000	0.935
82	83	0.0112	0.0367	0.0380	-
82	96	0.0162	0.0530	0.0544	-
83	84	0.0625	0.1320	0.0258	-
83	85	0.0430	0.1480	0.0348	-
84	85	0.0302	0.0641	0.0123	-
85	86	0.0350	0.1230	0.0276	-
85	88	0.0200	0.1020	0.0276	-
85	89	0.0239	0.1730	0.0470	-
86	87	0.0283	0.2074	0.0445	-
88	89	0.0139	0.0712	0.0193	-
89	90	0.0163	0.0651	0.1588	-
89	92	0.0079	0.0383	0.0962	-

90	91	0.0254	0.0836	0.0214	-
91	92	0.0387	0.1272	0.0327	-
92	93	0.0258	0.0848	0.0218	-
92	94	0.0481	0.1580	0.0406	-
92	100	0.0648	0.2950	0.0472	-
92	102	0.0123	0.0559	0.0146	-
93	94	0.0223	0.0732	0.0188	-
94	95	0.0132	0.0434	0.0111	-
94	96	0.0269	0.0869	0.0230	-
94	100	0.0178	0.0580	0.0604	-
95	96	0.0171	0.0547	0.0147	-
96	97	0.0173	0.0885	0.0240	-
98	100	0.0397	0.1790	0.0476	-
99	100	0.0180	0.0813	0.0216	-
100	101	0.0277	0.1262	0.0328	-
100	103	0.0160	0.0525	0.0536	-
100	104	0.0451	0.2040	0.0541	-
100	106	0.0605	0.2290	0.0620	-
101	102	0.0246	0.1120	0.0294	-
103	104	0.0466	0.1584	0.0407	-
103	105	0.0535	0.1625	0.0408	-
103	110	0.0391	0.1813	0.0461	-
104	105	0.0099	0.0378	0.0099	-
105	106	0.0140	0.0547	0.0143	-
105	107	0.0530	0.1830	0.0472	-
105	108	0.0261	0.0703	0.0184	-
106	107	0.0530	0.1830	0.0472	-
108	109	0.0105	0.0288	0.0076	-
109	110	0.0278	0.0762	0.0202	-
110	111	0.0220	0.0755	0.0200	-
110	112	0.0247	0.0640	0.0620	-
114	115	0.0023	0.0104	0.0028	-

Appendix B: Distributed Generation Dynamic Data

Table B.1. Dynamic data for synchronous machine based DG

T'do	T''do	T'qo	T''qo	H	D	Xd	Xq	X'd	X'q	X''d	Xl	S(1.0)	S(1.2)
5	0.05	1	0.04	4	0	1.75	1.65	0.3	0.75	0.2	0.175	0.2	0.4

Table B.2. Dynamic data for induction machine based DG

T'	H	X	X'	Xl	E1	S(E1)	E2	S(E2)
0.98	3	3.1	0.18	0.1	1	0	1.2	0